NITROGEN'S ROLE IN CHANGING KERNEL WEIGHT IN MAIZE: RELEVANT PHYSIOLOGICAL MECHANISMS DURING REPRODUCTIVE STAGES

by

Lía Belén Olmedo Pico

A Dissertation

Submitted to the Faculty of Purdue University

In Partial Fulfillment of the Requirements for the degree of

Doctor of Philosophy

Department of Agronomy

West Lafayette, Indiana

May 2021

THE PURDUE UNIVERSITY GRADUATE SCHOOL

STATEMENT OF COMMITTEE APPROVAL

Dr. Tony J. Vyn, Chair

Department of Agronomy

Dr. James J. Camberato

Department of Agronomy

Dr. Jeffrey J. Volenec

Department of Agronomy

Dr. Cankui Zhang

Department of Agronomy

Dr. Ravi P. Sripada

Bayer Crop Science

Approved by:

Dr. Ronald Turco

Dedicated to little Lía, a curious, driven, bookish young girl growing up in a very small town of a little-populated province in a developing country. For her, and for all the little girls that she might represent and inspire.

ACKNOWLEDGMENTS

First, I wish to thank my advisor, Dr. Tony Vyn for the opportunity to pursue my Ph.D. studies under his guidance. Besides his academic mentorship, I am grateful for Dr. Vyn's persistent confidence in me and in this research project, even when the journey was full of challenges. I would also like to thank Dr. James Camberato, Dr. Jeffrey Volenec, Dr. Ravi Sripada, and Dr. Cankui Zhang for serving on my academic committee. In particular, thanks to Dr. Zhang for his enthusiastic support in the endosperm section of this dissertation.

Secondly, I wish to thank all the graduate students, the undergraduate workers, the visitant scholars, and the research associates who have been part of the Cropping Systems lab over the course of my Ph.D. Thanks for their help in field sampling, sample processing, and research discussions. Special thanks to Garrett V. for his key role in every field and lab measurement that I took, and to Monica O. for the invaluable study sessions, both in English and Spanish.

I also wish to thank people from the Department of Agronomy who have significantly contributed to this dissertation. Thanks to the Crop Molecular Physiology lab for their help in the endosperm analysis, especially Jing H. Thanks to Jason A., Sherry F.B., and the Cover Crop lab for lending me equipment that allowed me to collect data for Chapter 4. And special thanks to Connie F., Cheryl L., and Patti D. for helping me navigate the administrative intricacies of being an international graduate student.

I am very grateful to all the friends that I made throughout my Ph.D. journey, especially Diana S., Alyssa B., Lau O.Z., Linh P., and Jorge D.V. I was fortunate to connect with people from all over the world thanks to Fulbright, the program that funded my first two years of Ph.D. studies, and for that I will be always grateful. Thanks to the Purdue Fulbright Association, the Purdue Musical Organizations, and the Younger Women Task Force of Greater Lafayette, for providing me with opportunities to balance to my Ph.D. student life.

I also wish to thank people from Argentina that supported me throughout this journey. Thanks to Dr. Luis Erazzú, who has been a long-time career mentor. Thanks to all my friends who were constantly rooting for me, and who also took the time to visit with me in the few occasions that I was back in Argentina. Among them, special thanks to Cons C., Ale P., Lau P., Andrés P., Gabriel G., Lucas S., Nelsis N., Johana A., Lau C., Vane V., Tania B., Juli S., Ceci C., Jessi F., Lau B., Nati B. and Carla B.

Lastly, to my family. Especially, to my mum, Mony Pico Zossi, for the values that she raised me with, and to my sisters, Pía y Paula Olmedo Pico, for our unbreakable bond, even when I am always far away. Thank you to the three of you, your endless love and support have been the foundations that this dissertation was built on.

TABLE OF CONTENTS

LIST OF TABLES

LIST OF FIGURES

ABSTRACT

Although grain yield (GY) in maize (*Zea mays* L.) is the product of both kernel number (KN) per unit area and kernel weight (KW), the latter has historically been considered the least variable component. However, as a result of sink strength enhancement by genetic improvement, KW in modern genotypes has become more responsive to changes in environmental and management conditions. Furthermore, KW has recently been proven to play a bigger role in the genetic improvement of maize GY -in temperate U.S. germplasm- than it had before. Therefore, the prospect of KW becoming a more important driver behind GY variability warrants embarking on more intensive research into the physiological mechanisms underlying when post-flowering stress conditions can limit KW. In pursuit of that goal, this dissertation evaluated the effects of N availability on: 1) the sources of dry matter (DM) and N assimilates for the growing kernels during the reproductive period; 2) the determination of potential KW (i.e., potential kernel sink capacity) during the lag phase of grain filling; and 3) the realization of final KW (i.e., actual sink capacity) during the linear phase of grain filling.

To investigate how N availability affected source capacity during reproductive growth, a 2-year field study that combined N timing and N rate treatments (under a common density of 8.3 plants m^{-2}) was conducted at the Purdue Rice Farm (LaCrosse, IN) in 2016 and 2017. The timing applications included: all N applied at planting, split application between planting and early sidedress, and split application between planting and V12 (for the last 56 kg N ha^{-1}). The five N rates tested were 0, 112, 168, 224, and 280 kg N ha^{-1}. Biomass samples of plant components at R1, R3, and R6 enabled DM and N sources (i.e., post-silking DM production, post-silking N uptake, DM and N remobilization) to be calculated separately for the two main grain-filling phases: from R1 to R3 (i.e., lag phase) and from R3 to R6 (i.e., linear phase). Since N timing and its interaction with N rate had no impact on the majority of evaluated parameters, the much larger N rate impacts were therefore averaged across N timing treatments. In both seasons, lag-phase DM production ($PostDM_{R1.R3}$) was much less responsive to N rates than that during the linear-phase ($PostDM_{R3.R6}$). In the lag phase, substantial DM gains in leaves and stems occurred in both years, while N content gains were mostly detected in reproductive tissues. Differential seasonal patterns in post-silking N uptake were observed, with plants either achieving net above-ground N content gains only during the lag phase ($PostN_{R1.R3}$) in 2016, or during the linear phase ($PostN_{R3.R6}$) in 2017). Both GY and

KW were gradually increased by N supply, with reproductive tissues proving to be relatively stronger sinks for N than for DM during the lag phase.

To understand how N availability affected the determination of potential KW, three field experiments testing N rates, plant densities and N timing applications on a single commercial hybrid (DKC63-60) were conducted over a 3-year period. The second season (2017) of the previously described study was used as Experiment 1, considering the original three N timings and a sub-set of N rates (0, 112, and 224 kg N ha^{-1}). Experiments 2 (2018) and 3 (2019) were conducted at the Purdue Agronomy Center of Research and Education (West Lafayette, IN) and each one involved four N rates (0, 84, 168, and 224 kg N ha^{-1}, all applied at planting) and two plant densities (7.9 and 10.4 plants m^{-2}). Endosperm cell number (ECN), an indicator of potential KW, was determined at different timings (from 9 to 17 days after silking -DAS-). Biomass samples taken at V12, R1 and R3 enabled calculations of plant and ear growth and N accumulation rates were calculated. High GY (15.7-16.6 Mg ha^{-1}) were achieved at maximum N in the first two years (2017-2018), and average GY increased 8.1 Mg ha^{-1} in response to N (i.e., from 0N to 224N) over the 3-year period. In addition, GY variability was largely explained by KW in all experiments. Low N treatments consistently reduced ECN at 9, 10, 13, and 17 DAS. Final KW responses to N rates were always explained by ECN, though the strength of the relation changed with the experiment and the relative DAS sampling time. For each sampling date, ECN was highly correlated with ear N allocation rate during the lag phase. The N rate effects on potential KW were not associated with plant growth rate per kernel during the critical period bracketing silking, and a positive relationship (rather than a trade-off) was found between KW and KN. We concluded that N played a direct role in potential KW determination as this process seemed to be highly dependent on N assimilates. Under higher plant N availability, individual kernel sink capacity was found to increase via gains in ECN (independently of N timing and plant density).

To investigate how N availability affected the realization of final KW at maturity, intensive data were collected during the linear grain-filling period from same three field experiments. Since kernels accumulate both DM and N assimilates during the linear phase, kernels were removed from ears of all treatments on a weekly basis over the entire 9-10-week interval from the early R3 stage. Linear plateau models were then fitted to the resulting kernel DM and N values on a thermal time basis to obtain characterizing parameters. Increases in N supply, regardless of N application timing or plant density, improved final DM accumulation in kernels by either increasing both the

effective grain-filling rate (EGFR) and grain filling duration (GFD), or by increasing GFD alone. Kernel N content (KNC) increased consistently under higher N availability because of gains in both kernel N accumulation rate (KNAR) and duration (KNAD). Kernels actively accumulated N until late in the season, as shown by the similar durations to peak DM and peak KNC (averaging ~1140$^{o}Cd^{-1}$ for GFD and ~1120$^{o}Cd^{-1}$ for KNAD). While EGFR was less impacted by N rate differences, KNAR was much more responsive, showing a strong correlation with final KW (r=0.96). Furthermore, KNAR was highly correlated with whole-plant N uptake by R3 (PNU_{R3}) (r=0.80). We concluded that kernel DM accumulation during the linear phase, and therefore final KW, was limited by N assimilate remobilization to kernels from N reserves accumulated prior to R3.

Overall, this dissertation provides new evidences for the distinct indirect and direct roles that N plays in the physiological mechanisms that determine final KW in maize at high potential GY. Indirectly, leaf N is responsible for post-silking photosynthesis, the major source of carbohydrates for the kernels, while stem N works as a reserve buffer to delay leaf senescence resulting from an early N remobilization to developing kernels. Directly, N assimilates are highly demanded by reproductive tissues during the lag phase to fulfill the endosperm cell division requirements that establish potential KW. Similarly, during the linear phase, N assimilate availability may limit DM deposition in kernels as differences in final KW were strongly associated with the kernel N accumulation rate.

CHAPTER 1. GENERAL INTRODUCTION

Maize grain yield is a function of the number of kernels harvested per unit area and the average individual kernel weight (Poneleit and Egli, 1979). The critical period for yield determination in maize is a time period of ±15 days around silking when optimum physiological conditions are required to prevent sink-related limitations that are often associated with constraints in kernel number (Early et al., 1967; Daynard and Duncan, 1969; Claassen and Shaw, 1970; Tollenaar, 1977; Edmeades and Daynard, 1979; Frey, 1981; Uhart and Andrade, 1991; Andrade and Ferreiro, 1996; Cerrudo et al., 2013). While kernel number is strongly sensitive to adverse conditions during this critical period, kernel weight has been considered a more stable trait due to its relatively smaller impact on overall grain yield decreases (Cirilo and Andrade, 1994; Andrade, 1995; Otegui, 1995). However, in recent years, the question of kernel weight becoming a more important driver behind in-field grain yield variability than it was before has received growing attention as stress conditions occurring during the grain-filling period limited potential yields more frequently (Cerrudo et al., 2013; Chen et al., 2016a; Mueller et al., 2019). Moreover, kernel weight has recently been proven to play a bigger role in the genetic improvement of grain yield than it had before, as reported by studies comparing maize hybrids released in different decades, i.e., ERA studies (Chen et al., 2016a; Mueller et al., 2019). In addition, the fact that these ERA studies, working with hybrids from two separate major genetic pools (Dekalb and Pioneer, respectively) and different nitrogen (N) conditions, reached similar conclusions on kernel weight's key role reinforces the importance of studying the physiological mechanisms behind this yield component and its tight relationship with both dry matter (DM) and N dynamics during the reproductive period.

In order to better understand how post-flowering stress conditions are now limiting grain yield by affecting kernel development, growth and nutrient uptake, grain filling should be studied in the most integrative manner possible, considering that it constitutes a long period within the crop cycle: from silking (i.e., R1 stage) to physiological maturity (i.e., R6 stage). Once fertilization occurs, grains go through a three-phase developing process based on their pattern of dry matter accumulation: a) the lag phase, b) the linear phase, and c) the maturation phase (Johnson and Tanner, 1972). During the lag phase, lasting around 15 days from R1 stage (silking) to the end of R2 or onset of R3 stage, active cell division takes place, with negligible dry matter accumulation, i.e., less than 10% of final kernel weight (Johnson and Tanner, 1972; Reddy and Daynard, 1983).

After the end of R2 or onset of R3, kernels accumulate biomass at a constant rate during the linear phase. Because approximately 90% of final kernel weight is accumulated throughout this phase (Johnson and Tanner, 1972; Tollenaar, 1977), it is known as the effective grain-filling period. Finally, in the maturation phase, kernel growth rate decreases until the accumulation of dry matter stops and physiological maturity is reached (R6 stage) (Johnson and Tanner, 1972).

1.1 Source Dynamics During the Grain-filling Period in Maize

Throughout the whole maize reproductive period, source capacity, i.e. the potential to produce photosynthates for the grain to grow (Tollenaar, 1977), depends on the growth, function, and remobilization dynamics of other plant tissues. The main source of carbohydrates for the grain to grow is current photosynthesis (Tollenaar, 1977; Rajcan and Tollenaar, 1999b; Borrás et al., 2004; Lee and Tollenaar, 2007) produced in the leaves, and when that is not enough to meet sink demands, remobilization of stem reserves plays a role (D'Andrea et al., 2016). Similarly, N allocation to the grain will be the result of a balanced combination between post-silking N uptake and N remobilization from leaves and stems (Ciampitti and Vyn, 2013; Chen et al., 2015). Furthermore, given that these physiological dynamics (dry matter and N) are co-regulated (Lemaire and Millard, 1999; Paul and Foyer, 2001; Masclaux-Daubresse et al., 2010; Fernie et al., 2020), grain-filling C and N supplies are strongly interlinked.

Since the physiological feedbacks between sink and source capacities during the grain-filling period end up defining grain yield, source-sink relations have been widely studied. However, many of those studies have estimated reproductive biomass, reproductive N uptake, and remobilization on an overall silking-to-maturity basis (Pan et al., 1995; Rajcan and Tollenaar, 1999b, 1999a; Uribelarrea et al., 2009; Ning et al., 2013; Chen et al., 2015; Mueller et al., 2017), without considering the specific growth dynamics of the kernels, the main reproductive sink tissues allocating both C and N. As described above, a key inflection point for the reproductive period is the one that marks the end of the lag phase and the onset of the effective grain-filling period (i.e., R3 stage), due to the drastic change in the kernel's dry matter accumulation. Since the effects of environmental factors (e.g. soil N availability) on the DM and/or N partitioning patterns could differentially impact the supply of C and/or N assimilates to kernels during these two developmental phases, they should be addressed separately (i.e., R1-R3 and R3-R6) in order to obtain a more appropriate analysis of resource allocation to reproductive tissues.

1.2 Lag Phase of the Grain-filling Period in Maize: Potential Sink Capacity

Although little dry matter accumulation occurs during the lag phase, it plays a key role in grain development since it is the timeframe where kernel storage capacity is established (Jones et al., 1985, 1996). During this early phase, both embryo and endosperm are under active cell division. While the embryo comprises only 10-15% of the total grain weight at maturity, endosperm cells are the major source of stored reserves within the mature seed, being responsible for almost 80-90% of final kernel weight (Jones and Brenner, 1987; Myers et al., 1990; Singletary and Below, 1990). Thus, kernel sink capacity, i.e. the potential to accommodate photosynthates (Tollenaar, 1977), is determined by the number and size of endosperm cells formed in this phase (Reddy and Daynard, 1983; Jones et al., 1985, 1996; Leroux et al., 2014) since the extent of cell division may place an upper limit on the amount of storage material synthesized at subsequent stages of endosperm development (Setter and Flannigan, 1989; Olsen, 2020). Because final kernel weight is related to this potential sink capacity, the lag phase is known for being the period when potential kernel weight is determined.

Endosperm development is highly sensitive to changes in temperature (Jones et al., 1981, 1985), water potential (Westgate and Boyer, 1985; Grant et al., 1989; Artlip et al., 1995), and intercepted radiation (Jones and Simmons, 1983; Setter and Flannigan, 1989) during the lag phase. Any resulting declines in endosperm cell number from these stress factors during the lag phase have been shown to be well correlated with decreases in final kernel weight (Egharevba et al., 1976; Jones and Simmons, 1983; Reddy and Daynard, 1983; Jones et al., 1985, 1996). However, plant nutritional status, and specifically N availability, effects on grain development during the lag phase have been less studied. Following the model proposed by Lemaire and Millard (1999) for sink organs, N substrates are firstly required for cell division processes such as DNA replication and protein synthesis (Berger, 1999; Olsen et al., 1999); in turn, the number of divided cells will be responsible for the later-season C substrate demand for expansion. Therefore, N deficiency would be expected to influence endosperm cell number, limiting final kernel weight at this early stage. While this outcome has already been reported for kernels cultured in vitro (Cazetta et al., 1999), studies based on grain samples from field-grown maize are less frequent and usually reflect a small range of N conditions, such as in Lemcoff and Loomis (1994).

1.3 Linear Phase of the Grain-filling Period in Maize: Actual Sink Capacity

After the lag phase ends, kernels increase their mass by accumulating dry matter, a process highly correlated with the deposit of starch in endosperm cells (Tollenaar and Daynard, 1978; Jones et al., 1981, 1985; Sabelli and Larkins, 2009), which ultimately relies on sucrose supply coming from the plant phloem. Both the rate and the duration of dry matter accumulation in grain during this phase constitute the determining factors of final kernel weight (Johnson and Tanner, 1972; Poneleit and Egli, 1979). In addition, kernel water content increases to reach a maximum around mid-filling and then decreases as dry matter continues to increase (Westgate and Boyer, 1986; Borrás et al., 2003).

Final kernel weight can be lowered by reductions in the grain-filling duration due to shading (Uhart and Andrade, 1991; Andrade and Ferreiro, 1996), defoliation (Egharevba et al., 1976; Frey, 1981; Echarte et al., 2006), water deficit (Claassen and Shaw, 1970; Ouattar et al., 1987), and higher plant densities (Poneleit and Egli, 1979; Wei et al., 2019). Regarding plant nutritional status, N effects during grain filling have been widely analyzed from a whole-crop perspective. However, only a few studies have focused on how dry matter (Melchiori and Caviglia, 2008; Wei et al., 2019) or nutrient dynamics (Chen et al., 2016b) on a per kernel basis are affected by N availability, despite this nutrient's key roles in the determination of final kernel weight. During the linear phase, a portion of the N allocated to the grain is used to form enzymes for the conversion of soluble sugars and amino acids into starch and protein, respectively (Below et al., 1981, 2000; Crawford et al., 1982; Rendig and Crawford, 1985; Lemaire and Millard, 1999). Therefore, deficient ear N can limit starch deposition in maize endosperms by affecting the synthesis of key proteins (Singletary and Below, 1990; Cazetta et al., 1999; Below et al., 2000). Furthermore, as leaf-N is required for photosynthesis (Novoa and Loomis, 1981; Ta and Weiland, 1992; Lemaire and Millard, 1999; Gastal and Lemaire, 2002; Mi et al., 2003; Pommel et al., 2006; Ning et al., 2017), which is the main source of carbohydrates for kernel growth (Tollenaar, 1977; Rajcan and Tollenaar, 1999b; Borrás et al., 2004; Lee and Tollenaar, 2007), the lack of N can lower source capacity during the grain-filling period (Uhart and Andrade, 1995; Lemaire and Millard, 1999; Cirilo et al., 2009), ultimately lowering final kernel weight. In addition, differences in N availability could also affect grain nutrient allocation dynamics, resulting in changes in nutrient concentration and/or content during grain filling.

1.4 Objectives

Based on all of the above, a better understanding of the physiology of grain development under a wide soil mineral N gradient with respect to plant N availability (e.g. due to more N rates, different application timings, and different plant populations) would be helpful in the design of maize management and breeding programs to maintain potential grain weight -and thus reduce yield losses- under low soil N availability during vegetative or reproductive stages. Given the current significance of kernel weight to final yields, source capacity (both DM and N) should be re-visited from a partitioning perspective as grains are competing for resources with the remaining plant tissues with more or less strength depending on which phase of grain filling is unfolding. Likewise, physiological determinants such as endosperm cell number, grain-filling rate, grain-filling duration, nutrient allocation rates, and plant or ear growth rate should be better understood to determine their consequences for sink capacity (both potential and actual) on a per kernel basis, along with kernel number.

Determining dry matter and N allocation in each crop component from R1 to R6 would help improve our understanding of source-sink tradeoffs, especially when new N becomes available at different timings, and determine crop management practices that aim to maintain productive green leaf area later in the season. Furthermore, studying endosperm cell formation during the lag phase could be a key element when looking for traits to explain the variation in both sink capacity and final kernel weight under differences in N availability. Finally, analyzing dry matter and N dynamics in developing grains, together with endosperm cell number would provide an even stronger framework to study the physiological mechanisms involved in the role of N in grain development and growth.

Therefore, this dissertation has the following general objectives:

1. To better understand the physiological mechanisms behind DM and N dynamics during the reproductive period in maize under different soil N availability conditions by separately analyzing the two main periods of grain filling, i.e. the lag phase (R1-R3) and the effective grain-filling phase (R3-R6). [Chapter 2]
2. To determine the effect of soil N availability on potential kernel weight via the number of endosperm cells formed during the lag phase, and to study the relationship between endosperm cell number and indicators of resource availability per kernel during the lag phase in maize. [Chapter 3]

3. To study dry matter and N kernel dynamics during the linear phase of grain filling, to determine N effects on the characterizing parameters, and to study the relationships between the parameters underlying the two processes. [Chapter 4]

1.5 References

Andrade, F. H. (1995). Analysis of growth and yield of maize, sunflower and soybean grown at Balcarce, Argentina. *F. Crop. Res.* 41, 1–12. doi:10.1016/0378-4290(94)00107-N.

Andrade, F. H., and Ferreiro, M. A. (1996). Reproductive growth of maize, sunflower and soybean at different source levels during grain filling. *F. Crop. Res.* 48, 155–165.

Artlip, T. S., Madison, J. T., and Setter, T. L. (1995). Water deficit in developing endosperm of maize: cell division and nuclear DNA endoreduplication. *Plant. Cell Environ.* 18, 1034–1040. doi:10.1111/j.1365-3040.1995.tb00614.x.

Below, F. E., Cazetta, J. O., and Seebauer, J. R. (2000). Carbon/nitrogen interactions during ear and kernel development of maize. *Crop Sci.*, 15–24. doi:10.2135/cssaspecpub29.c2.

Below, F. E., Christensen, L. E., Reed, A. J., and Hageman, R. H. (1981). Availability of reduced N and carbohydrates for ear development of maize. *Plant Physiol.* 68, 1186–1190. doi:10.1104/pp.68.5.1186.

Berger, F. (1999). Endosperm development. *Curr. Opin. Plant Biol.* 2, 28–32. doi:10.1016/S1369-5266(99)80006-5.

Borrás, L., Slafer, G. A., and Otegui, M. E. (2004). Seed dry weight response to source-sink manipulations in wheat, maize and soybean: A quantitative reappraisal. *F. Crop. Res.* 86, 131–146. doi:10.1016/j.fcr.2003.08.002.

Borrás, L., Westgate, M. E., and Otegui, M. E. (2003). Control of kernel weight and kernel water relations by post-flowering source-sink ratio in maize. *Ann. Bot.* 91, 857–867. doi:10.1093/aob/mcg090.

Cazetta, J. O., Seebauer, J. R., and Below, F. E. (1999). Sucrose and nitrogen supplies regulate growth of maize kernels. *Ann. Bot.* 84, 747–754. doi:10.1006/anbo.1999.0976.

Cerrudo, A., Di Matteo, J., Fernandez, E., Robles, M., Olmedo Pico, L., and Andrade, F. H. (2013). Yield components of maize as affected by short shading periods and thinning. *Crop Pasture Sci.* 64, 580–587. doi:10.1071/CP13201.

Chen, K., Camberato, J. J., Tuinstra, M. R., Kumudini, S. V., Tollenaar, M., and Vyn, T. J. (2016a). Genetic improvement in density and nitrogen stress tolerance traits over 38 years of commercial maize hybrid release. *F. Crop. Res.* 196, 438–451. doi:10.1016/j.fcr.2016.07.025.

Chen, K., Kumudini, S. V., Tollenaar, M., and Vyn, T. J. (2015). Plant biomass and nitrogen partitioning changes between silking and maturity in newer versus older maize hybrids. *F. Crop. Res.* 183, 315–328. doi:10.1016/j.fcr.2015.08.013.

Chen, Q., Mu, X., Chen, F., Yuan, L., and Mi, G. (2016b). Dynamic change of mineral nutrient content in different plant organs during the grain filling stage in maize grown under contrasting nitrogen supply. *Eur. J. Agron.* 80, 137–153. doi:10.1016/J.EJA.2016.08.002.

Ciampitti, I. A., and Vyn, T. J. (2013). Grain nitrogen source changes over time in maize: A review. *Crop Sci.* 53, 366–377. doi:10.2135/cropsci2012.07.0439.

Cirilo, A. G., and Andrade, F. H. (1994). Sowing date and maize productivity: I. Crop growth and dry matter partitioning. *Crop Sci.* 34, 1039–1043. doi:10.2135/cropsci1994.0011183X003400040037x.

Cirilo, A. G., Dardanelli, J., Balzarini, M., Andrade, F. H., Cantarero, M., Luque, S., et al. (2009). Morpho-physiological traits associated with maize crop adaptations to environments differing in nitrogen availability. *F. Crop. Res.* 113, 116–124. doi:10.1016/j.fcr.2009.04.011.

Claassen, M. M., and Shaw, R. H. (1970). Water deficit effects on corn. II. Grain components. *Agron. J.* 62, 652–655. doi:10.2134/agronj1970.00021962006200050032x.

Crawford, T. W., Rendig, V. V., and Broadbent, F. E. (1982). Sources, fluxes, and sinks of nitrogen during early reproductive growth of maize (Zea mays L.). *Plant Physiol.* 70, 1654–1660. doi:10.1104/pp.70.6.1654.

D'Andrea, K. E., Piedra, C. V., Mandolino, C. I., Bender, R., Cerri, A. M., Cirilo, A. G., et al. (2016). Contribution of reserves to kernel weight and grain yield determination in maize: Phenotypic and genotypic variation. *Crop Sci.* 56. doi:10.2135/cropsci2015.05.0295.

Daynard, T. B., and Duncan, W. G. (1969). The black layer and grain maturity in corn. *Crop Sci.* 9, 473–476. doi:10.2135/cropsci1969.0011183x000900040026x.

Early, E. B., Mcllrath, W. O., Seif, R. D., and Hageman, R. H. (1967). Effects of shade applied at different stages of plant development on corn (Zea mays L.) production. *Crop Sci.* 7, 151–156.

Echarte, L., Andrade, F. H., Sadras, V. O., and Abbate, P. (2006). Kernel weight and its response to source manipulations during grain filling in Argentinean maize hybrids released in different decades. *F. Crop. Res.* 96, 307–312. doi:10.1016/j.fcr.2005.07.013.

Edmeades, G. O., and Daynard, T. B. (1979). The relationship between final yield and photosynthesis at flowering in individual maize plants. *Can. J. Plant Sciense* 601, 585–601.

Egharevba, P. N., Horrocks, R. D., and Zuber, M. S. (1976). Dry matter accumulation in maize in response to defoliation. *Agron. J.* 68, 40–43. doi:10.2134/agronj1976.00021962006800010011x.

Fernie, A. R., Bachem, C. W. B., Helariutta, Y., Neuhaus, H. E., Prat, S., Ruan, Y. L., et al. (2020). Synchronization of developmental, molecular and metabolic aspects of source–sink interactions. *Nat. Plants* 6, 55–66. doi:10.1038/s41477-020-0590-x.

Frey, N. M. (1981). Dry matter accumulation in kernels of maize. *Crop Sci.* 21, 118–122. doi:10.2135/cropsci1981.0011183x002100010032x.

Gastal, F., and Lemaire, G. (2002). N uptake and distribution in crops: An agronomical and ecophysiological perspective. *J. Exp. Bot.* 53, 789–799. doi:10.1093/jexbot/53.370.789.

Grant, R. F., Jackson, B. S., Kiniry, J. R., and Arkin, G. F. (1989). Water deficit timing effects on yield components in maize. *Agron. J.* 81, 61–65. doi:10.2134/agronj1989.00021962008100010011x.

Johnson, D. R., and Tanner, J. W. (1972). Calculation of the rate and duration of grain filling in corn (Zea mays L.). *Crop Sci.* 12, 485–486. doi:10.2135/cropsci1972.0011183x001200040028x.

Jones, R. J., and Brenner, M. L. (1987). Distribution of abscisic acid in maize kernel during grain filling. *Plant Physiol.* 83, 905–909. doi:10.1104/pp.83.4.905.

Jones, R. J., Gengenbach, B. G., and Cardwell, V. B. (1981). Temperature effects on in vitro kernel development of maize. *Crop Sci.* 21, 761–766. doi:10.2135/cropsci1981.0011183x002100050033x.

Jones, R. J., Roessler, J., and Ouattar, S. (1985). Thermal environment during endosperm cell division in maize: effects on number of endosperm cells and starch granules. *Crop Sci.* 25, 830–834. doi:10.2135/cropsci1985.0011183x002500050025x.

Jones, R. J., Schreiber, B. M. N., and Roessler, J. A. (1996). Kernel sink capacity in maize: Genotypic and maternal regulation. *Crop Sci.* 36, 301–306. doi:10.2135/cropsci1996.0011183X003600020015x.

Jones, R. J., and Simmons, S. R. (1983). Effect of altered source-sink ratio on growth of maize kernels. *Crop Sci.* 23, 129–134. doi:10.2135/cropsci1983.0011183x002300010038x.

Lee, E. A., and Tollenaar, M. (2007). Physiological basis of successful breeding strategies for maize grain yield. *Crop Sci.* 47. doi:10.2135/cropsci2007.04.0010IPBS.

Lemaire, G., and Millard, P. (1999). An ecophysiological approach to modelling resource fluxes in competing plants. *J. Exp. Bot.* 50, 15–28. doi:10.1093/jxb/50.330.15.

Lemcoff, J. H., and Loomis, R. S. (1994). Nitrogen and density influences on silk emergence, endosperm development, and grain yield in maize (Zea mays L.). *F. Crop. Res.* 38, 63–72. doi:10.1016/0378-4290(94)90001-9.

Leroux, B. M., Goodyke, A. J., Schumacher, K. I., Abbott, C. P., Clore, A. M., Yadegari, R., et al. (2014). Maize early endosperm growth and development: From fertilization through cell type differentiation. *Am. J. Bot.* 101, 1259–1274. doi:10.3732/ajb.1400083.

Masclaux-Daubresse, C., Daniel-Vedele, F., Dechorgnat, J., Chardon, F., Gaufichon, L., and Suzuki, A. (2010). Nitrogen uptake, assimilation and remobilization in plants: Challenges for sustainable and productive agriculture. *Ann. Bot.* 105, 1141–1157. doi:10.1093/aob/mcq028.

Melchiori, R. J. M., and Caviglia, O. P. (2008). Maize kernel growth and kernel water relations as affected by nitrogen supply. *F. Crop. Res.* 108, 198–205. doi:10.1016/j.fcr.2008.05.003.

Mi, G., Liu, J. A., Chen, F., Zhang, F., Cui, Z., and Liu, X. (2003). Nitrogen uptake and remobilization in maize hybrids differing in leaf senescence. *J. Plant Nutr.* 26, 237–247. doi:10.1081/PLN-120016507.

Mueller, S. M., Camberato, J. J., Messina, C., Shanahan, J., Zhang, H., and Vyn, T. J. (2017). Late-split nitrogen applications increased maize plant nitrogen recovery but not yield under moderate to high nitrogen rates. *Agron. J.* 109, 2689. doi:10.2134/agronj2017.05.0282.

Mueller, S. M., Messina, C. D., and Vyn, T. J. (2019). Simultaneous gains in grain yield and nitrogen efficiency over 70 years of maize genetic improvement. *Sci. Rep.* 9, 9095. doi:10.1038/s41598-019-45485-5.

Myers, P. N., Setter, T. L., Madison, J. T., and Thompson, J. F. (1990). Abscisic acid inhibition of endosperm cell division in cultured maize kernels. *Plant Physiol.* 94, 1330–1336. doi:10.1104/pp.94.3.1330.

Ning, P., Fritschi, F. B., and Li, C. (2017). Temporal dynamics of post-silking nitrogen fluxes and their effects on grain yield in maize under low to high nitrogen inputs. *F. Crop. Res.* 204, 249–259. doi:10.1016/j.fcr.2017.01.022.

Ning, P., Li, S., Yu, P., Zhang, Y., and Li, C. (2013). Post-silking accumulation and partitioning of dry matter, nitrogen, phosphorus and potassium in maize varieties differing in leaf longevity. *F. Crop. Res.* 144, 19–27. doi:10.1016/j.fcr.2013.01.020.

Novoa, R., and Loomis, R. S. (1981). Nitrogen and plant production. *Plant Soil* 58, 177–204. doi:10.1007/BF02180053.

Olsen, O. A. (2020). The modular control of cereal endosperm development. *Trends Plant Sci.* 25, 279–290. doi:10.1016/j.tplants.2019.12.003.

Olsen, O., Linnestad, C., and Nichols, S. (1999). Developmental biology of the cereal endosperm. *Trends Plant Sci.* 4, 253–257. doi:10.1007/7089_2007_106.

Otegui, M. E. (1995). Prolificacy and grain yield components in modern Argentinian maize hybrids. *Maydica* 40, 371–376.

Ouattar, S., Jones, R. J., and Crookston, R. K. (1987). Effect of water deficit during grain filling on the pattern of maize kernel growth and development. *Crop Sci.* 27, 726–730. doi:10.2135/cropsci1987.0011183x002700040025x.

Pan, W. L., Camberato, J. J., Moll, R. H., Kamprath, E. J., and Jackson, W. A. (1995). Altering source-sink relationships in prolific maize hybrids: Consequences for nitogen uptake and remobilization. *Crop Sci.* 35, 836–845. doi:10.2135/cropsci1995.0011183X003500030034x.

Paul, M. J., and Foyer, C. H. (2001). Sink regulation of photosynthesis. *J. Exp. Bot.* 52, 1383–1400. doi:10.1093/jexbot/52.360.1383.

Pommel, B., Gallais, A., Coque, M., Quilleré, I., Hirel, B., Prioul, J. L., et al. (2006). Carbon and nitrogen allocation and grain filling in three maize hybrids differing in leaf senescence. *Eur. J. Agron.* 24, 203–211. doi:10.1016/j.eja.2005.10.001.

Poneleit, C. G., and Egli, D. B. (1979). Kernel growth rate and duration in maize as affected by plant density and genotype. *Crop Sci.* 19, 385–388. doi:10.2135/cropsci1979.0011183x001900030027x.

Rajcan, I., and Tollenaar, M. (1999a). Source: Sink ratio and leaf senescence in maize: II. Nitrogen metabolism during grain filling. *F. Crop. Res.* 60, 255–265. doi:10.1016/S0378-4290(98)00143-9.

Rajcan, I., and Tollenaar, M. (1999b). Source:sink ratio and leaf senescence in maize: I. Dry matter accumulation and partitioning during grain filling. *F. Crop. Res.* 60, 255–265. doi:10.1016/s0378-4290(98)00143-9.

Reddy, V., and Daynard, T. (1983). Endosperm characteristics associated with rate of grain filling and kernel size in corn. *Maydica* 28, 339–355. doi:10.11693/hyhz20181000233.

Rendig, V. V., and Crawford, T. W. (1985). Partitioning into maize grain N fractions of N absorbed through the roots before and after pollination. *J. Sci. Food Agric.* 36, 645–650. doi:10.1002/jsfa.2740360804.

Sabelli, P. A., and Larkins, B. A. (2009). The development of endosperm in grasses. *Plant Physiol.* 149, 14–26. doi:10.1104/pp.108.129437.

Setter, T. L., and Flannigan, B. A. (1989). Relationship between photosynthate supply and endosperm development in maize. *Ann. Bot.* 64, 481–487. doi:10.1093/oxfordjournals.aob.a087867.

Singletary, G. W., and Below, F. E. (1990). Nitrogen-induced changes in the growth and metabolism of developing maize kernels grown in vitro. *Plant Physiol.* 92, 160–167. doi:10.1104/pp.92.1.160.

Ta, C. T., and Weiland, R. T. (1992). Nitrogen partitioning in maize during ear development. *Crop Sci.* 32, 443–451. doi:10.2135/cropsci1992.0011183x003200020032x.

Tollenaar, M. (1977). Sink-source relationships during reproductive development in maize. A review. *Maydica* 22, 49–75.

Tollenaar, M., and Daynard, T. B. (1978). Relationship between assimilate source and reproductive sink in maize grown in a short-season environment. *Agron. J.* 70, 219–223. doi:10.2134/agronj1978.00021962007000020003x.

Uhart, S. A., and Andrade, F. H. (1995). Nitrogen and carbon accumulation and remobilization during grain filling in maize under different source/sink ratios. *Crop Sci.* 35, 183–190. doi:10.2135/cropsci1995.0011183X003500010034x.

Uhart, S., and Andrade, F. (1991). Source-sink relationships in maize grown in a cool-temperate area. *Agronomie* 11, 863–875. doi:10.1051/agro:19911004.

Uribelarrea, M., Crafts-Brandner, S. J., and Below, F. E. (2009). Physiological N response of field-grown maize hybrids (Zea mays L.) with divergent yield potential and grain protein concentration. *Plant Soil* 316, 151–160. doi:10.1007/s11104-008-9767-1.

Wei, S., Wang, X., Li, G., Qin, Y., Jiang, D., and Dong, S. (2019). Plant density and nitrogen supply affect the grain-filling parameters of maize kernels located in different ear positions. *Front. Plant Sci.* 10, 180. doi:10.3389/fpls.2019.00180.

Westgate, M. E., and Boyer, J. S. (1985). Carbohydrate reserves and reproductive development at low leaf water potentials in maize. *Crop Sci.* 25, 762–769. doi:10.2135/cropsci1985.0011183x0025000500010x.

Westgate, M. E., and Boyer, J. S. (1986). Water status of the developing grain of maize. *Agron. J.* 78, 714–719. doi:10.2134/agronj1986.00021962007800040031x.

CHAPTER 2. REVISITING DRY MATTER AND NITROGEN SOURCE DYNAMICS DURING GRAIN FILL IN MAIZE AT WIDELY RANGING NITROGEN SUPPLIES

2.1 Abstract

While maize dry matter (DM) and N dynamics during reproductive growth have been widely studied, our understanding of the origin and supply of C and N assimilates to kernels during the lag versus linear phases of grain filling remain obscured by the typical component-based approaches of analyzing either critical period intervals (centered on silking) or the net silking-to-maturity timeframe. Our primary objective was to study DM and N reproductive dynamics under different N availability conditions by separating the two main grain-filling phases. A 2-year field study was conducted at the Purdue Rice Farm (LaCrosse, IN) during the 2016 and 2017 growing seasons. Maize with supplemental irrigation was grown under a split-plot design, with N timing (main plot) and N rate (sub-plot) treatments. The timing applications included: all N applied at planting, split application between planting and early sidedress, and split application between planting and the last 56 kg N ha^{-1} applied at V12. The five N rates tested were 0, 112, 168, 224, and 280 kg N ha^{-1}. In addition to the standard metrics of grain yield (GY), yield components, N efficiencies, and harvest indices at R6, both biomass and N contents in plant components were determined at R1, at the onset of linear grain fill (R3), and at R6. Post-silking DM production (PostDM), post-silking N uptake (PostN), and remobilization of DM (RemDM) and N (RemN) from leaf and stem were calculated separately for the periods R1-R3 (lag phase) and R3-R6 (effective grain filling). Nitrogen timing had virtually no impact on evaluated parameters; the much larger N rate impacts were therefore averaged across N timing treatments. In both seasons, $PostDM_{R1.R3}$, was much less responsive to N rates than PostDM. Substantial DM gains in leaves and stems occurred from R1 to R3 at all N rates in both years, and in 2016 those DM gains exceeded the ear DM gain in the same interval. Differential seasonal patterns in post-silking N uptake were observed, with plants either taking up net new N only during the lag phase (2016), or during the linear grain-filling phase (2017). In both years, the nitrogen nutrition index (NNI) at R1 and R3 explained over 80% of the per-plot variability in subsequent RemN, but had little influence on PostN. Both grain yield (GY) and kernel weight (KW) were gradually increased by N supply, with reproductive tissues proving to be relatively stronger sinks for N than for DM

during the lag phase. Results from this work highlight the importance of assessing DM and N in maize plant components at R3, instead of just at the R1 and R6 stages, when studying reproductive-period dynamics for relative source supply gains and losses arising from new versus remobilized DM and N.

2.2 Introduction

Maize grain yield is the final result of multiple physiological processes responding to genotype by environment by management interactions throughout the growing season. Among those processes, carbon (C) economy dynamics during reproductive stages are useful to explain grain yield variations by defining the pool of available assimilates produced by the crop (source) to fulfill the carbohydrate demand of the growing kernels (sink) (Tollenaar, 1977). Nitrogen (N) assimilates are also demanded by sink tissues during grain filling (Crawford et al., 1982). The analysis of N economy dynamics that define N supply to the kernels and their ultimate N content can, in the context of plant component dry matter changes, improve understanding of physiological processes driving changes in grain yield, N use efficiency, and grain composition (Triboi and Triboi-Blondel, 2002).

Since crop dry matter (DM) and N dynamics are co-regulated (Lemaire and Millard, 1999; Paul and Foyer, 2001; Masclaux-Daubresse et al., 2010; Fernie et al., 2020), grain-filling C and N assimilate supplies are strongly interlinked. Pre-silking leaf-stored N is associated with both post-silking photosynthesis, the primary source of C substrates for the kernels (Rajcan and Tollenaar, 1999b; Borrás et al., 2004), and N remobilization, a source of N substrates (Rajcan and Tollenaar, 1999a; Chen et al., 2015; Yang et al., 2016) via protein turnover (Masclaux-Daubresse et al., 2010). Provided that C supply to the roots is sufficient (Tolley-Henry and Raper, 1991) and soil solution N supplies adequate, absorption of new N after silking becomes another N source for the kernels (Ciampitti and Vyn, 2013; Chen et al., 2015). In addition, stem remobilization of previously-stored non-structural reserves provide the kernels with a supplementary supply of C (Uhart and Andrade, 1995; D'Andrea et al., 2016) and N substrates (Uhart and Andrade, 1995; Yang et al., 2016).

Given these tight physiological interactions, factors that alter C assimilate production also impact N assimilation dynamics, and vice versa (Paul and Foyer, 2001; Fernie et al., 2020). Among those factors, soil N availability places a direct limit on plant N uptake (Lemaire and Gastal, 2009). Under low mineral N soil conditions, leaf area, intercepted radiation, and thus biomass

accumulation, are reduced (Uhart and Andrade, 1995; Echarte et al., 2008; Ciampitti and Vyn, 2011). Deficient N nutrition reduces not only C assimilation but its partitioning to reproductive sink tissues, ultimately lowering grain yield (Uhart and Andrade, 1995; D'Andrea et al., 2008; Nasielski and Deen, 2019). In these N limiting conditions, partitioning of carbohydrates to the roots is also decreased, exacerbating a lower N uptake, especially after silking (Chen et al., 2015; Mueller et al., 2017). This leads to a shorter period of post-silking DM production (i.e. C source) because limited N uptake triggers early senescence and N remobilization, which consequently becomes a more important N source for the grain under such conditions (Tsai et al., 1991; Abe et al., 2013). Changes in grain-filling N dynamics in response to differences in N rate can also vary with the genotype (Pommel et al., 2006; Ciampitti and Vyn, 2013; Chen et al., 2015) and the timing of fertilizer application (Mueller et al., 2017; Fernandez et al., 2019).

Despite the abundant research in DM and/or N dynamics under soil N availability differences, many of those studies have calculated reproductive biomass, reproductive N uptake, and remobilization on an overall silking-to-maturity basis (Pan et al., 1995; Rajcan and Tollenaar, 1999b, 1999a; Uribelarrea et al., 2009; Ning et al., 2013; Chen et al., 2015; Antonietta et al., 2016; Mueller et al., 2017) without considering the specific growth dynamics of the kernels, the main reproductive sink tissues allocating both C and N. From a grain-filling perspective, a key inflection point for the reproductive period is the one that marks the end of the lag phase and the onset of the effective grain-filling period. While kernels gain little DM during the lag phase (Johnson and Tanner, 1972; Reddy and Daynard, 1983), assimilate supply is needed for the determination of both kernel number (Andrade et al., 2002) and potential kernel weight (Gambín et al., 2006). Based on the potential sink strength thus determined, kernel DM accumulation during effective grain filling then relies on the active supply of assimilates (from the sources previously described) to achieve final kernel weight. Therefore, changes in DM and/or N partitioning patterns in response to environmental factors (e.g. soil N availability) that could affect final grain yield by differentially impacting the supply of C and/or N assimilates to kernels during these two developmental phases, remain hidden under the R1-to-R6 net analysis, especially for N.

When predictions of lag phase length are not available for specific genotype x environment x management combinations, the beginning of milk stage (i.e. R3) has been used as a close estimator in the few studies that assessed dry matter and N reproductive dynamics at this key point (Uhart and Andrade, 1995; Ciampitti et al., 2013). Uhart and Andrade (1995) reported non-

structural carbohydrate remobilization and N remobilization from stems between R3 and R5, but this study did not account for processes happening during the lag phase (i.e., R1 to R3) as a stand-alone period as it considered the whole critical period (i.e., V11-12 to R3). Similarly, the analysis of the complete critical period plus the effective grain filling has also been used by Ciampitti et al. (2013) when determining plant N uptake and total-shoot N remobilization rates under three N soil levels and three densities, as well as by other studies determining dry matter source-sink dynamics in inbred lines and hybrids under only two soil N levels (D'Andrea et al., 2008; Hisse et al., 2019).

Given the possible trade-offs between potential kernel set and potential KW definition during the lag phase, and the limited information regarding this period among studies conducted in field conditions, a thorough analysis of resource allocation to reproductive tissues over that period (R1-R3) and the effective grain-filling phase (R3-R6) is warranted. Evaluating both pre-silking, vegetative-stored and post-silking, newly produced DM and N substrates at R3 under a wide gradient of soil N availability conditions can help address this knowledge gap and identify potential physiological constraints to grain yields and crop N utilization. Physiological information resulting from such an analysis could then be used as input for improvements in crop simulation models (Messina et al., 2009), breeding programs (Lemaire and Gastal, 2009), and N fertilization practices aiming to lower N losses (Cassman et al., 2002). Therefore, the primary objective of this study was to better understand the physiological mechanisms behind DM and N dynamics during the reproductive period in maize under different soil N availability conditions by separately analyzing the two main periods of grain filling, i.e. the lag phase (R1-R3) and the effective grain-filling phase (R3-R6).

2.3 Materials and Methods

2.3.1 Experimental Site and Design

A two-year field study was conducted during the 2016 and 2017 growing seasons at the Purdue Rice Farm in LaCrosse, IN on a Gilford fine sandy loam soil (coarse-loamy, mixed, superactive, mesic Typic Endoaquolls) (USDA Web Soil Survey). Maize followed normally-fertilized maize each year in adjacent field sites centered on a 40-ha field with center pivot irrigation. The tillage system consisted of fall chisel plowing and spring secondary tillage. Supplementary sprinkler irrigation was applied when needed, considering that a target yield of

12.5 Mg ha^{-1} requires 508 mm of water during the growing season (Licht et al., 2017). Information on soil fertility (Table A.1) and soil N availability at planting (Table A.2) and at V6 stage (Table A.3) for each experimental site can be found in Appendix A.

Plots were arranged in a split-plot design with three N timing applications as main plots and five N rates as subplots, in a four-replicate RCBD. The sole N source was 28% urea ammonium nitrate (UAN). The three N timings were: all N applied at planting, half of the total N rate applied at planting plus the other half applied at the V6 stage, and the majority of N applied at planting with the last 56 kg N ha^{-1} applied at the V12 stage. The total N rates for each timing main treatment were 0, 112, 168, 224, and 280 kg N ha^{-1}. Both at planting and V6 N applications were coulter-injected into soil between rows, while V12 sidedress was surface-banded along both sides of maize rows using 360 Yield Center Y-Drops (360 Yield Center, Morton, IL) on a high clearance applicator. Starter fertilizer (19-17-0) was band-applied to all plots while planting at 17 kg N ha^{-1} and 6 kg P ha^{-1}.

Two maize hybrids were used in the study. Hybrid DKC66-42 GENSS (Dekalb) was planted on April 26th, 2016 (Season 1), and DKC63-60RIB GENSS (Dekalb) was planted on May 16th, 2017 (Season 2). The hybrid change was necessitated since DKC66-42 GENSS, released in 2013, was phased out of commercial sales in 2017; its replacement was DKC63-60RIB GENSS, released in 2015. Although these hybrids have no direct parents in common, both their respective male and female parents have similar genetic backgrounds. Thus, these hybrids would fall into a similar "germplasm bucket" and similar responses to management practices would be expected (personal communication with Bayer maize breeders).

The study used a common seeding rate of 8.3 plants m^{-2}, and plots were 12 rows wide (0.76 m rows) and 228-m long. The at-plant N treatments were applied within a day of planting. Pesticide management practices followed Purdue University recommendations, and all plots were maintained in a weed-free condition. No fungicide was applied.

2.3.2 Measurements and Calculations

Final plant populations were determined at the V4 stage using 4 subsample areas per plot. Both vegetative and reproductive stages were recorded utilizing the scale proposed by Ritchie and Hanway (1982). Daily anthesis and silk emergence notes were taken during flowering on 20 pre-

tagged plants in each plot. Each phenological stage was determined by the day when 50% of those 20 marked plants reached it.

Above-ground biomass samples were taken at R1, R3, and R6 stages. Biomass sampling at R1 matched 50% silking in 2016, and it occurred only two days after 50% silking in 2017. Each time, 10 consecutive plants were cut off at ground level from rows 3 or 4 of each plot, and the linear length between plants was measured to account for plant component DM per unit area. Plants were separated into leaves (plus husks and silks), stems (plus tassels), and ears at R1 stage in both seasons, and at R3 stage in 2016. Plants were dissected into leaves, stems, kernels, and cobs at R3 stage in 2017, and at R6 stage in both seasons. In 2017, ears were separated into kernels and cobs for the R3 sampling in order to better understand organ-specific partitioning patterns at this stage. Once partitioned, plants were dried at 60°C to constant weight, weighed, ground to pass through a 1-mm sieve and analyzed for N by combustion methods (Etheridge et al., 1998) at A&L Great Lakes Laboratories, Inc. (Fort Wayne, IN).

Kernel number (KN) and kernel weight (KW) estimations were based on the R6 biomass samples. KN was expressed on an area basis by counting kernels per ear from each plant, totaling the kernels from the 10-plant sample from each plot, and relating that number to the sampling area. KW was expressed on an individual-grain DM basis after averaging the weight of 1000 kernels per plot (5 sub-samples of 200 kernels), and adjusting those weights to 0% moisture content.

Grain yield was determined by an 8-row combine harvesting the 8-center rows of each plot. Grain yield monitor data were corrected by cropping 21 m of border at both ends of the original plot length in order to only consider the yield points recorded when the combine reached a stable harvesting flow. Combine monitor data outliers which were higher/lower than 2.5 standard deviations were removed. Grain yield was then adjusted to 15.5% moisture content.

Post-silking biomass production (PostDM) was calculated as the difference in whole-plant DM between two consecutive sampling stages:

$$PostDM_{R1.R3} = DM_{R3} - DM_{R1} \qquad PostDM_{R3.R6} = DM_{R6} - DM_{R3} \qquad \text{Equation 2.1}$$

Dry matter remobilized from leaves (L), stems (S), and cobs (C) was calculated by the difference in their respective DM values between two consecutive sampling stages as shown in equations 2.2, 2.3, and 2.4.

$$RemDM\_L_{R1.R3} = DML_{R1} - DML_{R3} \qquad RemDM\_L_{R3.R6} = DML_{R3} - DML_{R6} \qquad \text{Equation 2.2}$$

$$RemDM\_S_{R1.R3} = DMS_{R1} - DMS_{R3} \qquad RemDM\_S_{R3.R6} = DMS_{R3} - DMS_{R6} \quad \text{Equation 2.3}$$

$$RemDM\_C_{R1.R3} = DMC_{R1} - DMC_{R3} \qquad RemDM\_C_{R3.R6} = DMC_{R3} - DMC_{R6} \quad \text{Equation 2.4}$$

Total-plant biomass remobilization (RemDM) was computed as the sum of each component's remobilization values:

$$RemDM_{R1.R6} = RemDM\_L_{R1.R3} + RemDM\_L_{R3.R6} + RemDM\_S_{R1.R3} + RemDM\_S_{R3.R6} + RemDM\_C_{R1.R3} + RemDM\_C_{R3.R6} \quad \text{Equation 2.5}$$

Similarly, post-silking N uptake (PostN) was calculated as the difference in whole-plant N uptake (NU) between two consecutive sampling stages:

$$PostN_{R1.R3} = NU_{R3} - NU_{R1} \qquad PostN_{R3.R6} = NU_{R6} - NU_{R3} \quad \text{Equation 2.6}$$

N remobilized from leaves (L), stems (S), and cobs (C) was calculated by the difference in their respective N tissue contents (NC) between two consecutive sampling stages as shown in equations 2.7, 2.8, and 2.9.

$$RemN\_L_{R1.R3} = NCL_{R1} - NCL_{R3} \qquad RemN\_L_{R3.R6} = NCL_{R3} - NCL_{R6} \quad \text{Equation 2.7}$$

$$RemN\_S_{R1.R3} = NCS_{R1} - NCS_{R3} \qquad RemN\_S_{R3.R6} = NCS_{R3} - NCS_{R6} \quad \text{Equation 2.8}$$

$$RemN\_C_{R1.R3} = NCC_{R1} - NCC_{R3} \qquad RemN\_C_{R3.R6} = NCC_{R3} - NCC_{R6} \quad \text{Equation 2.9}$$

Total-plant N remobilization (RemN) was computed as the sum of each component's remobilization values:

$$RemN = RemN\_L_{R1.R3} + RemN\_L_{R3.R6} + RemN\_S_{R1.R3} + RemN\_S_{R3.R6} + RemN\_C_{R1.R3} + RemN\_C_{R3.R6} \quad \text{Equation 2.10}$$

Given that respiration costs and remobilization efficiencies were not taken into account in this study, both DM and N remobilization values should be considered apparent.

Nitrogen Nutrition Index (NNI) (Lemaire and Gastal, 1997) was calculated on a whole-plant basis at both R1 and R3 stages by following equation 2.11:

$$NNI = \frac{\%N_a}{\%N_c} \quad \text{Equation 2.11}$$

Where $\%N_a$ is the whole-plant N concentration at either R1 or R3 stage and $\%N_c$ is the critical N concentration for that biomass. $\%N_c$ was obtained by applying the coefficients proposed

for maize by Plénet and Lemaire (1999) on each plot's whole-plant biomass (W) for each stage as follows:

$$\%N_c = 3.4\, W^{-0.37} \qquad \text{Equation 2.12}$$

Nitrogen Recovery Efficiency (NRE) was computed according to equation 2.13, where NRE is the ratio between the difference in total N uptake (NU) at R6 between the 0N plots and the non-0N plots, over the total N amount applied:

$$NRE = \frac{[NU_{XN} - NU_{0N}]_{R6}}{NApplied} \qquad \text{Equation 2.13}$$

Nitrogen Internal Efficiency (NIE) was calculated by following equation 2.14, where NIE is the ratio of the difference between the 0N plots and the non-0N plots in grain dry matter (GW) and nitrogen uptake (NU).

$$NIE = \frac{[GW_{XN} - GW_{0N}]_{R6}}{[NU_{XN} - NU_{0N}]_{R6}} \qquad \text{Equation 2.14}$$

2.3.3 Statistical Analysis

Statistical analysis was performed using R (R Core Team, 2019). For the majority of measured variables, F-tests based on the mean square error between the two seasons (2016 and 2017) were significant at α=0.05 (Carmer et al., 1969), indicating lack of homogeneity of variances. Thus, seasons were analyzed separately. Factor and interaction effects on individual variables were tested by ANOVA following the common nested blocking structure of a split-plot model, where main plots (i.e., N timings) are nested within the blocks, and sub-plots (i.e., N rates) are nested within the main plots. Means separation was tested by LSD at α=0.05. Both ANOVA and LSD were conducted using the *agricolae* R package (de Mendiburu, 2020), via the *sp.plot* and *LSD.test* functions, respectively. *LSD.test* function was run under the appropriate mean square errors for each comparison. Linear regression analysis was conducted to determine relationships between pairs of variables via the *lm* function.

2.4 Results

2.4.1 Weather Conditions

Overall maximum and minimum temperature patterns were consistent among years (Fig. 2.1). While a longer growing season occurred in 2016 due to its earlier planting date (April 27, 2016 versus May 17, 2017), 50% of silk emergence happened around the same chronological date (July 18, 2016 versus July 19, 2017). From planting to silking, the 2016 growing season received both higher cumulative thermal units (853 growing degree days, GDD) and cumulative available water, i.e. rainfall and irrigation events added up together (290 mm), compared to 2017 (822 GDD and 213 mm, respectively). A similar trend was found from silking to the end of the growing season (Table 2.1). Nevertheless, when considering only the period between V12 and R3 stages as an indicator of the critical period for yield determination, 2017 environmental conditions were superior to those of 2016 since the former received 22 mm more water while accumulating almost the same thermal units.

2.4.2 Biomass Accumulation, Partitioning, and Remobilization

For the majority of the dry matter variables evaluated at three stages in both seasons, the N rate main effect was usually the only significant factor detected, with the N timing main effect occasionally present in only a few variables and with none of the 2-way interactions being significant (Table 2.2). Dry matter accumulation in all plant components increased with N availability to varying rates depending mainly on year, growth stage and plant component.

In 2016, leaf and total-plant dry matter at R1 and R3 increased gradually with N rate until 168N, while stem and ear biomass responded to even higher N rates. Following this pattern, at maturity, all plant components except cob showed significant incremental gains in biomass up to 224N (Table 2.2). Interestingly, harvest index, i.e., the ratio between grain biomass and total-plant biomass at R6, was similar among N fertilized treatments (Table 2.4), indicating that this partitioning index only changed when there was no N applied. Both grain and total-plant DM at R6 decreased when N was split-applied between planting and V6, but the V12 split treatment yielded similar to the 100% N applied at planting (Table 2.2).

In 2017, the DM response to N rate in most plant components at R1 and R3 was positive to 112N, although grain biomass at R3 was highest at the 280N rate. When plants reached R6 stage,

N rate had a greater impact, and biomass increases in all plant components mirrored increases in N availability until 224N (grain) or 280N (leaf, stem, cob, and total-plant). Dry matter partitioning to grain at R6 (i.e., harvest index), also responded positively to N availability, but only until 168N (Table 2.5). Timing of application effects on DM accumulation were even smaller than they had been for 2016 (Table 2.2).

Both leaf and stem components achieved substantial DM gains from R1 to R3 at all N rates in both years, as shown by the negative remobilization values in Figure 2.2 (A and C). The average gain (across years and N treatments) in leaf DM after R1 was 0.9 Mg ha^{-1} and the average gain in stem DM was 1.3 Mg ha^{-1}. Total-plant DM accumulation over the lag period was reduced only at 0N (Fig. 2.2, A and C), and the average DM gains during this period were 4.3 Mg ha^{-1} (2016) and 4.8 Mg ha^{-1} (2017).

Conversely, total-plant DM accumulation from R3 to R6 increased gradually with N rate (Fig. 2.2, B and D). In addition, stem DM remobilization during the linear grain-fill period occurred at all N rates with no changes observed relative to soil N availability, averaging 3.3 Mg ha^{-1} (2016) and 2.8 Mg ha^{-1} (2017). Leaf DM remobilization was negligible in both years at all N rates (Fig. 2.2, B and D).

2.4.3 Nitrogen Concentration in Plant Components

In both years, N rate treatments strongly affected leaf, stem, and total-plant N concentration values at R1, R3 and R6 stages, while neither N application timing nor its interaction with rate proved significant (Table 2.3). At R1, ear N concentration was not affected by N rate in either 2016 nor 2017, averaging 3.3% N in the former and 3.13% N in the latter. Similarly, N concentration of R3 reproductive organs (i.e. ear in 2016, grain and cob in 2017) did not change with N availability. However, at maturity, strong N rate treatment effects on grain N concentration were observed, with mean values ranging (and positively with N rates as expected) from 0.74 to 1.10% in 2016 and 0.8 to 1.31% in 2017 (Table 2.3).

2.4.4 Nitrogen Uptake, Partitioning, and Remobilization

The N content in all plant components at the three phenological stages in both seasons were affected by N rate treatments, regardless of application timing (Table 2.4). In 2016, leaf, stem and

ear N contents at silking averaged 63%, 36% and 1% of total plant N uptake. Similarly, in 2017, the contribution of each component to total N uptake at R1 was 59%, 38% and 3%, respectively. R1 minimum values (i.e. under the 0N control) of leaf, stem and total N uptake were similar across years (around 44, 22, 67 kg N ha^{-1}, respectively), while the lowest ear N content value was observed in 2016 (0.43 kg N ha^{-1}).

By the R3 stage, ear N content averaged 15% and 26% of total R3 N uptake in 2016 and 2017, respectively. In 2016, leaf N content increased from R1 to R3, as shown by the negative leaf remobilization values presented (Fig. 2.3, A), especially under higher N rates. Stem N content decreased slightly (an average of 8.5%) from R1 to R3, but the amount of stem N remobilized during this period was not affected by N rate treatments (Fig. 2.3, A), despite the more than 3-fold variation in absolute R3 stem N contents from 0N to 280N (Table 2.4). Total-plant post-silking N uptake by R3 increased with N rates (Fig. 2.3, A), with noticeable gains ranging from 5 to 36 kg N ha^{-1} between R1 and R3 (Table 2.4). In 2017, N remobilization from R1 to R3 came from both leaf and stem components at all N rates except for leaf N at 280N (which had a small numerical N content gain). Despite similar dry matter increases in 2016 and 2017 from R1 to R3 (Fig. 2.2), there was no gain in whole-plant N content from R1 to R3 in 2017 except with the 280N treatment, which gained almost 30 kg N ha^{-1} (Fig. 2.3, C; Table 2.4).

From R3 to R6, though leaf and stem N remobilization occurred in both seasons, two different patterns were noticeable. In 2016, remobilization accounted for the majority of N allocated to the grain with negligible new N uptake happening during this period. Furthermore, remobilized N coming from both leaf and stem increased as N availability was higher (Fig. 2.3, B). In 2017, on the other hand, remobilization and new N uptake contributed almost equally to gains in grain N uptake. While leaf N remobilization did not change among fertilized treatments, both stem N remobilization and post-R3 N uptake increased gradually with N rate (Fig. 2.3, D; Table 2.4).

Although no application timing effects were detected, both final grain N content and total-plant N uptake were strongly affected by N rate in both seasons (Table 2.4). In 2016, incremental gains in N content with N rates were proportionally achieved in both grain and stover since N harvest index (NHI) did not change among fertilized treatments. Conversely, in 2017, NHI increased with N availability (Table 2.5).

2.4.5 Grain Yield, Kernel Number and Kernel Weight

In both seasons, grain yield (GY), kernel number (KN), and kernel weight (KW) were mostly affected by N rate, with the timing by rate interaction proving significant only for GY in 2017 (Table 2.5). In 2016, there was no further yield benefit after 168N, while GY responded significantly up to the 224N treatment in 2017. In terms of KN, no significant differences were found due to N rate treatments in either season, except for the 0N control, which resulted in the lowest values as anticipated.

Conversely to KN, individual KW showed a similar variability pattern to that of GY, increasing gradually (and significantly) with N rate (Table 2.5). Interestingly, KW had equivalent mean values across seasons (282.23 mg $grain^{-1}$ in 2016 and 281.43 mg $grain^{-1}$ in 2017).

2.4.6 Nitrogen Recovery Efficiency and Nitrogen Internal Efficiency

While N timing treatments did not affect either nitrogen recovery efficiency (NRE) or nitrogen internal efficiency (NIE), both efficiencies decreased as N rate increased (Table 2.5), as expected. In 2017, NRE (kg N uptake kg^{-1} N applied) averages across timing treatments ranged from 1.02 at 112N to 0.72 at 280N, while the 2016 average NRE levels were lower with means ranging from 0.83 to 0.57, respectively. The opposite trend was found for NIE (kg grain kg^{-1} N uptake), as higher values were observed in 2016 (from 74 to 52) than those in 2017 (from 59 to 46).

2.4.7 Nitrogen Nutrition Index

Although the zero N treatment resulted in >50% reduction in NNI at R1 (NNI_{R1}), the NNI in most treatments with N applied comfortably exceeded 1.0 and increased with N rate (Table 2.5). Overall, NNI_{R1} was 0.1 to 0.2 units higher than NNI at R3 (NNI_{R3}). In 2016, NNI_{R1} increased until 168N while NNI_{R3} did so until 224N. In 2017, NNI_{R1} values did not differ among fertilized treatments, whereas NNI_{R3} responded positively to N rates until 224N. More significant treatment differences in NNI were observed at R3 than at R1.

When N sources to the grain were regressed against NNI values, a common pattern was found across seasons. Total post-silking N uptake ($PostN_{R1.R6}$) and post-R3 N uptake ($PostN_{R3.R6}$), both expressed as percentage of total N uptake at R6, were not impacted by their respective NNI

values in either 2016 (Fig. 2.4, A and B) nor 2017 (Fig. 2.4, E and F). However, NNI was a strong predictor of apparent N remobilization in both seasons: NNI_{R1} explained 83% (2016) and 79% (2017) of the variability in N remobilization between silking and maturity ($RemN_{R1.R6}$) (Fig. 2.4, C and G), while NNI_{R3} explained 87% (2016) and 82% (2017) of the variability in N remobilization between milk stage and maturity ($RemN_{R3.R6}$) (Fig. 2.4, D and H). The N rate treatment separation patterns of NNI gains at R1 stage more closely reflected that of kernel number differences, while the NNI treatment differences at R3 stage more closely reflected treatment differences in kernel weight (Table 2.5).

2.5 Discussion

2.5.1 Overview of Experimental Factors and Environmental Conditions

Overall variability between seasons, probably the result of a confounding effect between environmental and genotypic differences, did not allow for a 2-year combined analysis (as previously explained in the Material and Methods section). Despite year-to-year variability, and according to the respective ANOVAs, the majority of the 133 variables evaluated in this study responded positively to increasing N rate regardless of the timing of N application. Among the relatively few parameters that reported a significant timing application effect (21 out of 133), no uniform trend was identified, indicating there was neither an advantage nor a disadvantage in splitting the same total N applied into at planting and later vegetative stages from a statistical point of view. Furthermore, since a timing by rate interaction was only detected once, there was little evidence, if any, that late-split applications resulted in higher N uptake and/or utilization when compared to at-planting applications, under the experimental conditions of this study.

The lack of N timing responses might be explained by favorable environmental factors. While there was variability in precipitation between seasons (Fig. 2.1), each experiment received supplementary irrigation in order to prevent any substantial water limitations from happening. This beneficial situation, alongside the well-drained soil that facilitated root growth and limited denitrification losses, might have diluted any advantage of a better synchrony between plant N demand and soil N supply that late-split fertilizer applications could have provided, similar to perspectives presented by Morris et al. (2018). From a crop management standpoint, this means that under sufficient water availability on a fine sandy loam soil, N applied at planting can be as

efficiently taken up and utilized by the crop as when it is split into later vegetative stages (see NRE and NIE in Table 2.5), giving farmers considerable latitude to apply N fertilizer when they see fit based on other factors such as labor/machinery availability, soil conditions and economic optimization. This outcome is in contrast to previous Indiana research which found enhanced NRE with late-split N applications (Mueller et al., 2017). However, overall NRE levels were high in this experiment, reaching or exceeding 70% of the N applied even with the 224N rate treatment. Furthermore, other Indiana research has confirmed that late-split N was less likely to realize reductions in associated nitrous oxide emissions when maize production systems achieve higher NRE (Omonode and Vyn, 2019).

2.5.2 Physiological Mechanisms of Biomass Dynamics During the Reproductive Period

Dry matter production responded positively to increasing N supply throughout the reproductive period in 2016, as most plant components evaluated at R1, R3 and R6 gained DM incrementally until 168N or 224N (Table 2.2). In 2017, on the other hand, a progressive spectrum of N treatment differences in DM were not realized until R6 as total-plant and individual plant-component DM at R1 and at R3 were not significantly changed among non-0N treatments (Table 2.2). Regardless of this difference, in both seasons, average total-plant DM response to increases in N supply became higher as the season progressed (30% and 42% increase at R1, 38% and 50% increase at R3, 82% and 100% increase at R6 in 2016 and 2017, respectively), indicating that post-silking crop responsiveness to soil N availability clearly depends on sink demands for carbohydrates. In addition, in both years, ear C demand was also affected by soil N supply, since ear DM at silking (especially in 2016) and at the onset of linear grain filling (both years) increased with N rate. These results contradict previous reports with Pioneer era hybrids (Mueller and Vyn, 2018b; Mueller et al., 2019b) that proposed that ear DM was highly conserved around silking and was unlikely to be affected by N availability, even under 0N, until the end of the critical period. However, in the latter research, average grain yields with 0N were in a higher range (especially for hybrids commercialized after 1990) indicating that the soil N deficiency may not have been as severe as at the current site.

In 2016, final DM partitioning to grain (i.e., HI) did not change among non-0N treatments (Table 2.5), implying that the increases in total-plant biomass were proportionally consistent to those of grain at R6, and thus increases in final grain yield in response to increasing N supply

(Table 2.5) were more related to higher total-plant biomass rather than to partitioning. In addition, the 26% incremental gain in HI with higher N supply in 2017 was lower proportionally than that of total-plant DM gain by R6, thus supporting the 2016 pattern as well as prior literature (Muchow, 1994; Massignam et al., 2009; Ciampitti and Vyn, 2011) that the dominant effect of N rate on grain yield increase was via total DM production rather than HI.

Although HI was not a strong factor in explaining GY changes due to N rate differences, partitioning to reproductive sink tissues was indeed important to explain seasonal differences in maize productivity since total-plant DM production was similar between years (Table 2.2) but GY was higher in 2017 (Table 2.5). Seasonal differences in GY were related to an overall lower kernel number (KN) in 2016 (Table 2.5), consistent with a lower ear DM at R1 in 2016 across all N rate levels (Table 2.2). Interestingly, despite sink capacity differences between years, overall biomass partitioning trends throughout the reproductive period were fairly similar across seasons, with average leaf contribution to total DM (35% and 36% at R1, 32% and 29% at R3, and 21% and 20% at R6 in 2016 and 2017, respectively) decreasing much less than that of stem (64% and 63% at R1, 56% and 49% at R3, and 25% and 20% at R6 in 2016 and 2017, respectively) as the season progressed. Despite a greater stem DM allocation at silking, average stem/leaf DM ratio (1.80 in 2016, 1.75 in 2017) was similar to the range shown by modern genotypes and lower than that of older genotypes reported by Chen et al. (2015). In that study, it was argued that a more balanced distribution of carbohydrates between these two vegetative organs at silking could benefit later DM and N dynamics during grain filling; the same was also confirmed by Mueller and Vyn (2018).

Maximum DM values in both leaves and stems were not realized until R3 (Table 2.2), indicating that they continued accumulating carbohydrates even during the early stages of grain development. This outcome is illustrated by the negative DM remobilization values found in both seasons for the period R1-R3 (Fig. 2.2, A and C), which should be understood as incremental DM gains in those plant components that contributed most of the total post-silking DM gain during that period. In both seasons, soil N availability had no impact on the increase in stem biomass from R1 to R3, indicating that even under N deficiency, this tissue gained carbohydrates (averaging 1.59 Mg ha^{-1} of DM in 2016, and 1.00 Mg ha^{-1} in 2017), regardless of ear sink capacity changes. Stem biomass increases from R1 to R3, also reported by previous authors (Tollenaar, 1977; Kiniry et al., 1992; Uhart and Andrade, 1995; Rajcan and Tollenaar, 1999b; Mueller and Vyn, 2018a), reflect this tissue's strong capacity of storing carbohydrates when DM production exceeds ear demands

(Daynard et al., 1969; Hume and Campbell, 1972). The latter phenomenon can occur under a wide range of physiological conditions given that during the lag phase kernels function as a weak sink gaining very little DM (Johnson and Tanner, 1972; Reddy and Daynard, 1983). In addition, the magnitude of leaf biomass gains from R1 to R3 within years was quite uniform among N treatments (with the exception of the small gain observed with 0N in 2016). These leaf biomass gains from R1 to R3 could be explained by their potential to store excessive photosynthates, as well as by the continued expansion of upper leaves after silking.

In both seasons, new dry matter production resulting from current photosynthesis between silking and the onset of linear grain fill ($PostDM_{R1.R3}$) was, on a net basis, the only source of carbohydrates to the ear during this early reproductive stage (Fig. 2.2, A and C). There was neither leaf nor stem DM remobilization during this period ($RemDM_{R1.R3}$), a unique observation that usually escapes notice when maize biomass component samples are only taken at silking and at physiological maturity. In addition, the fact that both vegetative tissues reported increases in DM from R1 to R3 under all N rates could mean that a reproductive sink limitation occurred at a pre-silking stage, in spite of differences in N availability, in both seasons. This was particularly noticeable in 2016, when stover DM increases (leaf plus stem together) accounted for 55-72% of post-silking dry matter production from R1 to R3. Pre-silking sink restrictions are more commonly associated with reduced kernel number (KN) rather with lower final kernel weight (KW) (Borrás and Otegui, 2001; Cerrudo et al., 2013).

Despite pre-silking conditions, soil N availability effects on post-silking sink determination are usually confounded by the fact that both kernel set and potential KW are defined during the lag phase. Since restrictions in N supply can decrease KN by reductions in plant growth rate and DM partitioning to the ear (Uhart and Andrade, 1995; D'Andrea et al., 2008), the lack of KN changes among the non-0N treatments in our study (Table 2.5) implies that the plants had reached optimum growing conditions for KN even under the lowest N rate (112N), thus preventing kernel abortion, the most sensitive mechanism regulating KN during the lag phase in limited N conditions (Monneveux et al., 2005). Potential KW, related to the number of endosperm cells determined over the lag phase (Jones et al., 1985, 1996), also depends on assimilate supply to the ear during this period (Gambín et al., 2006). Therefore, the fact that final KW increased gradually with N rate (Table 2.5) beyond optimum plant growth, suggests that increases in N supply actually changed

potential KW by different means than those affecting KN. Differential regulation mechanisms for KN and KW have recently been proposed by Paponov et al. (2020).

Once linear grain filling began, partitioning was clearly dominated by kernels, with an average of 85% and 84% of final grain DM achieved from R3 to R6 in 2016 and 2017, respectively (Table 2.2). Conversely to what happened during the lag phase, DM allocated to kernels during linear grain fill came from both photosynthetic source capacity, i.e. total-plant DM accumulation from R3 to R6 ($PostDM_{R3.R6}$), as well as from DM remobilization ($RemDM_{R3.R6}$), especially from stem, under all N rate treatments (Fig. 2.2. B and D). Even though $PostDM_{R3.R6}$ increased with N availability, it was never enough to fulfill the high grain DM demand at any N level, and its contribution to final grain biomass declined proportionally as mineral N decreased (28% and 24% of final grain DM under 0N, versus 61% and 64% of final grain DM under 280N in 2016 and 2017, respectively).

From R3 to R6, DM remobilization from stem compensated for the photosynthetic source limitation by an average net contribution to grain DM of 3.3 Mg ha^{-1} in 2016 and 2.8 Mg ha^{-1} in 2017. Stem DM remobilization, therefore, accounted for 53% and 56% of final grain DM at 0N and 25% and 21% of final grain DM in all non-0N treatments, respectively, in 2016 and 2017. In addition, 49% (2016) and 36% (2017) of total stem DM remobilization from R3 to R6 came from post-silking gains in stem biomass over the lag phase, while the remaining 51% (2016) and 64% (2017) came from stored carbohydrates in stem before silking. Remobilization of stem reserves when current photosynthesis is not enough to meet sink demands has been widely reported (Daynard et al., 1969; Hume and Campbell, 1972; Setter and Meller, 1984; Kiniry et al., 1992; Rajcan and Tollenaar, 1999b; Rattalino Edreira et al., 2014; D'Andrea et al., 2016). However, the fact that $PostDM_{R3.R6}$ was not enough to meet reproductive sink demands at any N rate level (even with luxury N rates), provides further confirmation that KN alone is an inadequate gauge of sink strength. While KN has frequently been used to estimate sink capacity (Andrade and Ferreiro, 1996; Otegui and Bonhomme, 1998; Borrás et al., 2004; D'Andrea et al., 2008; Chen et al., 2016; Hisse et al., 2019), grain yield (GY) changes due to N supply mirrored KW differences rather than those of KN under the conditions of this study, suggesting the need of a deeper analysis into KW physiological determinants in order to include them as sink parameters. A bigger KW role in GY determination for more recent hybrids compared to older genotypes has been reported in multiple ERA studies (Chen et al., 2016; Mueller et al., 2019a).

Most maize papers estimating remobilization versus new photosynthetic production sources for grain DM gain at maturity do so by measuring net DM loss from leaf and stems between R1 and R6 (Pan et al., 1995; Rajcan and Tollenaar, 1999b, 1999a; Uribelarrea et al., 2009; Ning et al., 2013; Chen et al., 2015; Antonietta et al., 2016; Mueller et al., 2017). This research confirms that the actual leaf and stem DM remobilization is underestimated by net silking-to-maturity approach because it doesn't account for the stem and leaf DM increases that commonly occur in modern hybrids during the lag phase.

2.5.3 Physiological Mechanisms of Nitrogen Dynamics During the Reproductive Period

As expected, plant N uptake responded positively to increasing N rate throughout the whole reproductive period in both seasons. Most plant components evaluated at R1, R3 and at R6 increased their respective N contents until 168N-224N (Table 2.4). Reproductive N uptake (Table 2.4) and partitioning (Fig. 2.3) showed strong differences between seasons despite similar total-plant biomass production at the three phenological stages (Table 2.2) and similar DM allocation patterns during both the lag and linear grain-filling phases (Fig. 2.2). While total-plant average N uptake at R1 was somewhat similar between years (153.2 kg N ha^{-1} in 2016 vs 147.1 kg N ha^{-1} in 2017), the much higher ear N contents achieved in 2017 were replaced by higher leaf N contents in 2016 (Table 2.4). Regardless of these seasonal differences, in both years, ear N content changes due to N availability at R1 as well as R3 were explained by changes in ear biomass (Table 2.2) rather than ear N concentration (Table 2.3).

The lack of N rate effect on ear N concentration at R1 and R3 in both seasons (Table 2.3) despite seasonal sink differences suggests that both DM and N allocation to reproductive sinks changed proportionally due to N availability differences during the early stages of kernel development. The conservative nature of ear N concentration found in our results, similar to what was proposed by D'Andrea et al. (2008), agrees with a concept, recently reviewed by Fernie et al. (2020), that plants are able to adjust C metabolism in response to both soil N availability and sink strength under N stress conditions as well as at high N supply.

In contrast to developments at early reproductive stages, grain N concentration at R6 was strongly affected by N supply (Table 2.3), indicating that at some point during linear grain filling, N supply began to have differential effects on grain carbohydrate and N allocation dynamics. This is reinforced by the fact that grain N uptake (average increase of 282% and 299% in 2016 and

2017, respectively) was much more affected by N supply than grain biomass (average increase of 171% and 157% in 2016 and 2017, respectively) at physiological maturity. In addition, both grain N content and total-plant N uptake at R6 were consistently lower in 2016, indicating that the seasonal difference in sink capacity via a lower KN (Table 2.5) demanded less total-plant N uptake (Table 2.4) but similar total-plant biomass production (Table 2.2). Furthermore, the bigger N sink demand in 2017 may be explained by a higher KN, as well as the kernels' capacity to accumulate more N while achieving the same DM [i.e. similar KW (Table 2.5) and greater grain N concentration (Table 2.3)].

Despite seasonal differences, total N uptake values in both years of this study were among the highest reported in Indiana maize research, which in turn explained the high NRE obtained (Table 2.5). Mueller et al. (2017) reported lower N uptake (214-209 kg N ha^{-1}) and NRE (70-50%) with similar biomass (22-24.3 Mg ha^{-1}) and grain yield (12-14.3 Mg ha^{-1}) for the first two years of a study conducted at a nearby location (13 km north of our experimental site) under a gradient of N availability realized by a combination of N rate and N timing application treatments. Our results are closer to those of Omonode and Vyn (2019), who reported 261.3-276.6 kg N ha^{-1} of N uptake and 85.5-96.8% of NRE for a study testing tillage practices under a common N rate of 220 kg N ha^{-1}. In addition, in both seasons of our study, crop N uptake exceeded fertilizer N applied until 224N, presumably because of soil N mineralization plus the small starter N application.

Nitrogen partitioning patterns among plant components reflected seasonal and N treatment differences (Fig. 2.3). In 2016, N allocated to the reproductive sink tissues from R1 to R3 came from both new N uptake ($PostN_{R1.R3}$) and N remobilization ($RemN_{R1.R3}$) (Fig. 2.3, A), with the former N source playing a bigger role (particularly in the non-0N treatments by accounting for 72-90% of the ear's N requirements during this period). While N availability positively affected $PostN_{R1.R3}$, it did not change total remobilized N but the tissue source for remobilized N. In fertilized treatments, stem was the source of remobilized N, but when severe stress prevented this tissue from doing so (i.e. at 0N) remobilized N came from leaves. Interestingly, under the opposite situation at high N rates, and even though stem remobilization continued, leaves also accumulated some N, as shown by the leaf negative N remobilization values in Fig. 2.3 (A).

In 2017, on the other hand, the net N allocated to the reproductive sink tissues during the lag phase apparently originated exclusively from N remobilization ($RemDM_{R1.R3}$) at most N rates (0N-224N) (Fig. 2.3, C). However, the losses in leaf and stem N content from R1 to R3 were higher

than the increases in ear N content for the same period (Table 2.4). In certain N treatments, this situation led to a decrease in total-plant N uptake between R1 and R3 (Table 2.4) associated with negative $PostN_{R1.R3}$ values in Fig. 2.3 (C). The latter might indicate that not only did plants fail to take-up new N, but that a net N loss occurred from above-ground vegetative tissues. While gaseous N losses from the canopy have previously been reported not only for maize (Francis et al., 1993), but also for soybean (Stutte et al., 1979) and winter wheat (Kanampiu et al., 1997), the decreases in N content from R1 to R3 that were detected might not reflect a "true" N loss but a variability in this parameter's measurement. Given the methodology employed in this study, it was not possible to tell which tissue might have been providing the ear with more N than the other, and which one might have been losing more N to the environment (if any), but at least it was clear that both leaf and stem N remobilization were required to fulfill ear N demands at 112N, 168N, and 224N (Table 2.4). Conversely, plants were only able to add net new N ($PostN_{R1.R3}$) under the highest soil supply (280N) (Fig. 2.3, C); however, even then, N remobilization from stems was also required.

Nitrogen source dynamics (Fig. 2.3, A and C) and dry matter source dynamics (Fig. 2.2, A and C) during the period between R1 and R3 seemed to have different roles. While ear's carbohydrate demand was always exceeded by current photosynthesis, and while vegetative tissues stored the "extra" C at all N supply levels, ear's N demand was exceeded by N sources only at higher N rates with leaf and/or stem N remobilization contributing to ear N gains under all soil N conditions. These observations confirm that reproductive sink strength manifests itself differently depending on the allocated substrate, with the ear behaving as a much stronger importer of N than for DM during the lag phase of grain development (when endosperm cells, and thus potential KW, are being determined). Our results are consistent to what Paponov et al. (2020) reported for the lag phase on hydroponic-grown maize, and to what Cazetta et al. (1999) found studying *in vitro*-cultured maize grains. This is also similar to the sink model proposed by Lemaire and Millard (1999) for meristem development, where N substrates are first required for cell division processes such as DNA replication and protein synthesis, and then the resultant divided cells will be responsible for the later-season C substrate demand.

Another common pattern across seasons was the fact that N accumulation in leaves and N remobilization from stem were apparently happening simultaneously under high N rates (168N-280N in 2016, 280N in 2017). This might be due to differential utilization rates by the ear, with remobilization from stem having a higher allocation rate to the grain than that of the new N uptake

being absorbed. In addition, contrary to other reports (Crawford et al., 1982; Swank et al., 1982; Yang et al., 2016), and conversely to our DM dynamics in this research, the stem was never a sink for N after silking (Fig. 2.2, A and C).

Once linear grain filling began, N was exclusively allocated to kernels, with an average of 76% and 79% of final grain N content being achieved from the R3 to R6 period in 2016 and 2017, respectively (Table 2.4). In 2016, the primary N source for the grain after R3 was remobilization ($RemN_{R3.R6}$), especially from leaves (Fig. 2.3, B). In non-0N treatments, leaves accounted for an average of 74% of total N remobilization, while it was the only tissue remobilizing N under severe stress (0N). Conversely to DM remobilization, the amount of N remobilized from both leaves and stem increased with N rate, indicating DM and N remobilization processes were relatively independent from one another. This was particularly evident for leaves, which experienced significant decreases in N content from R3 to R6 for remobilization (Table 2.4; Fig. 2.3, B) with negligible loss of biomass (Table 2.2; Fig. 2.2, B). Similar results on the differential contribution of leaves in terms of N and DM have been found by other authors (Rajcan and Tollenaar, 1999a; Chen et al., 2015). In addition, plants absorbed little net new N during linear grain fill; net gains in post-silking N uptake only occurred during the lag phase (Fig. 2.3, A), something that would have gone undetected without sampling at R3 stage. Since the majority of new N uptake from R1 to R3 was used to meet ear requirements, these results indicate that N accumulated in plant vegetative tissues before silking was indeed more responsible to sustain N reproductive sink demands during linear grain fill than during the lag period. Similar associations between pre-silking N uptake and N remobilization were also reported by Coque and Gallais (2007), Ciampitti and Vyn (2013), and Yang et al. (2016).

In 2017, by contrast, linear grain-filling N requirements were fulfilled by both new N uptake ($PostN_{R3.R6}$) and N remobilization ($RemN_{R3.R6}$) from all non-grain tissues at all N rate treatments (Fig. 2.3, D). Both $PostN_{R3.R6}$ and stem N remobilization increased with soil N availability. Therefore, the common trade-off between new N uptake and total N remobilization (Muchow and Sinclair, 1994; Coque and Gallais, 2007; Ciampitti and Vyn, 2013) was not noticed in this study, even under the wide gradient of soil N conditions present. Since plants did not absorb new N, and rather lost it, during the lag phase (except at 280N) (Fig. 2.3, C), the overall post-silking N uptake in 2017 happened only after R3, a phenomenon that would have escaped notice without R3 stage

sampling. Furthermore, this new N uptake from R3 to R6 not only enabled crop recovery, but it might also be responsible for the high N contents in grain and plant reported at R6 (Table 2.4).

Since this study resulted in two different patterns of reproductive N dynamics in maize, the resulting nitrogen nutrition index was then calculated at both silking (NNI_{R1}) and at the onset of linear grain fill (NNI_{R3}). NNI is an indicator of whether the crop is under N luxury (NNI>1), N optimum (NNI≅1), or N deficiency (NN<1) conditions at a specific stage (Lemaire and Gastal, 1997), and thus, NNI_{R1} has been used as an estimator of how well the photosynthetic apparatus could work after silking in order to delay senescence (Gallais and Coque, 2005) and increase post-silking N uptake (Fernandez et al., 2019). Contrary to those reports, our results showed that neither NNI_{R1} nor NNI_{R3} were good predictors of total post-silking N uptake ($PostN_{R1.R6}$) or post-R3 N uptake ($PostN_{R3.R6}$), respectively, in either season (Fig. 2.4, A, B, E and F). Instead, total N remobilization patterns in both seasons of our study, regardless of N translocation differences, were strongly related to NNI_{R1} and NNI_{R3}, with the former explaining 83% (2016) and 79% (2017) of N remobilization from silking to maturity ($RemN_{R1.R6}$) (Fig. 2.4, C and G), and the latter explaining 87% (2016) and 82% (2017) of N remobilization from the onset of linear grain fill to maturity ($RemN_{R3.R6}$) (Fig. 2.4, D and H). Under the conditions of our study, crop N status quantified by NNI was not a good indicator of the potential for new N uptake [a conclusion suggested by Fernandez et al. (2019) in the context of late-season N treatments]. Instead, NNI was a good indicator of the amount of N stored in vegetative tissues up to R1 or R3 that was available for remobilization at later stages. In that respect, our results are consistent with Coque et al. (2008), who found common QTLs for NNI_{R1} and N remobilization.

2.6 Conclusions

We studied maize DM and N dynamics during the reproductive period under a wide gradient of soil N availability conditions (5 N rates with 3 N timings) by splitting the analysis into the two main periods of grain filling, i.e. the lag phase (R1-R3) and the effective grain-filling phase (R3-R6). We sought to identify potential physiological mechanisms unique to each period that remain hidden under both the silking-to-maturity approach and the critical period approach. Nitrogen rate had much greater impact on all evaluated parameters than N timing treatments. In both seasons, net new C gains for the reproductive sink tissues during the lag phase ($PostDM_{R1.R3}$), was much less responsive to soil N availability than C gains associated with $PostDM_{R3.R6}$. Although

$PostDM_{R3.R6}$ was the primary source of C for kernels during effective grain filling, $RemDM_{R3.R6}$ from stem also occurred at all N rates. Plants took up new N after silking either during the lag phase (2016) or during the linear grain-fill (2017). Despite seasonal differences, PostN, as well as RemN, were both increased by soil N availability in both seasons. The nitrogen nutrition index (NNI) of maize plants at R1 and R3 explained over 80% of the per-plot variability in subsequent RemN, but had little influence on PostN uptake during both R1 to R6 and R3 to R6 periods. Both grain yield (GY) and kernel weight (KW) gradually increased with N rate, and given that kernel number (KN) did not change among fertilized treatments, increased N supply to the ear primarily increased potential KW as, especially since during the lag phase, reproductive tissues proved to be stronger sinks for N than DM. Results from this work highlight the importance of assessing DM and N components at the R3 stage when studying maize crop N dynamics during the reproductive period, the value of continued study on NNI as a predictor of RemN when no new N fertilizers are applied after V12, and the potential knowledge gains from further study of physiological determinants of KW and grain N content in maize hybrids at varying N levels.

2.7 References

Abe, A., Adetimirin, V. O., Menkir, A., Moose, S. P., and Olaniyan, A. B. (2013). Performance of tropical maize hybrids under conditions of low and optimum levels of nitrogen fertilizer application - Grain yield, biomass production and nitrogen accumulation. *Maydica* 58, 141–150.

Andrade, F. H., Echarte, L., Rizzalli, R., Della Maggiora, A., and Casanovas, M. (2002). Kernel number prediction in maize under nitrogen or water stress. *Crop Sci.* 42, 1173–1179. doi:10.2135/cropsci2002.1173.

Andrade, F. H., and Ferreiro, M. A. (1996). Reproductive growth of maize, sunflower and soybean at different source levels during grain filling. *F. Crop. Res.* 48, 155–165.

Antonietta, M., Acciaresi, H. A., and Guiamet, J. J. (2016). Responses to N deficiency in stay green and non-stay green Argentinean hybrids of maize. *J. Agron. Crop Sci.* 202, 231–242. doi:10.1111/jac.12136.

Borrás, L., and Otegui, M. E. (2001). Maize kernel weight response to postflowering source-sink ratio. *Crop Sci.* 41, 1816–1822. doi:10.2135/cropsci2001.1816.

Borrás, L., Slafer, G. A., and Otegui, M. E. (2004). Seed dry weight response to source-sink manipulations in wheat, maize and soybean: A quantitative reappraisal. *F. Crop. Res.* 86, 131–146. doi:10.1016/j.fcr.2003.08.002.

Carmer, S. G., Walker, W. M., and Seif, R. D. (1969). Practical suggestions on pooling variances for F tests of treatment effects. *Agron. J.* 61, 334–336. doi:10.2134/agronj1969.00021962006100020051x.

Cassman, K. G., Dobermann, A., and Walters, D. T. (2002). Agroecosystems, nitrogen-use efficiency, and nitrogen management. *Ambio* 31, 132–140. doi:10.1579/0044-7447-31.2.132.

Cazetta, J. O., Seebauer, J. R., and Below, F. E. (1999). Sucrose and nitrogen supplies regulate growth of maize kernels. *Ann. Bot.* 84, 747–754. doi:10.1006/anbo.1999.0976.

Cerrudo, A., Di Matteo, J., Fernandez, E., Robles, M., Olmedo Pico, L., and Andrade, F. H. (2013). Yield components of maize as affected by short shading periods and thinning. *Crop Pasture Sci.* 64, 580–587. doi:10.1071/CP13201.

Chen, K., Camberato, J. J., Tuinstra, M. R., Kumudini, S. V., Tollenaar, M., and Vyn, T. J. (2016). Genetic improvement in density and nitrogen stress tolerance traits over 38 years of commercial maize hybrid release. *F. Crop. Res.* 196, 438–451. doi:10.1016/j.fcr.2016.07.025.

Chen, K., Kumudini, S. V., Tollenaar, M., and Vyn, T. J. (2015). Plant biomass and nitrogen partitioning changes between silking and maturity in newer versus older maize hybrids. *F. Crop. Res.* 183, 315–328. doi:10.1016/j.fcr.2015.08.013.

Ciampitti, I. A., Murrell, S. T., Camberato, J. J., Tuinstra, M., Xia, Y., Friedemann, P., et al. (2013). Physiological dynamics of maize nitrogen uptake and partitioning in response to plant density and nitrogen stress factors: II. Reproductive phase. *Crop Sci.* 53, 2588–2602. doi:10.2135/cropsci2013.01.0041.

Ciampitti, I. A., and Vyn, T. J. (2011). A comprehensive study of plant density consequences on nitrogen uptake dynamics of maize plants from vegetative to reproductive stages. *F. Crop. Res.* 121, 2–18. doi:10.1016/J.FCR.2010.10.009.

Ciampitti, I. A., and Vyn, T. J. (2013). Grain nitrogen source changes over time in maize: A review. *Crop Sci.* 53, 366–377. doi:10.2135/cropsci2012.07.0439.

Coque, M., and Gallais, A. (2007). Genetic variation for nitrogen remobilization and postsilking nitrogen uptake in maize recombinant inbred lines: Heritabilities and correlations among traits. *Crop Sci.* 47, 1787–1796. doi:10.2135/cropsci2007.02.0096.

Coque, M., Martin, A., Veyrieras, J. B., Hirel, B., and Gallais, A. (2008). Genetic variation for N-remobilization and postsilking N-uptake in a set of maize recombinant inbred lines. 3. QTL detection and coincidences. *Theor. Appl. Genet.* 117, 729–747. doi:10.1007/s00122-008-0815-2.

Crawford, T. W., Rendig, V. V., and Broadbent, F. E. (1982). Sources, fluxes, and sinks of nitrogen during early reproductive growth of maize (Zea mays L.). *Plant Physiol.* 70, 1654–1660. doi:10.1104/pp.70.6.1654.

D'Andrea, K. E., Otegui, M. E., and Cirilo, A. G. (2008). Kernel number determination differs among maize hybrids in response to nitrogen. *F. Crop. Res.* 105, 228–239. doi:10.1016/j.fcr.2007.10.007.

D'Andrea, K. E., Piedra, C. V., Mandolino, C. I., Bender, R., Cerri, A. M., Cirilo, A. G., et al. (2016). Contribution of reserves to kernel weight and grain yield determination in maize: Phenotypic and genotypic variation. *Crop Sci.* 56, 697–706. doi:10.2135/cropsci2015.05.0295.

Daynard, T. B., Tanner, J. W., and Hume, D. J. (1969). Contribution of stalk soluble carbohydrates to grain yield in corn (Zea mays L.). *Crop Sci.* 9, 831–834. doi:10.2135/cropsci1969.0011183x000900060050x.

de Mendiburu, F. (2020). agricolae: Statistical Procedures for Agricultural Research. R package version 1.3-2. https://CRAN.R-project.org/package=agricolae.

Echarte, L., Rothstein, S., and Tollenaar, M. (2008). The response of leaf photosynthesis and dry matter accumulation to nitrogen supply in an older and a newer maize hybrid. *Crop Sci.* 48, 656–665. doi:10.2135/cropsci2007.06.0366.

Etheridge, R. D., Pesti, G. M., and Foster, E. H. (1998). A comparison of nitrogen values obtained utilizing the Kjeldahl nitrogen and Dumas combustion methodologies (Leco CNS 2000) on samples typical of an animal nutrition analytical laboratory. *Anim. Feed Sci. Technol.* 73, 21–28. doi:10.1016/S0377-8401(98)00136-9.

Fernandez, J. A., DeBruin, J., Messina, C. D., and Ciampitti, I. A. (2019). Late-season nitrogen fertilization on maize yield: A meta-analysis. *F. Crop. Res.*, 107586. doi:10.1016/J.FCR.2019.107586.

Fernie, A. R., Bachem, C. W. B., Helariutta, Y., Neuhaus, H. E., Prat, S., Ruan, Y. L., et al. (2020). Synchronization of developmental, molecular and metabolic aspects of source–sink interactions. *Nat. Plants* 6, 55–66. doi:10.1038/s41477-020-0590-x.

Francis, D. D., Schepers, J. S., and Vigil, M. F. (1993). Post-anthesis nitrogen loss from corn. *Agron. J.* 85, 659–663. doi:10.2134/agronj1993.00021962008500030026x.

Gallais, A., and Coque, M. (2005). Genetic variation and selection for nitrogen use efficiency in maize: A synthesis. *Maydica* 50, 531–547.

Gambín, B. L., Borrás, L., and Otegui, M. E. (2006). Source-sink relations and kernel weight differences in maize temperate hybrids. *F. Crop. Res.* 95, 316–326. doi:10.1016/j.fcr.2005.04.002.

Hisse, I. R., D'Andrea, K. E., and Otegui, M. E. (2019). Source-sink relations and kernel weight in maize inbred lines and hybrids: Responses to contrasting nitrogen supply levels. *F. Crop. Res.* 230, 151–159. doi:10.1016/J.FCR.2018.10.011.

Hume, D. J., and Campbell, D. K. (1972). Accumulation and translocation of soluble solids in corn stalks. *Can. J. Plant Sci.* 52, 363–368. doi:10.4141/cjps72-056.

Johnson, D. R., and Tanner, J. W. (1972). Calculation of the rate and duration of grain filling in corn (Zea mays L.). *Crop Sci.* 12, 485–486. doi:10.2135/cropsci1972.0011183x001200040028x.

Jones, R. J., Roessler, J., and Ouattar, S. (1985). Thermal environment during endosperm cell division in maize: effects on number of endosperm cells and starch granules. *Crop Sci.* 25, 830–834. doi:10.2135/cropsci1985.0011183x002500050025x.

Jones, R. J., Schreiber, B. M. N., and Roessler, J. A. (1996). Kernel sink capacity in maize: Genotypic and maternal regulation. *Crop Sci.* 36, 301–306. doi:10.2135/cropsci1996.0011183X003600020015x.

Kanampiu, F. K., Raun, W. R., and Johnson, G. V. (1997). Effect of nitrogen rate on plant nitrogen loss in winter wheat varieties. *J. Plant Nutr.* 20, 389–404. doi:10.1080/01904169709365259.

Kiniry, J. R., Tischler, C. R., Rosenthal, W. D., and Gerik, T. J. (1992). Nonstructural carbohydrate utilization by sorghum and maize shaded during grain growth. *Crop Sci.* 32, 131–137. doi:10.2135/cropsci1992.0011183x003200010029x.

Lemaire, G., and Gastal, F. (1997). “N uptake and distribution in plant canopies,” in *Diagnosis of the Nitrogen Status in Crops* (Berlin, Heidelberg: Springer Berlin Heidelberg), 3–43. doi:10.1007/978-3-642-60684-7_1.

Lemaire, G., and Gastal, F. (2009). “Quantifying crop responses to nitrogen deficiency and avenues to improve nitrogen use efficiency,” in *Crop Physiology: Applications for Genetic Improvement and Agronomy*, eds. V. O. Sadras and D. F. Calderini (San Diego, CA: Academic Press), 171–211. doi:10.1016/b978-0-12-374431-9.00008-6.

Lemaire, G., and Millard, P. (1999). An ecophysiological approach to modelling resource fluxes in competing plants. *J. Exp. Bot.* 50, 15–28. doi:10.1093/jxb/50.330.15.

Licht, M. A., Archontoulis, S., and Hatfield, J. L. (2017). Corn water use and evapotranspiration. *Integr. Crop Manag. News. Iowa State Univ. Ext. Outreach*, 1–6. Available at: https://crops.extension.iastate.edu/cropnews/2017/06/corn-water-use-and-evapotranspiration.

Masclaux-Daubresse, C., Daniel-Vedele, F., Dechorgnat, J., Chardon, F., Gaufichon, L., and Suzuki, A. (2010). Nitrogen uptake, assimilation and remobilization in plants: Challenges for sustainable and productive agriculture. *Ann. Bot.* 105, 1141–1157. doi:10.1093/aob/mcq028.

Massignam, A. M., Chapman, S. C., Hammer, G. L., and Fukai, S. (2009). Physiological determinants of maize and sunflower grain yield as affected by nitrogen supply. *F. Crop. Res.* 113, 256–267. doi:10.1016/j.fcr.2009.06.001.

Messina, C., Hammer, G., Dong, Z., Podlich, D., and Cooper, M. (2009). “Modelling crop improvement in a G×E×M framework via gene–trait–phenotype relationships,” in *Crop Physiology: Applications for Genetic Improvement and Agronomy*, eds. V. O. Sadras and D. F. Calderini (San Diego, CA: Academic Press), 235–581. doi:10.1016/b978-0-12-374431-9.00010-4.

Monneveux, P., Zaidi, P. H., and Sanchez, C. (2005). Population density and low nitrogen affects yield-associated traits in tropical maize. *Crop Sci.* 45, 535–545. doi:10.2135/cropsci2005.0535.

Morris, T. F., Murrell, T. S., Beegle, D. B., Camberato, J. J., Ferguson, R. B., Grove, J., et al. (2018). Strengths and limitations of Nitrogen rate recommendations for corn and opportunities for improvement. *Agron. J.* 110, 1–37. doi:10.2134/agronj2017.02.0112.

Muchow, R. C. (1994). Effect of nitrogen on yield determination in irrigated maize in tropical and subtropical environments. *F. Crop. Res.* 38, 1–13. doi:10.1016/0378-4290(94)90027-2.

Muchow, R. C., and Sinclair, T. R. (1994). Nitrogen response of leaf photosynthesis and canopy radiation use efficiency in field-grown maize and sorghum. *Crop Sci.* 34, 721–727. doi:10.2135/cropsci1994.0011183X003400030022x.

Mueller, S. M., Camberato, J. J., Messina, C., Shanahan, J., Zhang, H., and Vyn, T. J. (2017). Late-split nitrogen applications increased maize plant nitrogen recovery but not yield under moderate to high nitrogen rates. *Agron. J.* 109, 2689. doi:10.2134/agronj2017.05.0282.

Mueller, S. M., Messina, C. D., and Vyn, T. J. (2019a). Simultaneous gains in grain yield and nitrogen efficiency over 70 years of maize genetic improvement. *Sci. Rep.* 9, 9095. doi:10.1038/s41598-019-45485-5.

Mueller, S. M., Messina, C. D., and Vyn, T. J. (2019b). The role of the exponential and linear phases of maize (Zea mays L.) ear growth for determination of kernel number and kernel weight. *Eur. J. Agron.* 111, 125939. doi:10.1016/J.EJA.2019.125939.

Mueller, S. M., and Vyn, T. J. (2018a). Can late-split nitrogen application increase ear nitrogen accumulation rate during the critical period in maize? *Crop Sci.* 58, 1717–1728. doi:10.2135/cropsci2018.02.0118.

Mueller, S. M., and Vyn, T. J. (2018b). Physiological constraints to realizing maize grain yield recovery with silking-stage nitrogen fertilizer applications. *F. Crop. Res.* 228, 102–109. doi:10.1016/j.fcr.2018.08.025.

Nasielski, J., and Deen, B. (2019). Nitrogen applications made close to silking: Implications for yield formation in maize. *F. Crop. Res.* 243, 107621. doi:10.1016/j.fcr.2019.107621.

Ning, P., Li, S., Yu, P., Zhang, Y., and Li, C. (2013). Post-silking accumulation and partitioning of dry matter, nitrogen, phosphorus and potassium in maize varieties differing in leaf longevity. *F. Crop. Res.* 144, 19–27. doi:10.1016/j.fcr.2013.01.020.

Omonode, R. A., and Vyn, T. J. (2019). Tillage and nitrogen source impacts on relationships between nitrous oxide emission and nitrogen recovery efficiency in corn. *J. Environ. Qual.* 48, 421–429. doi:10.2134/jeq2018.05.0188.

Otegui, M. E., and Bonhomme, R. (1998). Grain yield components in maize I. Ear growth and kernel set. *F. Crop. Res.* 56, 257–264. doi:10.1016/s0378-4290(97)00094-4.

Pan, W. L., Camberato, J. J., Moll, R. H., Kamprath, E. J., and Jackson, W. A. (1995). Altering source-sink relationships in prolific maize hybrids: Consequences for nitogen uptake and remobilization. *Crop Sci.* 35, 836–845. doi:10.2135/cropsci1995.0011183X003500030034x.

Paponov, I., Paponov, M., Sambo, P., and Engels, C. (2020). Differential regulation of kernel set and potential kernel weight by nitrogen supply and carbohydrate availability in maize genotypes contrasting in nitrogen use efficiency. *Front. Plant Sci.* 11, 1–19. doi:10.3389/fpls.2020.00586.

Paul, M. J., and Foyer, C. H. (2001). Sink regulation of photosynthesis. *J. Exp. Bot.* 52, 1383–1400. doi:10.1093/jexbot/52.360.1383.

Plénet, D., and Lemaire, G. (1999). Relationships between dynamics of nitrogen uptake and dry matter accumulation in maize crops. Determination of critical N concentration. *Plant Soil* 216, 65–82. doi:10.1023/A:1004783431055.

Pommel, B., Gallais, A., Coque, M., Quilleré, I., Hirel, B., Prioul, J. L., et al. (2006). Carbon and nitrogen allocation and grain filling in three maize hybrids differing in leaf senescence. *Eur. J. Agron.* 24, 203–211. doi:10.1016/j.eja.2005.10.001.

R Core Team (2019). R: A language and environment for statistical computing. R Foundation for Statistical Computing, Vienna, Austria. https://www.R- project.org/.

Rajcan, I., and Tollenaar, M. (1999a). Source: Sink ratio and leaf senescence in maize: II. Nitrogen metabolism during grain filling. *F. Crop. Res.* 60, 255–265. doi:10.1016/S0378-4290(98)00143-9.

Rajcan, I., and Tollenaar, M. (1999b). Source:sink ratio and leaf senescence in maize: I. Dry matter accumulation and partitioning during grain filling. *F. Crop. Res.* 60, 255–265. doi:10.1016/s0378-4290(98)00143-9.

Rattalino Edreira, J. I., Mayer, L. I., and Otegui, M. E. (2014). Heat stress in temperate and tropical maize hybrids: Kernel growth, water relations and assimilate availability for grain filling. *F. Crop. Res.* 166, 162–172. doi:10.1016/j.fcr.2014.06.018.

Reddy, V., and Daynard, T. (1983). Endosperm characteristics associated with rate of grain filling and kernel size in corn. *Maydica* 28, 339–355. doi:10.11693/hyhz20181000233.

Ritchie, S. W., and Hanway, J. J. (1982). How a corn plant develops. Iowa State University of Science and Technology. Cooperative Extension Service, Iowa, EEUU. Special Report Nº48. 1982.

Setter, T. L., and Meller, V. H. (1984). Reserve carbohydrate in maize stem. *Plant Physiol.* 75, 617–622. doi:10.1104/pp.75.3.617.

Soil Survey Staff Web Soil Survey. Natural Conservation Service, USDA. http://websoilsurvey.sc.egov.usda.gov/.

Stutte, C. A., Weiland, R. T., and Blem, A. R. (1979). Gaseous nitrogen loss from soybean foliage. *Agron. J.* 71, 95–97. doi:10.2134/agronj1979.00021962007100010024x.

Swank, J. C., Below, F. E., Lambert, R. J., and Hageman, R. H. (1982). Interaction of carbon and nitrogen metabolism in the productivity of maize. *Plant Physiol.* 70, 1185–1190. doi:10.1104/pp.70.4.1185.

Tollenaar, M. (1977). Sink-source relationships during reproductive development in maize. A review. *Maydica* 22, 49–75.

Tolley-Henry, L., and Raper, D. (1991). Soluble carbohydrate allocation to roots, photosynthetic rate of leaves, and nitrate assimilation as affected by nitrogen stress and irradiance. *Bot. Gaz.* 152, 23–33.

Triboi, E., and Triboi-Blondel, A. M. (2002). Productivity and grain or seed composition: A new approach to an old problem - Invited paper. *Eur. J. Agron.* 16, 163–186. doi:10.1016/S1161-0301(01)00146-0.

Tsai, C. Y., Huber, D. M., Warren, H. L., and Lyznik, A. (1991). Nitrogen uptake and redistribution during maturation of maize hybrids. *J. Sci. Food Agric.* 57, 175–187. doi:10.1002/jsfa.2740570204.

Uhart, S. A., and Andrade, F. H. (1995). Nitrogen and carbon accumulation and remobilization during grain filling in maize under different source/sink ratios. *Crop Sci.* 35, 183–190. doi:10.2135/cropsci1995.0011183X003500010034x.

Uribelarrea, M., Crafts-Brandner, S. J., and Below, F. E. (2009). Physiological N response of field-grown maize hybrids (Zea mays L.) with divergent yield potential and grain protein concentration. *Plant Soil* 316, 151–160. doi:10.1007/s11104-008-9767-1.

Yang, L., Guo, S., Chen, Q., Chen, F., Yuan, L., and Mi, G. (2016). Use of the stable nitrogen isotope to reveal the source-sink regulation of nitrogen uptake and remobilization during grain filling phase in maize. *PLoS One* 11, 1–16. doi:10.1371/journal.pone.0162201.

2.8 Tables and Figures

Table 2.1. Cumulative thermal time (growing degree days, GDD) and cumulative available water (rainfall plus irrigation, mm) for four key periods during the 2016 and 2017 growing seasons. R1 and R3 data reflect the biomass sampling date, while R6 data was estimated by black layer observations. Data shown correspond to daily records averaged from two nearby weather stations: WANATAH 2 WNW (La Porte, IN) and KNOX WWTP (Starke, IN).

	Planting-V12			**V12-R1**			**R1-R3**			**R3-R6**		
	days	GDD	mm	days	GDD	mm	days	GDD	mm	days	GDD	mm
2016	65	614	224	18	239	66	14	225	87	40	585	365
2017	51	611	134	15	211	79	19	247	96	47	493	84

Table 2.2. ANOVA for plant components and total-plant dry matter at silking (R1), at the onset of linear grain fill (R3), and at maturity (R6) in 2016 and 2017. All grain data is expressed at 0% moisture. Whole-ear data (grains and cob together) is reported at R3 for 2016. Grain and cob data are reported separately at R3 for 2017.

	Dry Matter at Silking (Mg ha^{-1})				**Dry Matter at R3 Stage (Mg ha^{-1})**					**Dry Matter at Maturity (Mg ha^{-1})**				
	Leaf	**Stem**	**Ear**	**Total**	**Leaf**	**Stem**	**Ear/Grain**	**Cob**	**Total**	**Leaf**	**Stem**	**Grain**	**Cob**	**Total**
Season 2016														
N Timing Application														
Planting	3.81	6.81	0.04	10.7	4.82	8.61 a	1.77	-	15.2	4.34	5.12	10.8 ab	1.28	21.5 a
Planting_V6	3.70	6.75	0.04	10.5	4.68	8.19 b	1.72	-	14.6	4.23	5.13	10.1 b	1.26	20.7 b
Planting_V12	3.68	6.55	0.05	10.3	4.75	8.07 b	1.81	-	14.6	4.22	5.15	11.1 a	1.30	21.8 a
N Rate (kg N ha^{-1})														
0N	3.03 c	5.57 c	0.02 c	8.6 c	3.63 c	7.05 c	0.82 c	-	11.5 c	3.58 c	4.38 c	4.5 c	0.76 c	13.2 c
112N	3.62 b	6.67 b	0.04 b	10.2 b	4.79 b	8.20 b	1.81 b	-	14.8 b	4.10 b	5.09 b	11.1 b	1.27 b	21.5 b
168N	3.98 a	7.12 ab	0.05 ab	11.2 a	5.05 a	8.71 ab	1.96 ab	-	15.7 a	4.43 ab	5.31 ab	12.0 ab	1.42 a	23.1 ab
224N	4.01 a	7.03 ab	0.06 a	11.1 a	5.21 a	8.83 a	2.14 a	-	16.2 a	4.58 a	5.53 a	12.9 a	1.48 a	24.5 a
280N	4.02 a	7.14 a	0.05 ab	11.2 a	5.06 a	8.66 ab	2.10 ab	-	15.8 a	4.64 a	5.37 ab	12.9 a	1.50 a	24.4 a
F-test														
N Timing (T)	ns	ns	ns	ns	ns	0.013	ns	-	ns	ns	ns	0.04	ns	0.003
N Rate (R)	<.001	<.001	<.001	<.001	<.001	<.001	<.001	-	<.001	<.001	<.001	<.001	<.001	<.001
T x R	ns	ns	ns	ns	ns	ns	ns	-	ns	ns	ns	ns	ns	ns
Season 2017														
N Timing Application														
Planting	3.50	6.11 a	0.18	9.78	4.19	6.94	1.94	1.26	14.3	4.03 a	4.23	11.5	1.25	21.0
Planting_V6	3.46	6.02 ab	0.17	9.65	4.15	7.01	1.95	1.28	14.4	4.10 a	4.25	11.9	1.24	21.5
Planting_V12	3.22	5.58 b	0.14	8.93	4.18	6.75	1.88	1.28	14.1	3.73 b	3.96	11.3	1.22	20.2
N Rate (kg N ha^{-1})														
0N	2.45 b	4.61 b	0.04 b	7.1 b	3.10 b	5.61 b	0.68 c	0.73 b	10.1 b	2.85 c	2.77 c	5.1 d	0.64 c	11.4 d
112N	3.68 a	6.43 a	0.21 a	10.3 a	4.41 a	7.18 a	2.09 ab	1.38 a	15.1 a	4.14 b	4.24 b	11.7 c	1.30 b	21.4 c
168N	3.55 a	6.05 a	0.18 a	9.8 a	4.29 a	7.23 a	1.95 b	1.37 a	14.8 a	4.10 b	4.50 ab	12.8 b	1.38 ab	22.8 bc
224N	3.71 a	6.27 a	0.22 a	10.2 a	4.54 a	7.22 a	2.44 ab	1.44 a	15.3 a	4.21 ab	4.51 ab	13.8 a	1.41 ab	24.0 ab
280N	3.57 a	6.16 a	0.16 a	9.9 a	4.54 a	7.27 a	2.46 a	1.45 a	15.7 a	4.45 a	4.71 a	14.3 a	1.45 a	24.9 a
F-test														
N Timing (T)	ns	0.095	ns	ns	ns	ns	ns	ns	ns	0.038	ns	ns	ns	ns
N Rate (R)	<.001	<.001	<.001	<.001	<.001	<.001	<.001	<.001	<.001	<.001	<.001	<.001	<.001	<.001
T x R	ns	ns	ns	ns	ns	ns	ns	ns	ns	ns	ns	ns	ns	ns

ns: not significant at α=0.05, p-value for F-test is >0.05. Means separation determined by Fisher's least significant difference (LSD) at α=0.05. Same letter or absence of letter means no significant differences were found among levels. For all variables, three replicates were collected (n=3), except for those at R6 in 2016 (n=4).

Table 2.3. ANOVA for plant components and total-plant N concentration at silking (R1), at the onset of linear grain fill (R3), and at maturity (R6) in 2016 and 2017. Whole-ear data (grains and cob together) is reported at R3 for 2016. Grain and cob data are reported separately at R3 for 2017.

	N Concentration at Silking (%)				**N Concentration at R3 Stage (%)**					**N Concentration at Maturity (%)**				
	Leaf	**Stem**	**Ear**	**Total**	**Leaf**	**Stem**	**Ear/Grain**	**Cob**	**Total**	**Leaf**	**Stem**	**Grain**	**Cob**	**Total**
Season 2016														
N Timing Application														
Planting	2.58	0.80	3.22	1.44	1.99	0.57	1.54	-	1.13	0.94	0.60	0.98	0.53	0.85
Planting_V6	2.46	0.84	3.28	1.42	2.04	0.61	1.44	-	1.15	0.90	0.63	0.99	0.52	0.86
Planting_V12	2.56	0.77	3.39	1.42	2.09	0.61	1.45	-	1.18	0.82	0.58	0.98	0.54	0.82
N Rate (kg N ha^{-1})														
0N	1.45 c	0.39 d	3.36	0.77 c	1.07 c	0.30 d	1.42	-	0.62 d	0.53 d	0.47 b	0.74 c	0.65	0.59 d
112N	2.60 b	0.69 c	3.35	1.37 b	1.99 b	0.48 c	1.51	-	1.09 c	0.81 c	0.51 b	0.97 b	0.44	0.80 c
168N	2.86 a	0.89 b	3.22	1.60 a	2.31 a	0.65 b	1.50	-	1.29 b	0.96 b	0.64 a	1.05 a	0.55	0.91 b
224N	2.85 a	1.01 a	3.26	1.68 a	2.36 a	0.77 a	1.54	-	1.38 a	1.06 ab	0.67 a	1.10 a	0.47	0.96 a
280N	2.90 a	1.02 a	3.30	1.71 a	2.46 a	0.77 a	1.42	-	1.40 a	1.09 a	0.72 a	1.09 a	0.54	0.98 a
F-test														
N Timing (T)	ns	ns	ns	ns	ns	ns	ns	-	ns	ns	ns	ns	-	ns
N Rate (R)	<.001	<.001	ns	<.001	<.001	<.001	ns	-	<.001	<.001	<.001	<.001	-	<.001
T x R	ns	ns	ns	ns	ns	ns	ns	-	ns	ns	ns	ns	-	ns
Season 2017														
N Timing Application														
Planting	2.48	0.86	3.15	1.47	1.66	0.47	1.48	0.83	0.97 c	0.89	0.43	1.13	0.54	0.91
Planting_V6	2.52	0.94	3.10	1.54	1.68	0.53	1.47	0.80	0.99 b	0.95	0.47	1.16	0.49	0.94
Planting_V12	2.45	0.93	3.13	1.51	1.74	0.50	1.47	0.85	1.02 a	0.92	0.43	1.15	0.56	0.93
N Rate (kg N ha^{-1})														
0N	1.75 b	0.48 c	3.13	0.93 c	0.90 c	0.27 d	1.46	0.83	0.58 c	0.61 d	0.33 c	0.80 d	0.56	0.62 d
112N	2.66 a	0.81 b	3.01	1.51 b	1.80 b	0.42 c	1.44	0.80	0.99 b	078 c	0.38 bc	1.11 c	0.45	0.86 c
168N	2.69 a	1.03 a	3.24	1.67 ab	1.75 b	0.49 b	1.54	0.87	1.02 b	0.92 b	0.42 b	1.21 b	0.50	0.96 b
224N	2.84 a	1.10 a	3.07	1.79 a	1.82 ab	0.65 a	1.47	0.81	1.16 a	1.13 a	0.53 a	1.29 a	0.54	1.08 a
280N	2.49 a	1.14 a	3.18	1.64 ab	2.09 a	0.68 a	1.47	0.83	1.23 a	1.15 a	0.55 a	1.31 a	0.60	1.10 a
F-test														
N Timing (T)	ns	ns	ns	ns	ns	ns	ns	ns	0.006	ns	ns	ns	-	ns
N Rate (R)	<.001	<.001	ns	<.001	<.001	<.001	ns	ns	<.001	<.001	<.001	<.001	-	<.001
T x R	ns	ns	ns	ns	ns	ns	ns	ns	ns	ns	ns	ns	-	ns

ns: not significant at α=0.05, p-value for F-test is >0.05. Means separation determined by Fisher's least significant difference (LSD) at α=0.05. Same letter or absence of letter means no significant differences were found among levels. Cob N concentration was analyzed in only one rep at R6. For all variables, three replicates were collected (n=3), except for those at R6 in 2016 (n=4).

Table 2.4. ANOVA for plant components and total-plant N content at silking (R1), at the onset of linear grain fill (R3), and at maturity (R6) in 2016 and 2017. Whole-ear data (grains and cob together) is reported at R3 for 2016. Grain and cob data are reported separately at R3 for 2017.

	N Uptake at Silking (kg N ha^{-1})				N Uptake at R3 Stage (kg N ha^{-1})					N Uptake at Maturity (kg N ha^{-1})				
	Leaf	**Stem**	**Ear**	**Total**	**Leaf**	**Stem**	**Ear/Grain**	**Cob**	**Total**	**Leaf**	**Stem**	**Grain**	**Cob**	**Total**
Season 2016														
N Timing Application														
Planting	100.6 a	55.5	1.40	157.5	98.2	49.5	27.3	-	175.0	41.8	31.2	109.9	6.78	189.7
Planting_V6	92.6 b	58.0	1.29	151.9	98.6	51.2	24.8	-	174.5	39.0	33.1	104.5	6.72	183.0
Planting_V12	96.8 ab	51.8	1.53	150.2	102.4	50.4	25.9	-	178.6	35.5	30.2	113.9	6.46	186.3
N Rate (kg N ha^{-1})														
0N	44.0 c	21.9 d	0.43 c	66.3 c	39.3 c	20.9 d	11.5 c	-	71.7 d	18.8 d	20.7 b	33.6 d	4.85 d	77.9 d
112N	94.7 b	46.5 c	1.36 b	142.5 b	95.3 b	39.3 c	26.9 b	-	161.5 c	33.7 c	26.0 b	107.2 c	5.57 c	172.5 c
168N	113.8 a	63.4 b	1.61 b	178.8 a	116.7 a	56.9 b	28.9 ab	-	202.5 b	42.5 b	34.2 a	125.4 b	7.72 a	209.7 b
224N	114.0 a	70.8 ab	1.66 ab	186.7 a	122.6 a	67.7 a	29.7 ab	-	223.1 a	48.6 ab	37.4 a	139.2 ab	7.01 b	234.9 a
280N	116.9 a	73.1 a	1.98 a	191.7 a	124.6 a	66.9 a	32.9 a	-	221.2 a	50.4 a	39.2 a	141.9 a	8.12 a	236.8 a
F-test														
N Timing (T)	0.077	ns	ns	ns	ns	ns	ns	-	ns	ns	ns	ns	ns	ns
N Rate (R)	<.001	<.001	ns	<.001	<.001	<.001	<.001	-	<.001	<.001	<.001	<.001	<.001	<.001
R x T	ns	ns	ns	ns	ns	ns	ns	-	ns	ns	ns	ns	ns	ns
Season 2017														
N Timing Application														
Planting	89.6	54.3	5.39	149.3	72.0	33.5	28.2	10.3	144.1	36.9	18.7 b	136.2	6.67 a	198.5
Planting_V6	89.7	57.9	5.34	153.0	72.1	38.0	28.3	10.2	148.6	39.9	20.3 a	144.8	6.08 b	211.1
Planting_V12	81.2	53.7	4.28	139.2	74.3	34.9	27.9	10.9	147.9	35.0	17.3 c	134.5	6.84 a	193.7
N Rate (kg N ha^{-1})														
0N	44.2 b	22.2 c	1.18 b	67.7 b	28.1 d	14.9 c	9.8 d	5.9 c	58.7 c	17.4 d	9.0 c	40.8 d	3.59 d	70.8 d
112N	98.2 a	52.4 b	6.26 a	156.8 a	79.1 bc	30.0 b	29.8 bc	10.9 b	149.9 b	32.5 c	16.1 b	130.2 c	5.85 c	184.6 c
168N	96.0 a	62.4 ab	5.85 a	164.3 a	75.2 c	35.4 b	29.1 c	11.9 a	151.6 b	37.9 b	18.5 b	155.1 b	6.99 b	218.5 b
224N	105.1 a	70.9 a	6.57 a	182.5 a	86.8 ab	47.0 a	35.9 ab	11.6 ab	181.3 a	47.6 a	24.2 a	178.6 a	7.62 b	258.0 a
280N	90.7 a	68.7 a	5.16 a	164.5 a	94.9 a	50.0 a	36.1 a	12.0 a	193.0 a	51.1 a	25.9 a	187.7 a	8.62 a	273.4 a
F-test														
N Timing (T)	ns	ns	ns	ns	ns	ns	ns	ns	ns	ns	0.004	ns	0.026	ns
N Rate (R)	<.001	<.001	<.001	<.001	<.001	<.001	<.001	<.001	<.001	<.001	<.001	<.001	<.001	<.001
R x T	ns	ns	ns	ns	ns	ns	ns	ns	ns	ns	ns	ns	ns	ns

ns: not significant at α=0.05, p-value for F-test is >0.05. Means separation determined by Fisher's least significant difference (LSD) at α=0.05. Same letter or absence of letter means no significant differences were found among levels. For all variables, three replicates were collected (n=3), except for those at R6 in 2016 (n=4).

Table 2.5. ANOVA for nitrogen nutrition index at silking (NNI_{R1}), nitrogen nutrition index at the onset of linear grain fill (NNI_{R3}), grain yield at 15.5% moisture (GY), kernel number (KN), kernel weight at 0% moisture (KW), harvest index (HI), nitrogen harvest index (NHI), nitrogen recovery efficiency (NRE), and nitrogen internal efficiency (NIE) in 2016 and 2017.

	NNI_{R1}	**NNI_{R3}**	**GY (Mg ha^{-1})**	**KN (grain m^{-2})**	**KW (mg grain^{-1})**	**HI**	**NHI**	**NRE**	**NIE**
Season 2016									
N Timing Application									
Planting	1.03	0.91	9.9	3870	279	0.49	0.56	0.73	54
Planting_V6	1.00	0.93	10.4	3629	283	0.47	0.55	0.67	56
Planting_V12	0.99	0.95	11.0	3916	284	0.49	0.58	0.76	69
N Rate (kg N ha^{-1})									
0N	0.50 c	0.45 d	2.7 c	2033 b	232 d	0.34 b	0.42 b	-	-
112N	0.96 b	0.87 c	10.5 b	4170 a	276 c	0.51 a	0.62 a	0.83 a	74 a
168N	1.15 a	1.05 b	12.6 a	4080 a	297 b	0.52 a	0.60 a	0.78 a	57 b
224N	1.21 a	1.14 a	13.0 a	4352 a	293 b	0.53 a	0.60 a	0.70 a	54 b
280N	1.23 a	1.14 a	13.4 a	4391 a	314 a	0.52 a	0.59 a	0.57 b	52 b
F-test									
N Timing (T)	ns	ns	ns	ns	ns	ns	ns	ns	ns
N Rate (R)	<.001	<.001	<.001	<.001	<.001	<.001	<.001	<.001	<.001
T x R	ns	Ns	ns	ns	ns	ns	ns	ns	ns
Season 2017									
N Timing Application									
Planting	1.02	0.77 b	12.1	4198	277 b	0.54	0.67	0.84	53
Planting_V6	1.06	0.79 ab	12.9	4166	289 a	0.54	0.67	0.96	52
Planting_V12	1.01	0.81 a	12.6	4208	278 b	0.55	0.68	0.79	48
N Rate (kg N ha^{-1})									
0N	0.57 b	0.40 c	5.3 d	2552 b	213 d	0.45 c	0.57 c	-	-
112N	1.06 a	0.80 b	11.9 c	4547 a	271 c	0.54 b	0.70 ab	1.02 a	59 a
168N	1.14 a	0.81 b	14.1 b	4542 a	294 b	0.56 a	0.71 a	0.88 b	53 b
224N	1.24 a	0.94 a	15.7 a	4597 a	314 a	0.58 a	0.69 ab	0.84 bc	47 c
280N	1.13 a	1.00 a	15.6 a	4716 a	315 a	0.57 a	0.68 b	0.72 c	46 c
F-test									
N Timing (T)	ns	0.089	ns	ns	0.017	ns	ns	ns	ns
N Rate (R)	<.001	<.001	<.001	<.001	<.001	<.001	<.001	<.001	<.001
T x R	ns	ns	<.001	ns	ns	ns	ns	ns	ns

ns: not significant at α=0.05, p-value for F-test is >0.05. Means separation determined by Fisher's least significant difference (LSD) at α=0.05. Same letter or absence of letter means no significant differences were found among levels. For all 2017 variables, three replicates were collected (n=3). For all 2016 variables, four replicates were collected (n=4), except for NNI_{R1} and NNI_{R3} (n=4).

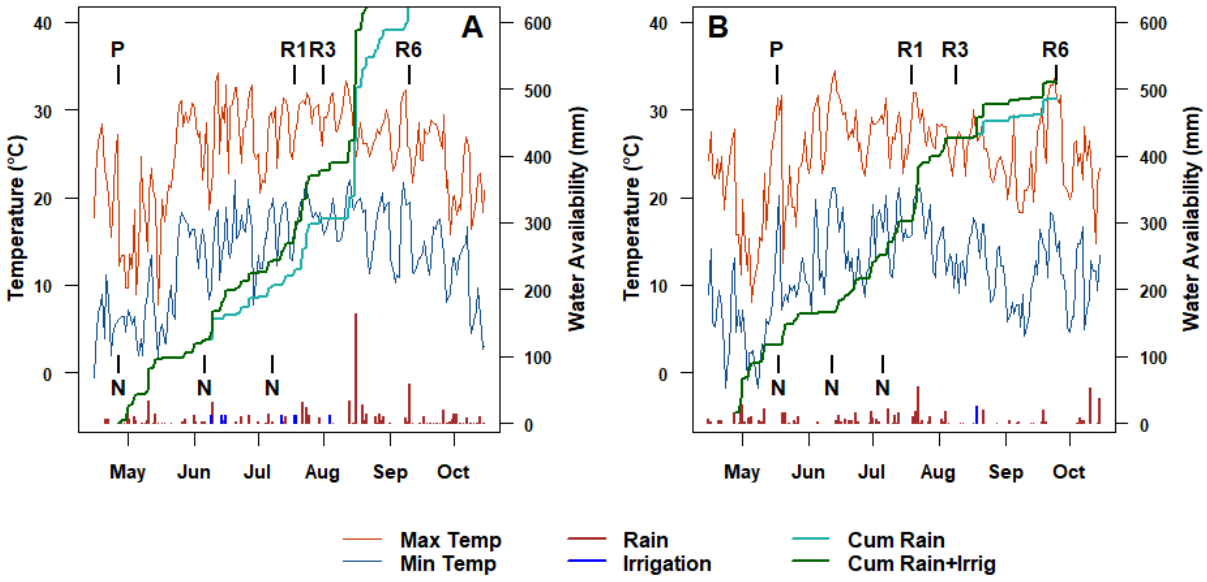

Figure 2.1. Weather conditions for the experimental site during the 2016 (A) and 2017 (B) growing seasons. Plotted are the daily records between April 15th and October 15th averaged from two nearby weather stations: WANATAH 2 WNW (La Porte, IN) and KNOX WWTP (Starke, IN). Top black, vertical lines point to planting (P) and reproductive phenological stages (R1, R3, R6), while bottom black, vertical lines point to the three N fertilizer applications performed. Red and blue thinner lines indicate maximum and minimum daily temperatures, respectively, sharing the left Y axis. Water availability is shown on the right Y axis. Daily rainfall and irrigation values are represented by thicker red and blue vertical bars, respectively. Cumulative precipitation (since April 27th) and cumulative total water availability (rainfall plus irrigation) are denoted by light green and dark green lines, respectively.

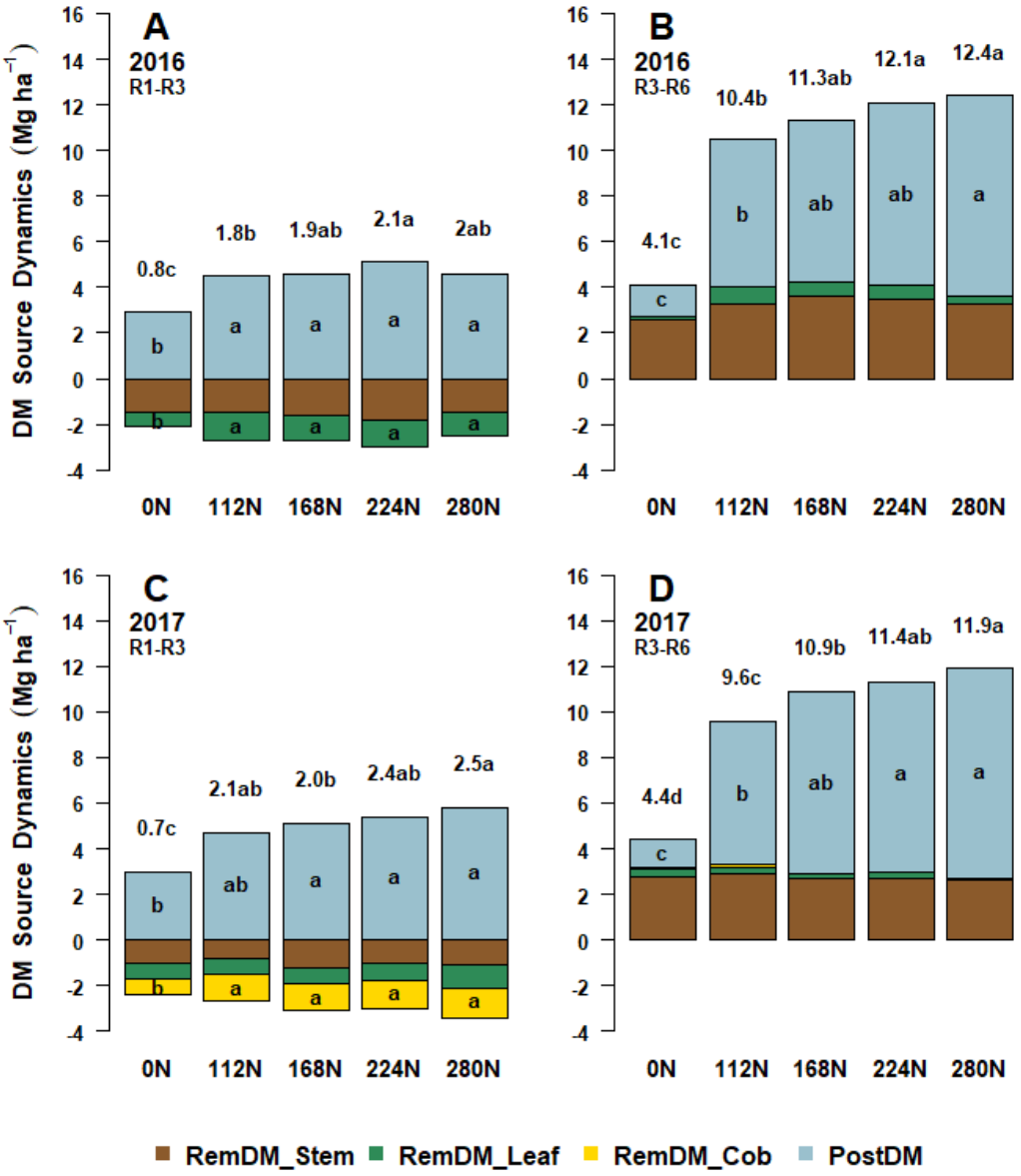

Figure 2.2. Effect of N rate on dry matter (DM) dynamics during the reproductive period in maize. Top figures show DM remobilization from leaf and stem and total-plant post-silking DM production from R1 to R3 (A) and from R3 to R6 (B) in 2016. Bottom figures show DM remobilization from leaf, stem, and cob, and total-plant post-silking DM accumulation from R1 to R3 (C) and from R3 to R6 (D) in 2017. Values on top of each bar represent DM balance, i.e., net dry matter allocated to the ear (2016) or the grain (2017) in each period. Plotted N rate means represent the average of three timing application treatments by three replications (n=9, N=45). Brown portions of the bars represent DM remobilization from stem (RemDM_Stem). Green portions of the bars represent DM remobilization from leaves (RemDM_Leaf). Only in 2017, yellow portions of the bars represent DM remobilization from cobs (RemDM_Cob). Blue portions of the bars represent total-plant post-silking DM accumulation (PostDM). Mean separation analyses were based on Fisher's LSD (α=0.05), and only those significant are shown.

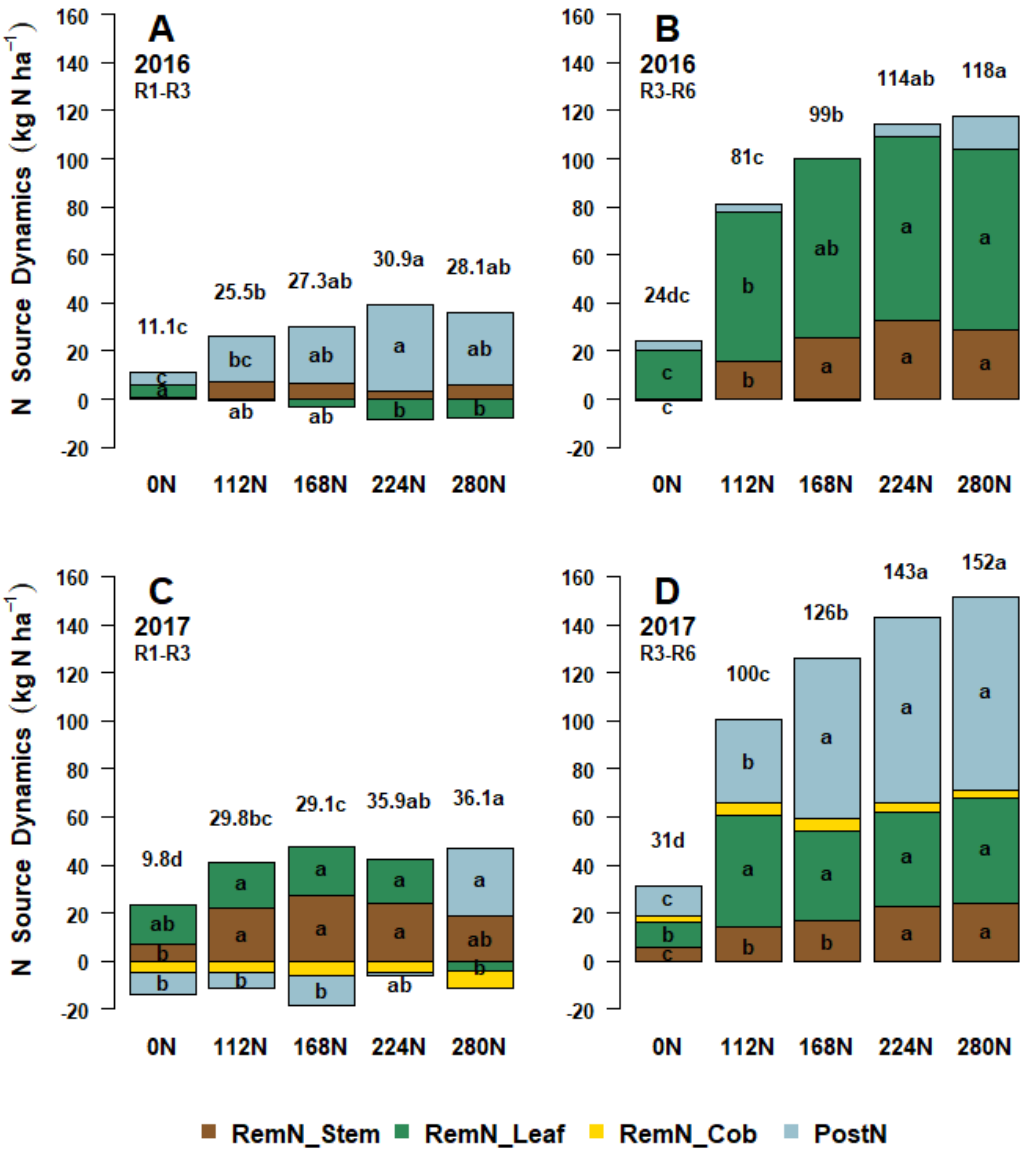

Figure 2.3. Effect of N rate on N dynamics during the reproductive period in maize. Top figures show N remobilization from leaf and stem and total-plant post-silking N uptake from R1 to R3 (A) and from R3 to R6 (B) in 2016. Bottom figures show N remobilization from leaf, stem, and cob, and total-plant post-silking N uptake from R1 to R3 (C) and from R3 to R6 (D) in 2017. Values on top of each bar represent N balance, i.e., net N allocated to the ear (2016) or the grain (2017) in each period. Plotted N rate means represent the average of three timing application treatments by three replications (n=9, N=45). Brown portions of the bars represent N remobilization from stem (RemN_Stem). Green portions of the bars represent N remobilization from leaves (RemN_Leaf). Only in 2017, yellow portions of the bars represent N remobilization from cobs (RemDM_Cob). Blue portions of the bars represent total-plant post-silking N uptake (PostN). Mean separation analyses were based on Fisher's LSD (α=0.05), and only those significant are shown.

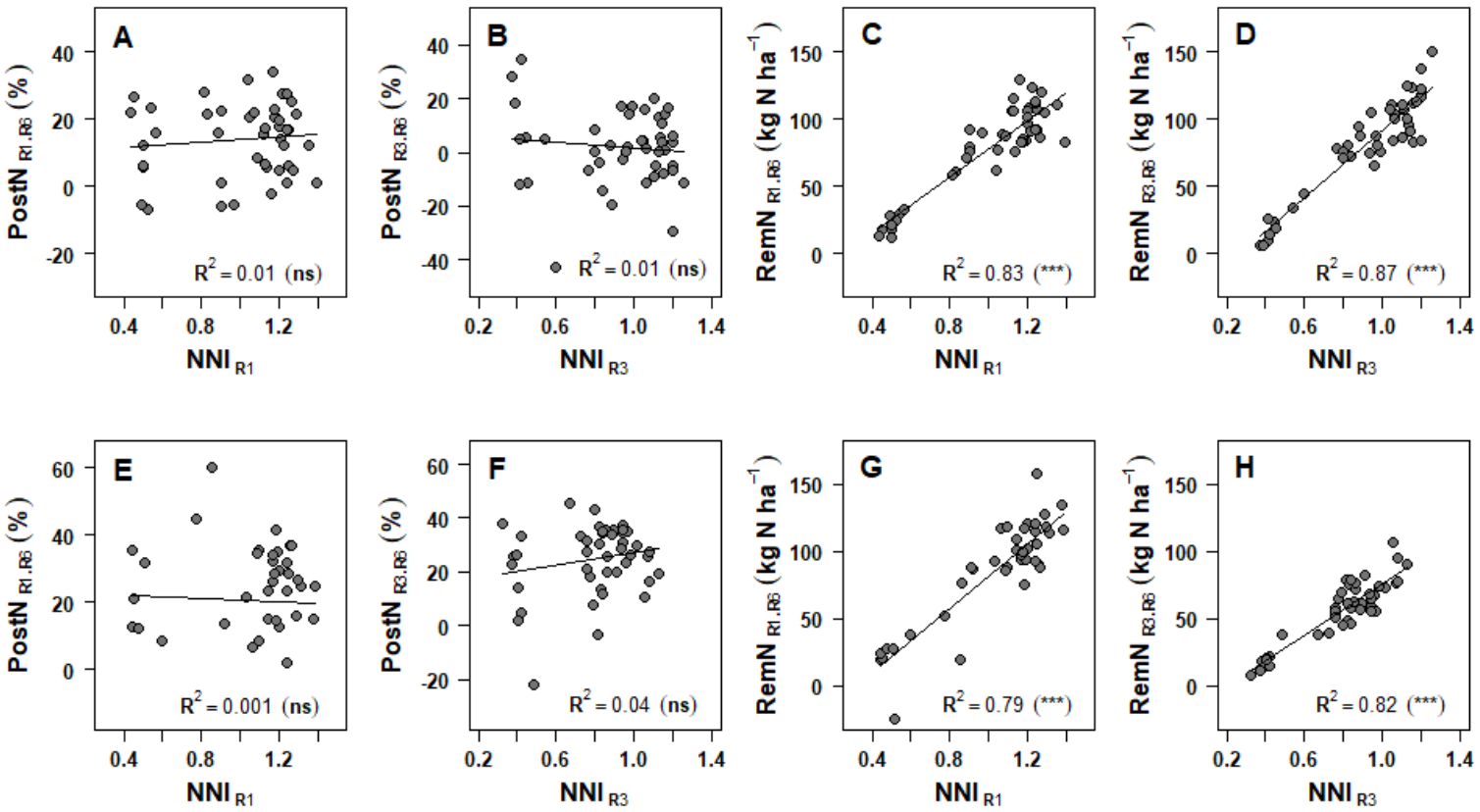

Figure 2.4. Relationship between nitrogen nutrition index and N dynamics during the reproductive period in maize. Top figures (A, B, C, D) show relationships for the 2016 growing season. Bottom figures (E, F, G, H) show relationships for the 2017 growing season. $PostN_{R1.R6}$: total-plant post-R1 N uptake expressed as percentage of total N uptake. $PostN_{R3.R6}$: total-plant post-R3 N uptake expressed as percentage of total N uptake. $RemN_{R1.R6}$: apparent N remobilization from R1 to R6. $RemN_{R3.R6}$: apparent N remobilization from R3 to R6. Points represent data on a per plot basis from (N=45), coming from each combination of three N timing applications with five N rates over three replicates. Lines represent the linear fit obtained by regression analysis. R^2 for each regression is shown, as well as the significance of whether the slope is different from zero shown between brackets. (ns): p-value>0.05. (***): p-value<0.001.

CHAPTER 3. NITROGEN'S ROLE IN ENDOSPERM CELL AND ASSOCIATED KERNEL WEIGHT DETERMINATION DURING THE LAG PHASE DEVELOPMENT IN MAIZE

3.1 Abstract

As kernel weight (KW) has proven to be an increasingly important driver behind grain yield (GY) variability in modern maize hybrids, nitrogen's (N) role in the determination of individual sink capacity (i.e., potential KW) during the lag phase of reproductive development remains unclear. The research objective was to study the relationship between endosperm cell number (ECN) during the lag phase and final KW under field experiments testing 3 to 4 N rates at different plant densities or N timing applications over a 3-year period. Low N treatments consistently reduced ECN at 9, 10, 13, and 17 days after silking (DAS), thereby limiting KW during this early post-silking stage. Final KW responses to N management were always explained by ECN, though the strength of the relation changed with the experiment and the relative DAS sampling time. Nitrogen rate effects on potential KW were not associated with plant growth rate per kernel during the critical period bracketing silking. ECN was highly correlated with ear N allocation rate during the lag phase. Overall, these results show that higher N availability, independently of N timing and plant density, increased final KW by enhancing individual kernel sink capacity via gains in ECN during lag-period development.

Keywords: critical period, ear nitrogen allocation rate, endosperm cell number, kernel weight, lag period, maize, nitrogen, plant growth rate.

Abbreviations: EGR, ear growth rate; ENAR, ear nitrogen allocation rate; ECN, endosperm cell number; DAS, days after silking; GY, grain yield; KW, kernel weight; N, nitrogen; PGR, plant growth rate; PNUR, plant nitrogen uptake rate.

3.2 Introduction

Maize grain yield (GY) is determined by the number of kernels harvested per unit area and the individual kernel weight (Poneleit and Egli, 1979). Although genetic yield improvement over time has historically been mostly attributed to increases in kernel number (KN) (Tollenaar et al., 1992; Echarte et al., 2000; Luque et al., 2006; Haegele et al., 2013; Di Matteo et al., 2016), recent ERA studies testing U.S. maize germplasm have revealed a bigger role for kernel weight (KW). For example, Chen et al. (2016) compared Dekalb hybrids released over a 38-year time span (1967-2005) and found that KW, rather than KN, was the primary component driving yield improvement. Furthermore, other ERA studies involving Pioneer hybrids over a 79-year period (1934-2013; DeBruin et al., 2017) and a 70-year time span (1946-2015; Mueller et al., 2019) showed that KW was more responsible than KN for the GY increases in the last 3-4 decades. This change in the main component associated with yield improvement raises several questions concerning how management and environmental factors may impact the enhanced kernel weights in those more recently released maize hybrids. In that context, the potential to accommodate assimilates by reproductive tissues (i.e. sink capacity) (Tollenaar, 1977) at the individual kernel scale (i.e. potential KW) is of particular interest to further understand the resource dynamics that lead to changes in grain yield by adjusting KW.

Potential KW is determined during the lag phase, the first stage of the grain-filling period occurring right after fertilization (Duncan et al., 1965; Johnson and Tanner, 1972). Final KN determination therefore overlaps with establishing their potential weights. During this early phase, grain tissues undergo active cell division and differentiation (Olsen et al., 1999; Sabelli and Larkins, 2009b; Leroux et al., 2014) with rapid increase in water content but negligible grain dry matter gain. While the embryo comprises only 10-15% of the total KW at maturity, the endosperm is the major source of stored reserves within the mature maize grain, being responsible for almost 80-90% of final kernel weight (Jones and Brenner, 1987; Myers et al., 1990; Singletary and Below, 1990; Zhang and Kaeppler, 2017). Because the level of cell division during this early stage places an upper limit on the amount of storage material synthesized at subsequent stages of grain development (Setter and Flannigan, 1989; Zhang and Kaeppler, 2017; Olsen, 2020), the number of endosperm cells (ECN) formed in this phase is a determinant of kernel sink capacity (Reddy and Daynard, 1983; Jones et al., 1985, 1996; Zhang and Kaeppler, 2017).

Although potential sink capacity is genetically determined, endosperm development has proven to be highly sensitive to changes in environmental conditions during the lag phase (Jones and Simmons, 1983; Setter and Flannigan, 1989; Ober et al., 1991; Artlip et al., 1995; Commuri and Jones, 2001; Engelen-Eigles et al., 2001). In addition, declines in ECN have been well correlated with decreases in final KW (Egharevba et al., 1976; Jones and Simmons, 1983; Reddy and Daynard, 1983; Jones et al., 1985, 1996). Despite that background literature, few studies have considered nitrogen (N) availability effects on potential KW via endosperm analysis. Based on the Lemaire and Millard (1999) sink model for meristems, N substrates are first required for cell division processes such as DNA replication and protein synthesis (Berger, 1999; Olsen et al., 1999), and then the cells thus divided are responsible for the later-season C substrate demand for expansion (i.e. linear grain filling in kernels). Hence, N supply may have a direct influence on endosperm development during the lag phase, affecting final kernel weight at this early stage. While Cazetta et al. (1999) found evidence of this direct N effect by detecting increases in ECN at 14 days after pollination, this was found in *in-vitro* cultured kernels grown under increasing N concentration media. Under field experimental conditions, Lemcoff and Loomis (1994) tested N rate and plant density treatments on ECN, though a common density used at planting was only lowered at silking by thinning in half of the plots. These authors found increases in ECN only at 25 DAS (days after silking), with the higher of the two N rates they investigated, under the higher plant density (i.e., 7.3 plants m^{-2}). N rate effects on ECN were not detected at the lower density (i.e., 3.7 plants m^{-2}).

Results from field studies on N consequences for potential KW, examined from a crop scale or via linear grain-filling period parameters, are inconsistent. In one example of the crop-scale approach, Hisse et al. (2019) found that soil N availability differences did not change potential KW when they analyzed source-sink interactions during the critical period employing the Gambín et al. (2006) model (i.e., relationship between KW and plant growth rate -PGR- per kernel during the critical period). In an example of the second approach, Melchiori and Caviglia (2008) reported increases in maximum kernel water content, a predictor of potential KW (Borrás and Westgate, 2006), under higher soil N supply. Additionally, Nasielski and Deen (2019), utilizing both approaches, found that potential KW could be reduced by soil N deficits resulting from low N rates and late N timing applications. To the best of our knowledge, there have been no prior studies on potential KW determination in field-grown maize that addressed both the direct N availability

effects on endosperm cell development and the indirect N impacts on resource availability per kernel during the critical period. Therefore, the objectives of this study were: 1) to determine the effect of soil N availability on potential KW via the analysis of ECN during the lag phase, and 2) to test the effects of N availability on potential KW through resource availability per kernel during the critical period centered on silk emergence.

3.3 Materials and Methods

3.3.1 Field Experiments

Three field experiments were conducted to determine the effect of soil N availability on ECN formed during the lag phase, resource availability per grain during the critical period, and final KW in one common genotype (hybrid DKC63-60RIB GENSS, Dekalb, commercially released in 2015). In order to generate a wide gradient of N conditions around the lag phase, the experiments involved combinations of N rate, N timing application and plant density treatments in two locations and three seasons.

Experiment 1 was planted on 16 May 2017 at the Purdue Rice Farm in LaCrosse, IN on a Gilford fine sandy loam soil (coarse-loamy, mixed, superactive, mesic Typic Endoaquolls) (USDA Web Soil Survey). The field had center pivot irrigation. This study used a common seeding rate of 8.3 plants m^{-2}, and plots were 12 rows wide (0.76 m rows) and 228-m long. Plots also received 17 kg N ha^{-1} and 6 kg P ha^{-1} as band-applied starter fertilizer (19-17-0), and were provided with supplementary sprinkler irrigation when needed.

Experiments 2 and 3 were part of a two-year field study conducted during the 2018 and 2019 growing seasons, respectively, at the Purdue Agronomy Center of Research and Education (ACRE) in West Lafayette, IN. To guarantee genetic purity for each plant subsequently sampled, the 5% refuge seed (i.e. without the transgenic insect tolerance) was removed prior to planting. In 2018, the soil type was Chalmers silty clay loam (fine-silty, mixed, superactive, mesic Typic Endoaquolls). In 2019, the soil type was predominantly Drummer silty clay loam (fine-silty, mixed, superactive, mesic Typic Endoaquolls), with small portions of Raub-Brenton complex (fine-silty, mixed, superactive, mesic Aquic Argiudolls) and Toronto-Millbrook complex (fine-silty, mixed, superactive, mesic Udollic Epiaqualfs) (USDA Web Soil Survey). Experiment 2 was planted on 8 May 2018 and Experiment 3 was planted on 3 June 2019. Persistent precipitation

during May prevented us from planting on an earlier date in 2019. Plots were 4-row wide (0.76 m row spacing) and 14.5-m long. Neither irrigation nor starter fertilizer was supplied.

In all three experiments, plots were arranged in a split-plot structure in a three-replicate randomized complete block design (n=3). Experiment 1 tested three N timing applications as whole plots and three N rates as subplots (N=27). The N timing treatments were: all N applied at planting, half of the total N rate applied at planting plus the other half applied at the V6 stage, and the majority of N applied at planting with the last 56 kg N ha-1 applied at the V12 stage. The total N rates in all timing treatments were: 0, 112, and 224 kg N ha^{-1}. In Experiments 2 and 3, four N rate treatments (all applied at planting) were studied as whole plots and two plant densities as subplots (N=24). The N rates were: 0, 84, 168, and 224 kg N ha^{-1}. The plant densities were: 7.9 and 10.4 plants m^{-2}.

Across experiments, all N treatments were applied as 28% urea ammonium nitrate (UAN). At-planting and V6 N applications were coulter-injected into soil between rows, while V12 sidedress was surface-banded along both sides of maize rows using 360 Yield Center Y-Drops (360 Yield Center, Morton, IL) on a high clearance applicator. Pesticide management practices followed Purdue University recommendations, and all plots were kept weed-free.

Daily records of air maximum temperature (t_{max}), air minimum temperature (t_{min}), and precipitation were obtained for each growing season. Since the Purdue Rice Farm does not have a weather station, we utilized data from two nearby stations: "Wanatah 2 WNW" (La Porte, IN) and "Knox WWTP" (Starke, IN) (NOAA National Centers for Environmental Information) and averaged them in order to report weather data for Exp. 1. For Exp. 2 and 3, we collected data from the on-site station "ACRE-West Lafayette" (INClimate - The Indiana State Climate Office). Thermal time (*TT*, °Cd) was calculated on a daily basis (*Equation 3.1*) using 8°C as base temperature (t_b) (Ritchie and Nesmith, 1991) and then accumulated throughout the growing season starting at planting.

$$\boldsymbol{TT = \frac{(t_{max} - t_{min})}{2} - t_b} \qquad \text{Equation 3.1}$$

3.3.2 Field Measurements and Calculations

For each experiment, plant populations were determined at V4 stage by counting in four 4 sub-areas for each plot. Phenological stages were recorded over the course of the growing season

according to the scale by Ritchie and Hanway (1982). Each stage of interest was determined based on the day when 50% of 20 previously marked plants per plot reached that stage. In addition, around V12, another 60 plants per plot (from the respective center pair of rows in each experiment) were tagged and their silking date was recorded individually.

Above-ground biomass samples were taken at V12-V13, R1, R3, and R6 stages. The V12-V13 and R3 sampling dates were chosen to be representative of the critical period of yield determination (Table 1). Sampling at R1 was done two days after 50% silking in 2017, one day after 50% silking in 2018, and two days after 50% silking in 2019. At each sampling date, ten consecutive plants were cut off at ground level from center rows in each plot. Linear length between plants within the same row in the biomass removal zones was measured, and all data were expressed on a per plant basis. Plants were separated into their different components depending on the stage (leaf plus husks, stem plus tassels, ear, cob, grain), dried at 60°C to constant weight, and weighed. Dry matter samples were then ground to pass a 1-mm sieve and analyzed for N concentration by combustion methods (Etheridge et al., 1998) at A&L Laboratories, IN (Experiment 1) and at Ward Laboratories, NE (Experiments 2 and 3). In order to check for consistency in the analysis, a set of stored, back-up sub-samples of ground plant tissue from 2017 was sent to Ward Laboratories; similarly, stored back-up ground material from 2018/2019 was sent to A&L Laboratories.

Dry matter from all separate components was added up together to account for total-plant growth at each stage (PG, mg $plant^{-1}$). Similarly, N contents obtained from multiplying N concentration and biomass on a per tissue basis were then added together to account for total-plant N uptake (PNU, mg N $plant^{-1}$). R1 and R3 ear (without husks) dry matter and N content represented ear growth (EG, mg ear^{-1}) and ear N allocation (ENA, mg N ear^{-1}), respectively.

Plant and ear growth and N allocation rates were calculated in order to study dry matter and N allocation dynamics during the lag phase (R1-R3). Plant growth rate (PGR, mg $°Cd^{-1}$), plant N uptake rate (PNUR, mg N $°Cd^{-1}$), ear growth rate (EGR, mg $°Cd^{-1}$), and ear N allocation rate (ENAR, mg N $°Cd^{-1}$) were calculated as the difference in PG, PNU, EG, or ENA, respectively, between R3 and R1 stages divided by the difference in accumulated thermal time between those two dates. Onset of ear growth was assumed to occur at V12.

Grain yield (GY, Mg ha^{-1}) determination from plot areas varied with the experiment layout. In Exp. 1, GY was determined by an 8-row combine harvesting the 8-center rows of each plot. GY

monitor data were corrected by cropping 21 m of border at both ends of the original plot length in order to only consider the yield points recorded when the combine reached a stable harvesting flow. Combine monitor data outliers which were higher/lower than 2.5 standard deviations were removed. In Exp. 2 and Exp. 3, because of their much smaller plots, GY was obtained by hand-harvesting ears from properly bordered plants in a 3 m^2 area from the center 2 rows. For all three experiments, GY was adjusted to a 15.5% moisture content and expressed on a per area basis.

GY components were estimated from the R6 biomass sample. Kernel number per plant (KNP, grain $plant^{-1}$) was determined by counting kernels per ear from each of the ten plants sampled for biomass at R6. Final kernel weight (KW, mg $grain^{-1}$) resulted from averaging the weight of 1000 kernels (5 sub-samples of 200 kernels) from each of the ten plants sampled for biomass at R6. Final KW was then adjusted to 0% moisture content.

Finally, resource availability per kernel during the critical period (i.e., V12-R3) was estimated as the ratio between plant growth rate over that timeframe ($PGR_{V12.R3}$, mg $°Cd^{-1}$) and KNP (Gambín et al., 2006). $PGR_{V12.R3}$ was calculated as the difference in PG between R3 and V12 stages divided by the difference in accumulated thermal time between those two dates.

3.3.3 Endosperm Cell Number Determination

Tagged plants of known silking date corresponding to the 50% silking date of their specific treatment combination (across three blocks) were selected in the early stages of grain development. From these plants, three were randomly selected in each plot and their ears were removed for endosperm analysis at a consistent time interval from silk emergence. Since most treatment combinations had the same 50% silking date, these plants were exposed to the same environmental conditions during the lag phase. The only exception was maize in the 0N treatments, with 50% silking occurring 1 day later (i.e., relative to other N rate treatments) in Exp. 1 across all timings, 2 days later in Exp. 2 and 3 at the lower density, and 3 days later in Exp. 2 and 3 at the higher density. Nevertheless, all ears collected were developmentally at the same "age", and the environmental differences in the lag phase among treatments were assumed to be minimal. Sampled ears were always apical ears (viable secondary ears were never produced in any of the experiments).

Ear sampling times during the lag period doubled after the first experiment but the sample intensity was consistent at 3 ears per plot for each sampling. Ears were sampled at 13 days after

silking (DAS) in Exp. 1, at 9 DAS and 17 DAS in Exp. 2, and at 10 DAS and at 17 DAS in Exp. 3. Immediately after ear sampling, ten intact kernels were cautiously removed from the center of each ear, and placed in a fixing solution of 3:1 ethanol/acetic acid (v/v) for 24 hours at 20°C. Kernels were then transferred to 70% ethanol and stored at -20°C until further processing. In all cases, separate vials were used for each ear in order to account for plant variability within each plot. For endosperm analysis, one kernel was randomly collected from the stored vials of ears sampled at 13 and 17 DAS. Due to the small size of the kernels sampled at 9 and 10 DAS, two kernels were picked from ears sampled at those dates.

ECN was determined by adjusting methods from Rijven and Wardlaw (1966), Singh and Jenner (1982), and Jones et al. (1985). Kernels removed from the preserving solution were placed in 50% ethanol (v/v) for 5 minutes, and then transferred to deionized water for another 5 minutes. Thereafter, kernels were dissected and endosperms were separated from embryo and pericarp. Endosperms were then placed in 1 ml 1M HCl and incubated on ice for 30 minutes, followed by a second incubation in a 60ºC-water bath for 16 minutes. After a triple rinsing with deionized water, endosperms were placed in sealed test tubes containing 0.5 ml of basic Fuchsin reagent (Certified Biological Stain, Fisher Chemical) to incubate overnight. The next day, after a double rinsing with 95% ethanol (v/v), endosperms were digested at 37ºC with 30g/l Cellulysin (Cellulase, MilliporeSigma™ Calbiochem™) in 0.1 M NaOAc buffer (pH 4.7). From the resulting suspension, three sub-samples (technical reps) were loaded in a hemocytometer (Neubauer Counting Chamber, Hausser Scientific™) and digital pictures were taken from each sub-sample using a camera attached to a microscope (Microscope Digital Camera, MU1000, AmScope™). Suspensions were diluted when needed, and in such cases sub-samples were collected from the dilutions. In either case, both were always mixed by vortexing for 10 seconds before a sub-sample was collected in order to ensure uniform cell density. Cells were counted only when found inside the hemocytometer's central chamber unit (i.e., central square, 1-mm wide, 1-mm long, 0.1-mm deep, 0.0001-ml volume), following standard counting procedures (Absher, 1973; Hoffman, 2006). Four different pictures per sub-sample were taken to include the entire counting area at 10x magnification. Over counting due to picture overlapping was avoided by accurately delimiting the four different sections of the counting area using the grid ruling present in the Neubauer chamber. Cell counts coming from each of the four sections were added together to account for the total cell number (C, cells) in the counting area of the same sub-sample. Cells were counted using ImageJ

image processing software (Schneider et al., 2012) and the resulting numbers were related to the initial volume of suspension (V, ml), dilution (if any) (D, dimensionless factor), and number of endosperms (E, endosperms) digested each time to obtain the number of endosperm cells per kernel (ECN, cell grain^{-1}) (Equation 2). Overall, a total of 4428 pictures were analyzed: 972 in Exp. 1, 1728 in Exp. 2, and 1728 in Exp. 3.

$$\boldsymbol{ECN = \frac{C\ x\ D\ x\ V}{0.0001\ x\ E}} \qquad \text{Equation 3.2}$$

3.3.4 Statistical Analyses

Statistical analyses were conducted using R (R Core Team, 2019). Each experiment was analyzed separately. Factor and interaction effects on individual variables were tested by ANOVA applying the nested blocking structure of a split-plot model, where whole plots are nested within blocks, and subplots are nested within whole plots. As described earlier, whole plots were N timing treatments in Exp. 1 and N rate treatments in Exp. 2 and Exp. 3. Sub-plots were N rates in Exp. 1 and plant density treatments in Exp. 2 and Exp. 3. Means separation was tested by least significant difference (LSD) at α=0.05. Both ANOVA and LSD were conducted using the *agricolae* R package (de Mendiburu, 2020), via the *sp.plot* and *LSD.test* functions, respectively. *LSD.test* function was run under the appropriate mean square errors for each comparison. Relationships between variables were studied via linear regression and Pearson's correlation analyses.

3.4 Results

3.4.1 Environmental Conditions

Weather conditions varied across experiments (Table 3.1). Exp. 1 had slightly lower minimum and maximum air temperatures due to being located in a more northern location (LaCrosse, IN). It also had more water availability as it received 435 mm of total precipitation plus 25 mm of irrigation applied after R3 stage. Although Exp. 2 and Exp. 3 were conducted in the same location (West Lafayette, IN), seasonal variation resulted from the intrinsic variability of rainfed conditions. Exp. 2 presented characteristics of a typical growing season in a temperate location, accumulating 427 mm of precipitation. Conversely, maize productivity in Exp. 3 suffered

from a late planting due to excessive rains before and during May. Once planted, the crop experienced severe water stress, especially during the first part of the critical period, and the cumulative rainfall received in the 2019 growing season (265 mm) was approximately half of the previous season's rainfall.

3.4.2 Endosperm Cell Number Determined During the Lag Phase

The number of endosperm cells determined during the lag phase varied across experiments, confirming how responsive this trait was under different environment by management combinations. Overall ECN means by experiment and time of ear sampling resulted in the following ascending gradient: $6.1x10^5$ at 9 DAS in 2018, $11.6x10^5$ at 10 DAS in 2019, $22.6x10^6$ at 13 DAS in 2017, $82.3x10^6$ at 17 DAS in 2019, and $122.7x10^6$ at 17 DAS in 2018. Aside from the apparent increasing cell number over time associated with progressive plant development, an environmental effect was also evident in the overall 30% reduction in ECN from 2018 to 2019 at 17 DAS.

ECN during the lag phase increased with soil N availability (i.e. N rate) across experiments (Figure 3.1). The experiment conducted in 2017 reported the highest effect of N rate in ECN at 13 DAS as it increased gradually until 224N ($p<0.001$) (Appendix B, Table B.1), regardless of fertilizer timing ($p>0.05$). In Exp. 2, ECN was increased by N rate at both 9 DAS ($p<0.001$) and 17 DAS ($p<0.05$). At 9 DAS, ECN reached a peak at 168N, but at 17 DAS only 0N was different from other fertilized treatments. Main N rate effects also significantly impacted ECN at 10 DAS and at 17 DAS (each $p<0.05$) in Exp. 3, although the earlier sampling was less responsive (i.e., only 0N was different from all other fertilized treatments) than the later one (i.e., when ECN increased until 168N). Interestingly, a plant density main effect was never detected in either Exp. 2 or Exp. 3 ($p>0.05$) (Appendix B, Tables B.2 and B.3), suggesting that ECN was rather independent of differences in plant growth due to population.

3.4.3 Plant Growth Rate, Plant N Uptake Rate, Ear Growth Rate and Ear N Allocation Rate During the Lag Phase

Across experiments, the majority of dry matter and N allocation rates during the lag phase responded positively to N rate treatments without interacting with either N timing (Exp. 1, Table 3.2) or plant density (Exp. 2 and 3, Tables 3.3 and 3.4, respectively). At the whole-plant scale,

plant growth rate ($PGR_{R1.R3}$) had a more consistent response to N supply across experiments than that of plant nitrogen uptake rate ($PNUR_{R1.R3}$) (Tables 3.2, 3.3 and 3.4). While $PGR_{R1.R3}$ increased up to 112N (Exp. 1, Table 3.2) or 168N (Exp. 2 and 3, Tables 3.3 and 3.4, respectively), $PNUR_{R1.R3}$ was not affected by N rate in Exp. 1 (Table 3.2), had an inconsistent pattern in Exp. 2 (Table 3.3), and only changed under a much higher N rate (224N) in Exp. 3 (Table 3.4). Regarding the two additional experimental factors tested, N application timing had no effect on $PGR_{R1.R3}$ or $PNUR_{R1.R3}$ (Exp. 1, Table 3.2), while mean plant density effect was only significant for $PGR_{R1.R3}$ in Exp. 2 where, as expected, $PGR_{R1.R3}$ was reduced under an increase in population.

Conversely to whole-plant dynamics, lag-phase ear growth rate ($EGR_{R1.R3}$) and ear N allocation rate ($ENAR_{R1.R3}$) showed more similar responses to N supply across experiments (Tables 3.2, 3.3 and 3.4). Both parameters consistently increased until 168N in Exp. 2 and 3 (Tables 3.3 and 3.4), while in Exp. 1 $EGR_{R1.R3}$ increased until 112N and $ENAR_{R1.R3}$ gradually gained until 224N (Table 3.2). Main N timing effects were never detected in Exp. 1, but main plant density effects (Exp. 2 and 3) were always significant for both $EGR_{R1.R3}$ and $ENAR_{R1.R3}$. The decreases in dry matter and N fluxes to the ear under an increase in plant density (from 7.9 to 10.4 plants m^{-2}) were higher in Exp. 2 (32% decrease in $EGR_{R1.R3}$, 28% in $ENAR_{R1.R3}$) than in Exp. 3 (22% decrease in $EGR_{R1.R3}$, 19% in $ENAR_{R1.R3}$) (Tables 3.3 and 3.4).

3.4.4 Grain Yield, Kernel Number per Plant, Kernel Weight, and Source-sink Ratio During the Critical Period

Across experiments, grain yield (GY) was strongly affected by N rate (Tables 3.2, 3.3 and 3.4). In Exp. 1, N rate was the only significant factor for GY, while neither N timing application nor its interaction with rate were significant (Table 3.2). Similarly, kernel number per plant (KNP) and kernel weight (KW) were responsive to N rate but not to N timing. KNP did not increase above 112N, but KW means increased gradually up to the highest N rate.

In both Exp. 2 and 3, GY increased significantly with N rate, but plant density effects on GY weren't significant (Tables 3.3 and 3.4). Both KNP and KW increased until 168N, but KNP changed more gradually under lower N rates than KW in Exp. 2. Both yield components were significantly reduced under the higher density treatment in Exp. 2 (Table 3.3), while only KNP was affected by this factor in Exp. 3 (Table 3.4).

In terms of the source-sink relationship during the critical period, the ratio of plant growth rate during the critical period to KNP did not respond to any treatment in any experiment of this study (Tables 3.2, 3.3 and 3.4). This was explained by the fact that both components of the relationship (i.e., $PGR_{V12.R3}$ and KNP) experienced proportional changes in response to N treatments over the range of experimental conditions while maintaining their corresponding ratio.

3.4.5 Relationship Between Variables

When variables were regressed, both timing application (Exp. 1) and plant density (Exp. 2 and 3) effects were routinely considered in the corresponding models. However, when only one predicted line is presented, the timing and density factors were non-significant ($p>0.05$) for the specific parameter and a single model was sufficient to explain each experiment's relation, unless otherwise stated.

ECN determined during the lag phase significantly explained KW variability in all three experiments (Figure 3.2), although the strength of the relationship depended on the combination of experiment and ear sampling time. The highest R^2 value (0.77) was obtained when KW was regressed as a function of ECN at 13 DAS in Exp. 1, while the relationship of KW versus ECN was lowest at 10 DAS in Exp. 3 (R^2=0.35). Similarly, in Exp. 2, ECN at the earlier ear sampling date (9 DAS) explained less variability in KW (R^2=0.52) than at 17 DAS (R^2=0.63).

GY was strongly associated with KW in all experiments (Figure 3.3). In Exp. 1, KW explained a large portion of GY variability (R^2=0.91), with KNP playing a smaller role (R^2=0.80, Figure B.1). While KNP responded more gradually to N rate in Exp. 2, KW still explained 78% of GY variability. GY was also strongly related to KW in Exp. 3 (R^2=0.72), despite both yield component values reflecting smaller ranges in that site-year.

When yield components were related to each other, no trade-off was evident in any of the experiments (Figure 3.4). KW increased with KNP in a linear fashion in Exp. 2 and 3, while in Exp. 1 a curvilinear relationship was detected. Furthermore, no relationship was found between plant growth rate during the critical period per kernel -a common indicator of source sink relation- and KW (Figure 3.5). The one exception was a weak decreasing linear relationship detected in Exp. 2.

To examine how resource allocation to the ear related to KW, we considered ear growth rate during the lag phase (Figure 3.6) and ear N allocation rate during the same period (Figure 3.7) as

predictors. Although both parameters were good linear predictors for KW, the $ENAR_{R1.R3}$ resulted in higher R^2 values across all experiments (especially in Exp. 2). In addition, Pearson's correlation analysis between $ENAR_{R1.R3}$ and ECN resulted in high, significant, and positive correlation coefficients in all five ECN determinations (Table 3.5). Conversely, total-plant N uptake rate during the lag phase ($PNUR_{R1.R3}$) was never correlated with ECN (Table 3.5).

3.5 Discussion

Both potential KW, conceptually constrained by ECN achieved during the lag phase, and actual KW, as realized in the effective grain filling period, responses to N availability were studied under a wide range of growing conditions. Despite environmental differences among seasons, KW was always a significant predictor of grain yield (GY) variability (Figure 3.3). The strongest relation between GY and KW was found when KNP did not change among fertilized treatments (Exp. 1, Table 3.2). However, KW still explained more than 70% of GY variability even when N rate differences affected KNP more strongly (Exp. 2, Table 3.3) and even when there were relatively small GY responses to N rates (Exp. 3, Table 3.4). While KW is usually considered to be less responsive to environmental changes than KN (Sadras, 2007; Sadras and Slafer, 2012), our findings revealed a wide plasticity in KW that explained in-field grain yield variations under contrasting production scenarios, regardless of how much GY variability was explained by KNP (Figure B.1).

In order to elucidate whether KW variations could be related to changes in potential KW (i.e., potential sink capacity of individual kernels), we first studied endosperm cell numbers (ECN) established during the lag phase in response to N rate, N timing applications, and plant density treatments. That was followed by testing the relationship of KW versus ECN. Our analysis was focused on ECN due to its association with sink capacity of individual kernels (Reddy and Daynard, 1983; Jones et al., 1985, 1996; Zhang et al., 2016) given that cell division processes occurring in the endosperm tissue during this early stage limits the kernel's subsequent ability to import carbohydrates during the active phase of grain filling (Setter and Flannigan, 1989; Sabelli and Larkins, 2009a; Zhang and Kaeppler, 2017; Olsen, 2020). In our experiments, ECN was always affected by N rate treatments (Figure 3.1), regardless of N application timing (Exp. 1, Table A.1) or plant density (Exp. 2 and 3, Tables A.2 and A.3). Furthermore, ECN increased with soil N availability when determined at 9, 10, 13, and 17 DAS, although bigger effects (i.e., ECN changing

incrementally with N rate) were found in Exp. 1 and in the first sampling for Exp. 2 (Figure 3.1, Tables B.1 and B.2). Despite experimental differences in the degree of treatment effects, we consistently found that ECN changed with N availability, something that, to the best of our knowledge, had only been reported for 14-days-after-pollination, *in-vitro* cultured kernels grown under increasing N concentration media (Cazetta et al., 1999). Conversely, changes in ECN due to N rate treatments in a prior field experiment were only observed well beyond the lag phase (i.e. 25 DAS) while no ECN differences were evident at 11 or 18 DAS (Lemcoff and Loomis, 1994).

While we did not study cell division processes, phases, or components directly at the molecular level, cell numbers produced at fixed moments during endosperm development could be a good indicator of how cell division unfolded. Variations in ECN, both by season and N treatments, might be partly explained by the fact that this parameter depends on the mitotic phases of endosperm development (Sabelli and Larkins, 2009a; Dante et al., 2014; Leroux et al., 2014). Early endosperm development has two main mitoses stages separated by cellularization: first, mitoses of the primary endosperm nucleus without cytokinesis, cellularization of these nuclear domains, and then cell proliferation through mitotic activity coupled with cytokinesis (Sabelli and Larkins, 2009a, 2009b). The acytokinetic mitoses take place from 2-4 days after pollination (DAP) and the nuclei produced during that phase represent the founder cells that will ultimately divide and crowd the endosperm (Sabelli and Larkins, 2009a). Hence, one source of variation in ECN values can come from those original nuclei given that final nucleus number just before cellularization can vary considerably in the same genotype (Leroux et al., 2014). In addition, the extent of the acytokinetic mitosis, and thus the timing of cellularization, correlates with endosperm and kernel growth by defining the number of final nuclei (Sabelli, 2017). Fewer nuclei due to an early cellularization have been associated with smaller kernels (Dante et al., 2014), and vice versa (Sabelli, 2017). Furthermore, the longer lag phase usually detected in bigger kernels has been associated with higher ECNs (Zhang et al., 2016).

Besides seasonal and N treatment variation, we also found increases in ECN over time, i.e. from 9-10 DAS to 17 DAS (Figure 3.1). These increases are consistent with how the endosperm grows through the second type of mitoses, now coupled with cytokinesis. After cellularization takes place, mitotic cell division produces the majority of cells that can be found in the mature kernels from 4 to 10-12 DAP (Kowles and Phillips, 1985; Lur and Setter, 1993). Hence, ECN values that we determined early (i.e., 9-10 DAS) may not have shown final cell numbers since

major mitotic cycles can still take place a few days later. In addition, residual cell division has been detected in the more external layers of the endosperm even later (20-25 DAP) (Kowles and Phillips, 1988). Since our method for ECN determination is based on the digestion of the whole endosperm, without considering the different cell layers that contribute to this tissue, it is possible that the values obtained by the later sampling (i.e., 17 DAS) also contained cells derived from peripheral mitoses. Such separation may be warranted in future studies.

Our comprehensive approach to ECN determination during the lag phase enabled the simultaneous investigation of sink capacity response to N treatments at the individual kernel level. Prior studies of N effects on sink capacity formation have usually focused on whole-plant growth rate (PGR) responses during the critical period of yield determination and its relationship with KNP (Uhart and Andrade, 1995; Monneveux et al., 2005; Lemaire et al., 2008). Based on this acknowledged relationship, PGR per kernel was proposed as an indicator of source sink ratio during the critical period when studying potential KW (Gambín et al., 2006). Under this model, increases in potential KW would be expected when resource availability per kernel is increased by reductions in KNP. Recently, Hisse et al. (2019) applied this theoretical framework to study N availability effects on KW, and concluded that potential KW did not change under N differences given that the ranges in PGR per kernel were similar for 0N and fertilized treatments. In our study, however, we found differences in ECN in response to N availability (Figure 3.1) regardless of the wide ranges in PGR per kernel (Figure 3.5). Furthermore, we did not find any relationship between KW and PGR per kernel (Figure 3.5), which contrasts with previous research (Gambín et al., 2006, 2008; Hisse et al., 2019). The lack of relation between PGR per kernel and KW is consistent with the fact that, in our results, KW was reduced when KNP decreased, and vice versa (i.e., positive relation between the yield components, with no trade-off) (Figure 3.4). The latter suggests that potential KW may not be able to compensate for a reduction in KNP, or vice versa, when the stress constraining the plant's physiological condition occurs in the post-silking portion of the critical period (i.e., the lag phase), given that this phase is crucial to determination of both components. The fact that our results are similar to what was reported by Cerrudo et al. (2013) when they applied a short shading treatment during the lag phase hints at a broader physiological mechanism for yield determination specific to the lag phase worthy of further study under other experimental conditions. In terms of N treatments, in particular, Paponov et al. (2020) also concluded that potential KW and

KNP had different, independent mechanisms of regulation during the lag phase, providing opportunities for them to be increased simultaneously.

Assimilate availability per kernel, either during the critical period, or as more frequently analyzed during the effective grain filling period (Maddoni et al., 1998; Borrás and Otegui, 2001; D'Andrea et al., 2016; Hisse et al., 2019), has usually been the primary focus of studies exploring KW responses to N availability. Therefore, any direct N effects on KW would end up hidden under the broad umbrella of source-sink relations due to the interlinked nature of C and N crop dynamics (Paul and Foyer, 2001; Masclaux-Daubresse et al., 2010; Fernie et al., 2020). However, in our study, we found evidence of direct N effects on potential KW since variations in final KW were always at least partially explained by ECN (Figure 3.2). Furthermore, our findings suggest that N played a direct role in the establishment of individual kernel sink capacity by altering ECN (rather than indirectly via assimilate availability) since: 1) there was no relation between PGR per kernel and KW (Figure 3.5), 2) PGR per kernel was not affected by any combination of the experimental factors tested (Tables 3.2, 3.3 and 3.4), and 3) plant density treatments did not affect ECN at any of the sampling times in either Exp. 2 or Exp. 3 (Tables A.2 and A.3).

Besides what was reported for ECN in *in-vitro* cultured kernels (Cazetta et al., 1999), the bigger role of N -relative to that of carbohydrates- in the determination of the kernel weight component of sink capacity found in our study is also consistent with recent reports in plant-grown reproductive tissues using methods other than the analysis of ECN. Under field conditions, Ning et al. (2018) concluded that the supply of assimilates from source leaves was not the primary limitation under N deficiency since they detected higher starch concentrations in N-deficient apical cob tissue at both silking and 20 DAS. These authors also argue that sink limitation under N stress is the result of reduced utilization of these highly available sugars given that N deficiency leads to suppression of enzyme activity. Even more interesting, Paponov et al. (2020) concluded that potential KW was related to N flux per kernel rather independently of carbohydrate availability. This conclusion was supported by several of their findings, including significant increases in potential KW with a treatment of abrupt increase in N supply during the lag phase, the lack of change in plant biomass under that said treatment, and the close correlation between KW and the amount of N flux per kernel.

Direct N effects on potential KW and ECN during the lag phase of maize grain filling could be related to the fact that N substrates are needed by cell division processes such as DNA

replication and enzyme synthesis (Berger, 1999; Olsen et al., 1999). In terms of enzymes, two important stages in endosperm cell division cycle are controlled by the activity of different cyclin-dependent kinase (CDK) complexes (Sabelli, 2017). These structures, made of catalytic kinase and a protein-based cyclin subunit that works as regulator (Inzé and De Veylder, 2006), are controlled at the molecular level by different upstream kinases and phosphatases and CKIs inhibitors (Sabelli, 2017). Another group of enzymes that play a key role in the establishment of kernel sink strength are invertases (INVs), which are involved in the production of hexose signals that control cell cycle and cell division processes (Bihmidine et al., 2013; Koch and Ma, 2017). While enzyme activity was not measured in our study, it has already been hypothesized, based on *in-vitro* culture studies, that enzyme expression and/or activity could be one way for N to affect the establishment of kernel sink potential (Below et al., 2000).

Besides enzymes, N effects on cell division process during early endosperm development could also be attributed to cytokinins. Peak levels of these hormones, known for their role in regulating the proliferation and differentiation of plant cells (Sakakibara, 2006), have been detected in kernels between 4 and 12 DAP (Lur and Setter, 1993; Cheikh and Jones, 1994; Rijavec et al., 2011). Given that reductions in cytokinin levels have also been found under other stress conditions during the lag phase, such as heat stress (Cheikh and Jones, 1994), it is possible for N deficiency to work similarly, especially since cytokinin synthesis and metabolism are now known to be dependent on N supply (Sakakibara, 2006; Gu et al., 2018). More direct evidence would be helpful; future studies focused on maize kernel enzyme activity and hormonal concentration changes should be pursued to verify the underlying mechanisms of nitrogen's role in ECN during the lag phase.

Direct N effects on ECN, and thus on potential KW, in our field studies were associated with ear N allocation rates during the lag phase ($ENAR_{R1.R3}$) (Table 3.5). Across experiments, Pearson's correlation analysis showed a significant positive relationship between ECN (at multiple lag-phase sampling times) and $ENAR_{R1.R3}$, with coefficients ranging from 0.59 to 0.77. Hence, these results suggest that there may be a strong co-dependency between the establishment of individual kernel sink strength in early endosperm development and N fluxes to reproductive tissues during the lag phase. This is further supported by the fact that variations in final KW were explained by both $ENAR_{R1.R3}$ (Figure 3.7) and ECN (Figure 3.2). Our results also demonstrate that the role of N management in early endosperm development might be independent of aboveground plant N

uptake rate during the lag phase ($PNUR_{R1.R3}$), as evidenced by the lack of significance in the correlations between $PNUR_{R1.R3}$ and ECN (Table 3.5). Hence, the majority of actual N allocated to the ear during ECN formation, and when potential KW was being determined, might have originated from N remobilization.

Overall, we believe we found evidence that early endosperm development was indeed affected by N supply under the conditions of this study given that ECN always responded positively to main N rate effects. Furthermore, ECN always explained final KW changes, indicating that the establishment of individual sink capacity (i.e., potential KW) was modified by the N availability conditions imposed by these experiments. While changes in potential KW have previously been associated with carbohydrate availability per kernel during the critical period (i.e., PGR per kernel), we found no relationship between KW and PGR per kernel in our study. This result, combined with ECN's lack of response to plant density and PGR per kernel's lack of response to any of the experimental factors tested in this study, supports the idea that N played a direct role in potential KW determination during the lag phase. Finally, variation in ECN was highly correlated with ear N allocation rate during the lag phase ($ENAR_{R1.R3}$), whereas ECN's correlation with total-plant N uptake rate during the lag period was never significant.

3.6 References

Absher, M. (1973). "Hemocytometer Counting," in *Tissue Culture*, ed. P. F. Kruse (New York, NY: Academic Press, INC.), 395–397. doi:10.1016/b978-0-12-427150-0.50098-x.

Artlip, T. S., Madison, J. T., and Setter, T. L. (1995). Water deficit in developing endosperm of maize: cell division and nuclear DNA endoreduplication. *Plant. Cell Environ.* 18, 1034–1040. doi:10.1111/j.1365-3040.1995.tb00614.x.

Below, F. E., Cazetta, J. O., and Seebauer, J. R. (2000). Carbon/nitrogen interactions during ear and kernel development of maize. *Crop Sci.*, 15–24. doi:10.2135/cssaspecpub29.c2.

Berger, F. (1999). Endosperm development. *Curr. Opin. Plant Biol.* 2, 28–32. doi:10.1016/S1369-5266(99)80006-5.

Bihmidine, S., Hunter, C. T., Johns, C. E., Koch, K. E., and Braun, D. M. (2013). Regulation of assimilate import into sink organs: update on molecular drivers of sink strength. *Front. Plant Sci.* 4, 177. doi:10.3389/fpls.2013.00177.

Borrás, L., and Otegui, M. E. (2001). Maize kernel weight response to postflowering source-sink ratio. *Crop Sci.* 41, 1816–1822. doi:10.2135/cropsci2001.1816.

Borrás, L., and Westgate, M. E. (2006). Predicting maize kernel sink capacity early in development. *F. Crop. Res.* 95, 223–233. doi:10.1016/j.fcr.2005.03.001.

Cazetta, J. O., Seebauer, J. R., and Below, F. E. (1999). Sucrose and nitrogen supplies regulate growth of maize kernels. *Ann. Bot.* 84, 747–754. doi:10.1006/anbo.1999.0976.

Cerrudo, A., Di Matteo, J., Fernandez, E., Robles, M., Olmedo Pico, L., and Andrade, F. H. (2013). Yield components of maize as affected by short shading periods and thinning. *Crop Pasture Sci.* 64, 580–587. doi:10.1071/CP13201.

Cheikh, N., and Jones, R. J. (1994). Disruption of maize kernel growth and development by heat stress. *Plant Physiol.* 106, 45–51. doi:10.1104/pp.106.1.45.

Chen, K., Camberato, J. J., Tuinstra, M. R., Kumudini, S. V., Tollenaar, M., and Vyn, T. J. (2016). Genetic improvement in density and nitrogen stress tolerance traits over 38 years of commercial maize hybrid release. *F. Crop. Res.* 196, 438–451. doi:10.1016/j.fcr.2016.07.025.

Commuri, P. D., and Jones, R. J. (2001). High temperatures during endosperm cell division in maize: A genotypic comparison under in vitro and field conditions. *Crop Sci.* 41, 1122–1130. doi:10.2135/cropsci2001.4141122x.

D'Andrea, K. E., Piedra, C. V., Mandolino, C. I., Bender, R., Cerri, A. M., Cirilo, A. G., et al. (2016). Contribution of reserves to kernel weight and grain yield determination in maize: Phenotypic and genotypic variation. *Crop Sci.* 56. doi:10.2135/cropsci2015.05.0295.

Dante, R. A., Larkins, B. A., and Sabelli, P. A. (2014). Cell cycle control and seed development. *Front. Plant Sci.* 5, 493. doi:10.3389/fpls.2014.00493.

de Mendiburu, F. (2020). agricolae: Statistical Procedures for Agricultural Research. R package version 1.3-2. https://CRAN.R-project.org/package=agricolae.

DeBruin, J. L., Schussler, J. R., Mo, H., and Cooper, M. (2017). Grain yield and nitrogen accumulation in maize hybrids released during 1934 to 2013 in the US Midwest. *Crop Sci.* 57, 1431–1446. doi:10.2135/cropsci2016.08.0704.

Di Matteo, J. A., Ferreyra, J. M., Cerrudo, A. A., Echarte, L., and Andrade, F. H. (2016). Yield potential and yield stability of Argentine maize hybrids over 45 years of breeding. *F. Crop. Res.* 197, 107–116. doi:10.1016/j.fcr.2016.07.023.

Duncan, W. G., Hatfield, A. L., and Ragland, J. L. (1965). The growth and yield of corn. II. Daily growth of corn kernels. *Agron. J.* 57, 221–223. doi:10.2134/agronj1965.00021962005700020026x.

Echarte, L., Luque, S., Andrade, F. H., Sadras, V. O., Cirilo, A., Otegui, M. E., et al. (2000). Response of maize kernel number to plant density in Argentinean hybrids released between 1965 and 1993. *F. Crop. Res.* 68, 1–8. doi:10.1016/S0378-4290(00)00101-5.

Egharevba, P. N., Horrocks, R. D., and Zuber, M. S. (1976). Dry matter accumulation in maize in response to defoliation. *Agron. J.* 68, 40–43. doi:10.2134/agronj1976.00021962006800010011x.

Engelen-Eigles, G., Jones, R. J., and Phillips, R. L. (2001). DNA endoreduplication in maize endosperm cells is reduced by high temperature during the mitotic phase. *Crop Sci.* 41, 1114–1121. doi:10.2135/cropsci2001.4141114x.

Etheridge, R. D., Pesti, G. M., and Foster, E. H. (1998). A comparison of nitrogen values obtained utilizing the Kjeldahl nitrogen and Dumas combustion methodologies (Leco CNS 2000) on samples typical of an animal nutrition analytical laboratory. *Anim. Feed Sci. Technol.* 73, 21–28. doi:10.1016/S0377-8401(98)00136-9.

Fernie, A. R., Bachem, C. W. B., Helariutta, Y., Neuhaus, H. E., Prat, S., Ruan, Y. L., et al. (2020). Synchronization of developmental, molecular and metabolic aspects of source–sink interactions. *Nat. Plants* 6, 55–66. doi:10.1038/s41477-020-0590-x.

Gambín, B. L., Borrás, L., and Otegui, M. E. (2006). Source-sink relations and kernel weight differences in maize temperate hybrids. *F. Crop. Res.* 95, 316–326. doi:10.1016/j.fcr.2005.04.002.

Gambín, B. L., Borrás, L., and Otegui, M. E. (2008). Kernel weight dependence upon plant growth at different grain-filling stages in maize and sorghum. *Aust. J. Agric. Res.* 59, 280–290. doi:10.1071/AR07275.

Gu, J., Li, Z., Mao, Y., Struik, P. C., Zhang, H., Liu, L., et al. (2018). Roles of nitrogen and cytokinin signals in root and shoot communications in maximizing of plant productivity and their agronomic applications. *Plant Sci.* 274, 320–331. doi:10.1016/j.plantsci.2018.06.010.

Haegele, J. W., Cook, K. A., Nichols, D. M., and Below, F. E. (2013). Changes in nitrogen use traits associated with genetic improvement for grain yield of maize hybrids released in different decades. *Crop Sci.* 53, 1256. doi:10.2135/cropsci2012.07.0429.

Hisse, I. R., D'Andrea, K. E., and Otegui, M. E. (2019). Source-sink relations and kernel weight in maize inbred lines and hybrids: Responses to contrasting nitrogen supply levels. *F. Crop. Res.* 230, 151–159. doi:10.1016/J.FCR.2018.10.011.

Hoffman, T. L. (2006). Counting cells. *Cell Biol. Four-Volume Set* 1, 21–24. doi:10.1016/B978-012164730-8/50004-6.

INClimate - The Indiana State Climate Office Purdue Mesonet. https://ag.purdue.edu/indiana-state-climate/. Available at: https://iclimate.org/.

Inzé, D., and De Veylder, L. (2006). Cell cycle regulation in plant development. *Annu. Rev. Genet.* 40, 77–105. doi:10.1146/annurev.genet.40.110405.090431.

Johnson, D. R., and Tanner, J. W. (1972). Calculation of the rate and duration of grain filling in corn (Zea mays L.). *Crop Sci.* 12, 485–486. doi:10.2135/cropsci1972.0011183x001200040028x.

Jones, R. J., and Brenner, M. L. (1987). Distribution of abscisic acid in maize kernel during grain filling. *Plant Physiol.* 83, 905–909. doi:10.1104/pp.83.4.905.

Jones, R. J., Roessler, J., and Ouattar, S. (1985). Thermal environment during endosperm cell division in maize: effects on number of endosperm cells and starch granules. *Crop Sci.* 25, 830–834. doi:10.2135/cropsci1985.0011183x002500050025x.

Jones, R. J., Schreiber, B. M. N., and Roessler, J. A. (1996). Kernel sink capacity in maize: Genotypic and maternal regulation. *Crop Sci.* 36, 301–306. doi:10.2135/cropsci1996.0011183X003600020015x.

Jones, R. J., and Simmons, S. R. (1983). Effect of altered source-sink ratio on growth of maize kernels. *Crop Sci.* 23, 129–134. doi:10.2135/cropsci1983.0011183x002300010038x.

Koch, K. E., and Ma, F. (2017). "Determinants of kernel sink strength," in *Maize Kernel Development*, ed. B. A. Larkins (Boston, MA: CAB International), 190–203.

Kowles, R. V., and Phillips, R. L. (1985). DNA amplification patterns in maize endosperm nuclei during kernel development. *Proc. Natl. Acad. Sci.* 82, 7010–7014. doi:10.1073/pnas.82.20.7010.

Lemaire, G., and Millard, P. (1999). An ecophysiological approach to modelling resource fluxes in competing plants. *J. Exp. Bot.* 50, 15–28. doi:10.1093/jxb/50.330.15.

Lemaire, G., van Oosterom, E., Jeuffroy, M. H., Gastal, F., and Massignam, A. (2008). Crop species present different qualitative types of response to N deficiency during their vegetative growth. *F. Crop. Res.* 105, 253–265. doi:10.1016/j.fcr.2007.10.009.

Lemcoff, J. H., and Loomis, R. S. (1994). Nitrogen and density influences on silk emergence, endosperm development, and grain yield in maize (Zea mays L.). *F. Crop. Res.* 38, 63–72. doi:10.1016/0378-4290(94)90001-9.

Leroux, B. M., Goodyke, A. J., Schumacher, K. I., Abbott, C. P., Clore, A. M., Yadegari, R., et al. (2014). Maize early endosperm growth and development: From fertilization through cell type differentiation. *Am. J. Bot.* 101, 1259–1274. doi:10.3732/ajb.1400083.

Luque, S. F., Cirilo, A. G., and Otegui, M. E. (2006). Genetic gains in grain yield and related physiological attributes in Argentine maize hybrids. *F. Crop. Res.* 95, 383–397. doi:10.1016/j.fcr.2005.04.007.

Lur, H. S., and Setter, T. L. (1993). Endosperm development of maize defective kernel (dek) mutants. Auxin and cytokinin levels. *Ann. Bot.* 72, 1–6. doi:10.1006/anbo.1993.1074.

Maddoni, G. A., Otegui, M. E., and Bonhomme, R. (1998). Grain yield components in maize II. Post-silking growth and kernel weight. *F. Crop. Res.* 56, 247–256. doi:10.1016/S0378-4290(97)00093-2.

Masclaux-Daubresse, C., Daniel-Vedele, F., Dechorgnat, J., Chardon, F., Gaufichon, L., and Suzuki, A. (2010). Nitrogen uptake, assimilation and remobilization in plants: Challenges for sustainable and productive agriculture. *Ann. Bot.* 105, 1141–1157. doi:10.1093/aob/mcq028.

Melchiori, R. J. M., and Caviglia, O. P. (2008). Maize kernel growth and kernel water relations as affected by nitrogen supply. *F. Crop. Res.* 108, 198–205. doi:10.1016/j.fcr.2008.05.003.

Monneveux, P., Zaidi, P. H., and Sanchez, C. (2005). Population density and low nitrogen affects yield-associated traits in tropical maize. *Crop Sci.* 45, 535–545. doi:10.2135/cropsci2005.0535.

Mueller, S. M., Messina, C. D., and Vyn, T. J. (2019). Simultaneous gains in grain yield and nitrogen efficiency over 70 years of maize genetic improvement. *Sci. Rep.* 9, 9095. doi:10.1038/s41598-019-45485-5.

Myers, P. N., Setter, T. L., Madison, J. T., and Thompson, J. F. (1990). Abscisic acid inhibition of endosperm cell division in cultured maize kernels. *Plant Physiol.* 94, 1330–1336. doi:10.1104/pp.94.3.1330.

Nasielski, J., and Deen, B. (2019). Nitrogen applications made close to silking: Implications for yield formation in maize. *F. Crop. Res.* 243, 107621. doi:10.1016/j.fcr.2019.107621.

Ning, P., Yang, L., Li, C., and Fritschi, F. B. (2018). Post-silking carbon partitioning under nitrogen deficiency revealed sink limitation of grain yield in maize. *J. Exp. Bot.* 69, 1707–1719. doi:10.1093/jxb/erx496.

Ober, E. S., Setter, T. L., Madison, J. T., Thompson, J. F., and Shapiro, P. S. (1991). Influence of water deficit on maize endosperm development. *Plant Physiol.* 97, 154–164. doi:10.1104/pp.97.1.154.

Olsen, O. A. (2020). The modular control of cereal endosperm development. *Trends Plant Sci.* 25, 279–290. doi:10.1016/j.tplants.2019.12.003.

Olsen, O., Linnestad, C., and Nichols, S. (1999). Developmental biology of the cereal endosperm. *Trends Plant Sci.* 4, 253–257. doi:10.1007/7089_2007_106.

Paponov, I., Paponov, M., Sambo, P., and Engels, C. (2020). Differential regulation of kernel set and potential kernel weight by nitrogen supply and carbohydrate availability in maize genotypes contrasting in nitrogen use efficiency. *Front. Plant Sci.* 11, 1–19. doi:10.3389/fpls.2020.00586.

Paul, M. J., and Foyer, C. H. (2001). Sink regulation of photosynthesis. *J. Exp. Bot.* 52, 1383–1400. doi:10.1093/jexbot/52.360.1383.

Poneleit, C. G., and Egli, D. B. (1979). Kernel growth rate and duration in maize as affected by plant density and genotype. *Crop Sci.* 19, 385–388. doi:10.2135/cropsci1979.0011183x001900030027x.

R Core Team (2019). R: A language and environment for statistical computing. R Foundation for Statistical Computing, Vienna, Austria. https://www.R- project.org/.

Reddy, V., and Daynard, T. (1983). Endosperm characteristics associated with rate of grain filling and kernel size in corn. *Maydica* 28, 339–355. doi:10.11693/hyhz20181000233.

Rijavec, T., Jain, M., Dermastia, M., and Chourey, P. S. (2011). Spatial and temporal profiles of cytokinin biosynthesis and accumulation in developing caryopses of maize. *Ann. Bot.* 107, 1235–1245. doi:10.1093/aob/mcq247.

Rijven, A. H. G. C., and Wardlaw, I. F. (1966). A method for the determination of cell number in plant tissues. *Exp. Cell Res.* 328, 324–328.

Ritchie, S. W., and Hanway, J. J. (1982). How a corn plant develops. Iowa State University of Science and Technology. Cooperative Extension Service, Iowa, EEUU. Special Report N°48. 1982.

Sabelli, P. A. (2017). "Cell cycle and cell size regulation during maize seed development: Current understanding and challenging questions," in *Maize Kernel Development*, ed. B. A. Larkins (Boston, MA: CAB International), 119–133.

Sabelli, P. A., and Larkins, B. A. (2009a). The contribution of cell cycle regulation to endosperm development. *Sex. Plant Reprod.* 22, 207–219. doi:10.1007/s00497-009-0105-4.

Sabelli, P. A., and Larkins, B. A. (2009b). The development of endosperm in grasses. *Plant Physiol.* 149, 14–26. doi:10.1104/pp.108.129437.

Sadras, V. O. (2007). Evolutionary aspects of the trade-off between seed size and number in crops. *F. Crop. Res.* 100, 125–138. doi:10.1016/j.fcr.2006.07.004.

Sadras, V. O., and Slafer, G. A. (2012). Environmental modulation of yield components in cereals: Heritabilities reveal a hierarchy of phenotypic plasticities. *F. Crop. Res.* 127, 215–224. doi:10.1016/j.fcr.2011.11.014.

Sakakibara, H. (2006). Cytokinins: Activity, biosynthesis, and translocation. *Annu. Rev. Plant Biol.* 57, 431–449. doi:10.1146/annurev.arplant.57.032905.105231.

Schneider, C. A., Rasband, W. S., and Eliceiri, K. W. (2012). NIH Image to ImageJ: 25 years of image analysis. *Nat. Methods* 9, 671–675. doi:10.1038/nmeth.2089.

Setter, T. L., and Flannigan, B. A. (1989). Relationship between photosynthate supply and endosperm development in maize. *Ann. Bot.* 64, 481–487. doi:10.1093/oxfordjournals.aob.a087867.

Singh, B. K., and Jenner, C. F. (1982). A modified method for the determination of cell number in wheat endosperm. *Plant Sci. Lett.* 26, 273–278. doi:10.1016/0304-4211(82)90101-8.

Singletary, G. W., and Below, F. E. (1990). Nitrogen-induced changes in the growth and metabolism of developing maize kernels grown in vitro. *Plant Physiol.* 92, 160–167. doi:10.1104/pp.92.1.160.

Soil Survey Staff Web Soil Survey. Natural Conservation Service, USDA. http://websoilsurvey.sc.egov.usda.gov/.

Tollenaar, M. (1977). Sink-source relationships during reproductive development in maize. A review. *Maydica* 22, 49–75.

Tollenaar, M., Dwyer, L. M., and Stewart, D. W. (1992). Ear and kernel formation in maize hybrids representing three decades of grain yield improvement in Ontario. *Crop Sci.* 32, 432–438. doi:10.2135/cropsci1992.0011183x003200020030x.

Uhart, S. A., and Andrade, F. H. (1995). Nitrogen deficiency in maize: I. Effects on crop growth, development, dry matter partitioning, and kernel set. *Crop Sci.* 35, 1376–1383. doi:10.2135/cropsci1995.0011183X003500050020x.

Zhang, X., Hirsch, C. N., Sekhon, R. S., De Leon, N., and Kaeppler, S. M. (2016). Evidence for maternal control of seed size in maize from phenotypic and transcriptional analysis. *J. Exp. Bot.* 67, 1907–1917. doi:10.1093/jxb/erw006.

Zhang, X., and Kaeppler, S. (2017). "Natural variations in maize kernel size: A resource for discovering biological mechanisms," in *Maize Kernel Development*, ed. B. A. Larkins (Boston, MA: CAB International), 204–216.

3.7 Tables and Figures

Table 3.1. Environmental conditions for four key periods within the growing seasons of Experiment 1 (LaCrosse, IN, 2017), Experiment 2 (West Lafayette, IN, 2018), and Experiment 3 (West Lafayette, IN, 2019).

Climate Parameter	Growth Stage Interval	Experiment 1	Experiment 2	Experiment 3
Duration (days)	P-V12	51	48	49
	V12-R1	15	16	11
	R1-R3	19	15	21
	R3-R6	47	36	46
Cumulative Thermal Time ($^{o}Cdays^{-1}$)	P-V12	611	672	731
	V12-R1	211	257	141
	R1-R3	247	217	306
	R3-R6	493	504	543
Mean Minimum Temperature (^{o}C)	P-V12	13.3	16.2	17.5
	V12-R1	16.1	18.8	15.0
	R1-R3	15.5	16.9	16.4
	R3-R6	11.7	17.0	13.8
Mean Maximum Temperature (^{o}C)	P-V12	26.6	27.6	28.3
	V12-R1	26.8	29.2	27.6
	R1-R3	27.2	28.2	28.8
	R3-R6	25.1	27.3	26.1
Cumulative Rainfall (mm)	P-V12	201	201	127
	V12-R1	79	48	4
	R1-R3	96	14	29
	R3-R6	84*	164	105

**: 59 mm of rainfall plus 25 mm of irrigation.*

Table 3.2. ANOVA for grain yield (GY, Mg ha^{-1}, 15.5% moisture), kernel number per plant (KNP, grain $plant^{-1}$), kernel weight (KW, mg $grain^{-1}$), plant growth rate during the critical period ($PGR_{V12.R3}$, mg $^{o}Cd^{-1}$), $PGR_{V12.R3}$ per kernel (mg $^{o}Cd^{-1}$ $grain^{-1}$), plant growth rate during the lag phase ($PGR_{R1.R3}$, mg $^{o}Cd^{-1}$), ear growth rate during the lag phase ($EGR_{R1.R3}$, mg $^{o}Cd^{-1}$), plant N uptake rate during the lag phase ($PNUR_{R1.R3}$, mg N $^{o}Cd^{-1}$), and ear N allocation rate during the lag phase ($ENAR_{R1.R3}$, mg N $^{o}Cd^{-1}$) in Experiment 1 (LaCrosse, IN, 2017).

	GY	**KNP**	**KW**	**$PGR_{V12.R3}$**	**$PGR_{V12.R3}$ per kernel**	**$PGR_{R1.R3}$**	**$EGR_{R1.R3}$**	**$PNUR_{R1.R3}$**	**$ENAR_{R1.R3}$**
N Timing Application									
Planting	10.5	483	261.1	246.8	0.52	223.9	139.8	-0.29	1.54
Planting_V6	11.3	468	274.4	228.3	0.51	211.9	136.3	-0.10	1.44
Planting_V12	11.2	492	263.4	248.1	0.52	229.0	137.2	-0.40	1.50
N Rate **(kg N ha^{-1})**									
0N	5.3 c	314 b	213.3 c	175.3 b	0.57	153.3 b	68.1 b	-0.41	0.73 c
112N	11.9 b	560 a	271.3 b	274.5 a	0.49	244.1 a	162.9 a	-0.25	1.73 b
224N	15.7 a	569 a	314.3 a	273.4 a	0.48	267.3 a	182.4 a	-0.13	2.03 a
F-test									
N Timing (T)	ns	ns	ns	ns	ns	ns	ns	ns	ns
N Rate (N)	<.001	<.001	<.001	<.001	ns	0.024	<.001	ns	<.001
T x N	ns	ns	ns	ns	ns	ns	ns	ns	ns

ns: not significant at α=0.05, p-value for F-test is >0.05. Means separation determined by Fisher's least significant difference (LSD) at α=0.05. Same letter or absence of letter means no significant difference was found among levels. For all variables, three replicates were collected (n=3, N=27).

Table 3.3. ANOVA for grain yield (GY, Mg ha^{-1}, 15.5% moisture), kernel number per plant (KNP, grain $plant^{-1}$), kernel weight (KW, mg $grain^{-1}$), plant growth rate during the critical period ($PGR_{V12.R3}$, mg $^{o}Cd^{-1}$), $PGR_{V12.R3}$ per kernel (mg $^{o}Cd^{-1}$ $grain^{-1}$), plant growth rate during the lag phase ($PGR_{R1.R3}$, mg $^{o}Cd^{-1}$), ear growth rate during the lag phase ($EGR_{R1.R3}$, mg $^{o}Cd^{-1}$), plant N uptake rate during the lag phase ($PNUR_{R1.R3}$, mg N $^{o}Cd^{-1}$), and ear N allocation rate during the lag phase ($ENAR_{R1.R3}$, mg N $^{o}Cd^{-1}$) in Experiment 2 (West Lafayette, IN, 2018).

	GY	**KNP**	**KW**	**$PGR_{V12.R3}$**	**$PGR_{V12.R3}$ per kernel**	**$PGR_{R1.R3}$**	**$EGR_{R1.R3}$**	**$PNUR_{R1.R3}$**	**$ENAR_{R1.R3}$**
N Rate **(kg N ha^{-1})**									
0N	7.4 d	255 c	267.7 b	156.0 c	0.63	111.4 b	65.5 c	0.59 b	0.81 c
84N	11.4 c	356 b	283.9 b	195.1 b	0.56	177.9 ab	112.0 b	0.54 b	1.36 b
168N	15.3 b	475 a	309.6 a	236.6 a	0.50	285.0 a	169.3 a	2.14 a	2.20 a
224N	16.6 a	505 a	318.3 a	227.5 a	0.45	262.3 a	166.0 a	1.13 ab	2.24 a
Plant Density **(plant m^{-2})**									
7.9D	12.8	455 a	301.7 a	223.5 a	0.50	262.6 a	152.3 a	1.55	1.92 a
10.4D	12.5	340 b	288.0 b	184.0 b	0.57	155.8 b	104.1 b	0.65	1.38 b
F-test									
N Rate (N)	<.001	<.001	0.002	0.001	ns	0.025	0.002	0.090	<.001
Density (D)	ns	<.001	0.010	0.004	ns	0.001	<.001	ns	<.001
N x D	ns	ns	ns	ns	ns	ns	0.012	ns	0.013

ns: not significant at α=0.05, p-value for F-test is >0.05. Means separation determined by Fisher's least significant difference (LSD) at α=0.05. Same letter or absence of letter means no significant difference was found among levels. For all variables, three replicates were collected (n=3, N=24).

Table 3.4. ANOVA for grain yield (GY, Mg ha^{-1}, 15.5% moisture), kernel number per plant (KNP, grain $plant^{-1}$), kernel weight (KW, mg $grain^{-1}$), plant growth rate during the critical period ($PGR_{V12.R3}$, mg $^{o}Cd^{-1}$), $PGR_{V12.R3}$ per kernel (mg $^{o}Cd^{-1}$ $grain^{-1}$), plant growth rate during the lag phase ($PGR_{R1.R3}$, mg $^{o}Cd^{-1}$), ear growth rate during the lag phase ($EGR_{R1.R3}$, mg $^{o}Cd^{-1}$), plant N uptake rate during the lag phase ($PNUR_{R1.R3}$, mg N $^{o}Cd^{-1}$), and ear N allocation rate during the lag phase ($ENAR_{R1.R3}$, mg N $^{o}Cd^{-1}$) in Experiment 3 (West Lafayette, IN, 2019).

	GY	**KNP**	**KW**	**$PGR_{V12.R3}$**	**$PGR_{V12.R3}$ per kernel**	**$PGR_{R1.R3}$**	**$EGR_{R1.R3}$**	**$PNUR_{R1.R3}$**	**$ENAR_{R1.R3}$**
***N Rate* (kg N ha^{-1})**									
0N	7.5 c	288 c	264.9 c	164.1 b	0.58	133.0 b	88.3 b	0.25 b	0.95 b
84N	9.5 b	342 b	282.3 b	179.4 b	0.53	129.0 b	97.4 b	-0.02 b	1.11 b
168N	11.0 ab	406 a	295.3 ab	242.7 a	0.61	220.0 a	145.3 a	0.55 ab	1.69 a
224N	12.2 a	424 a	299.2 a	243.3 a	0.57	203.1 a	145.3 a	0.92 a	1.75 a
***Plant Density* (plant m^{-2})**									
7.9D	10.0	405 a	287.6	226.4 a	0.56	176.3	133.5 a	0.31	1.52 a
10.4D	10.1	325 b	283.2	188.3 b	0.58	166.3	104.7 b	0.55	1.23 b
F-test									
N Rate (N)	0.004	<.001	0.008	<.001	ns	0.005	0.002	0.037	<.001
Density (D)	ns	<.001	ns	<.001	ns	ns	<.001	ns	<.001
N x D	0.024	ns	ns	ns	ns	ns	ns	ns	ns

ns: not significant at α=0.05, p-value for F-test is >0.05. Means separation determined by Fisher's least significant difference (LSD) at α=0.05. Same letter or absence of letter means no significant difference was found among levels. For all variables, three replicates were collected (n=3, N=24).

Table 3.5. Correlation analysis between endosperm cell number (ECN, cells grain^{-1}) and plant N uptake rate ($PNUR_{R1.R3}$, mg N ºCd^{-1}) and ear N allocation rate ($ENAR_{R1.R3}$, mg N ºCd^{-1}) for the three experiments. Pearson's coefficient (r) is shown, alongside its significance between brackets. (ns): p>.05. (**): p<.01. (***): p<.001.

	ECN				
	2017	**2018**		**2019**	
	13 DAS	**9 DAS**	**17 DAS**	**10 DAS**	**17 DAS**
$PNUR_{R1.R3}$	-0.01 (ns)	0.24 (ns)	0.32 (ns)	0.19 (ns)	0.15 (ns)
$ENAR_{R1.R3}$	0.77 (***)	0.71 (***)	0.73 (***)	0.59 (**)	0.65 (***)

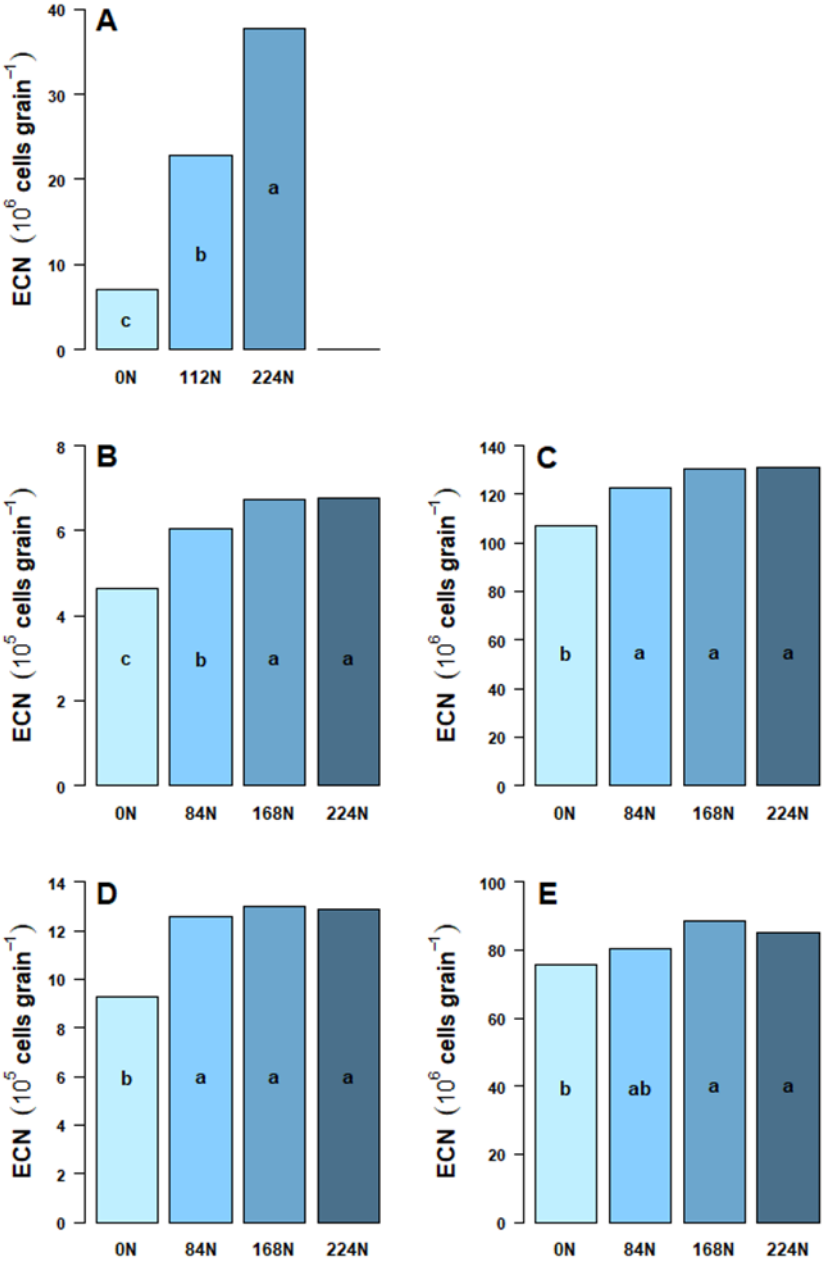

Figure 3.1. Effect of N rate on endosperm cell number (ECN) during early reproductive stages in maize. Panel A: ECN determined at 13 days after silking (DAS) in Experiment 1 (2017). Panels B and C: ECN determined at 9 and 17 DAS, respectively, in Experiment 2 (2018). Panels D and E: ECN determined at 10 and 17 DAS, respectively in Experiment 3 (2019). Plotted means were averaged over three timing application treatments in Exp. 1 (n=9), and two plant density treatments in Exp. 2 and Exp. 3 (n=8). Mean separation analyses were based on Fisher's LSD (α=0.05).

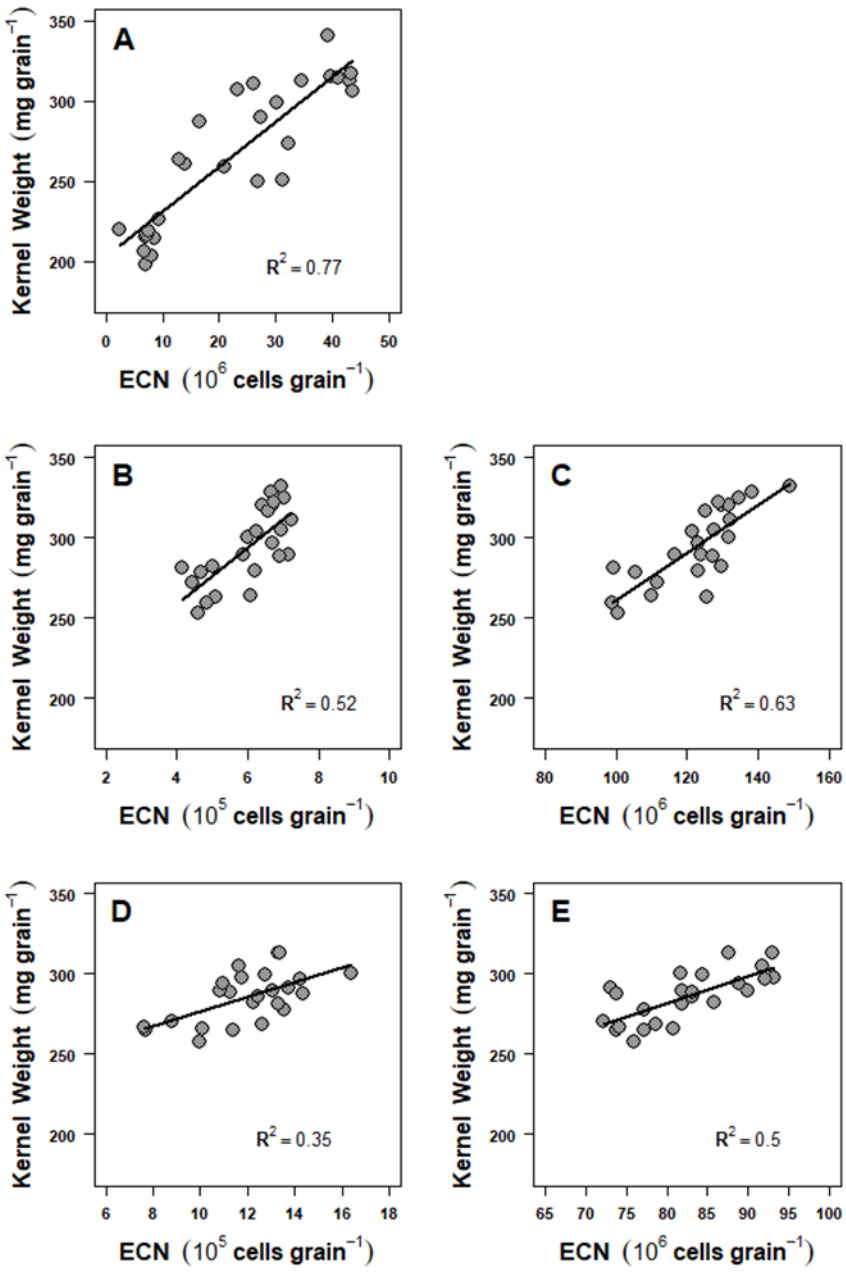

Figure 3.2. Relationship between endosperm cell number (ECN) and kernel weight in maize. Panel A: ECN determined at 13 days after silking (DAS) in Experiment 1 (2017). Panels B and C: ECN determined at 9 and 17 DAS, respectively, in Experiment 2 (2018). Panels D and E: ECN determined at 10 and 17 DAS, respectively, in Experiment 3 (2019). Points represent data on a per plot basis; each plot represents a combination of N timing by N rate treatment (Exp. 1) or N rate by plant density treatment (Exp. 2 and 3). Lines represent the linear fit obtained by regression analysis. R^2 for each significant regression ($p<0.05$) is shown.

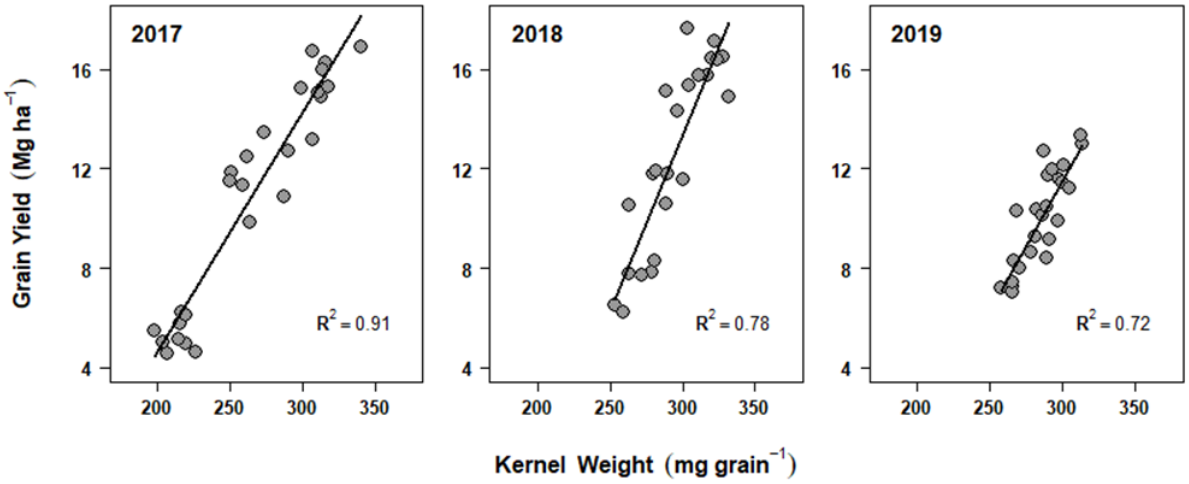

Figure 3.3. Relationship between kernel weight and grain yield in maize. Each panel shows data from a field experiment where N rate treatments were combined with timing application treatments (season 2017, Exp. 1) or plant density treatments (seasons 2018 and 2019, Exp. 2 and Exp. 3, respectively). Points represent data on a per plot basis. Lines represent the linear fit obtained by regression analysis. R^2 for each significant regression ($p<0.05$) is shown.

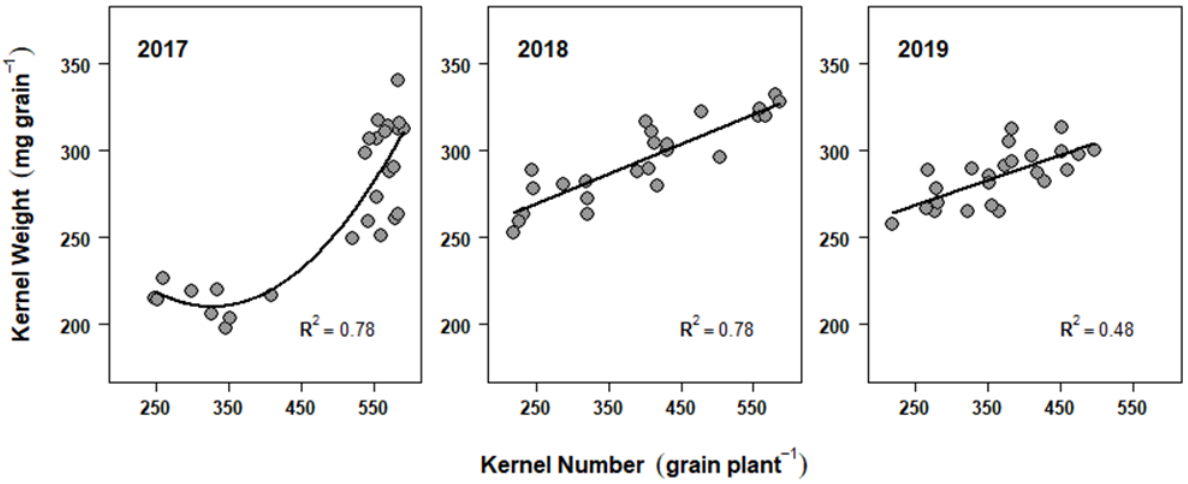

Figure 3.4. Relationship between kernel number and kernel weight in maize. Each panel shows data from a field experiment where N rate treatments were combined with timing application treatments (season 2017, Exp. 1) or plant density treatments (seasons 2018 and 2019, Exp. 2 and Exp. 3, respectively). Points represent data on a per plot basis. Lines represent the best fit obtained by regression analysis. R^2 for each significant regression ($p<0.05$) is shown.

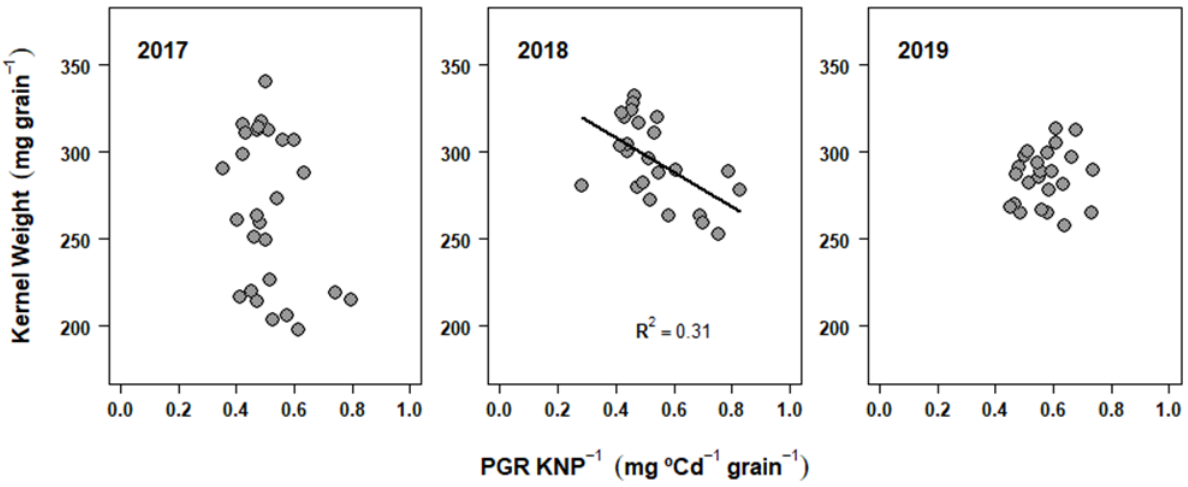

Figure 3.5. Relationship between plant growth rate during the critical period per kernel ($PGR_{V12.R3}$ KNP^{-1}) and kernel weight in maize. Each panel shows data from a field experiment where N rate treatments were combined with timing application treatments (season 2017, Exp. 1) or plant density treatments (seasons 2018 and 2019, Exp. 2 and Exp. 3, respectively). Points represent data on a per plot basis. Lines represent the linear fit obtained by regression analysis. R^2 for each significant regression ($p<0.05$) is shown.

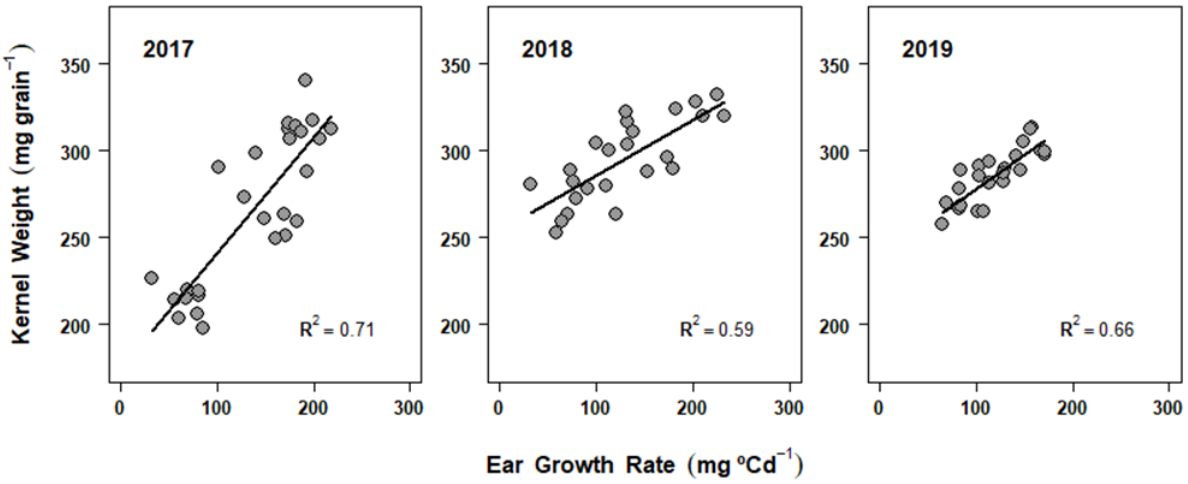

Figure 3.6. Relationship between ear growth rate during the lag phase ($EGR_{R1.R3}$) and kernel weight in maize. Each panel shows data from a field experiment where N rate treatments were combined with timing application treatments (season 2017, Exp. 1) or plant density treatments (seasons 2018 and 2019, Exp. 2 and Exp. 3, respectively). Points represent data on a per plot basis. Lines represent the linear fit obtained by regression analysis. R^2 for each significant regression ($p<0.05$) is shown.

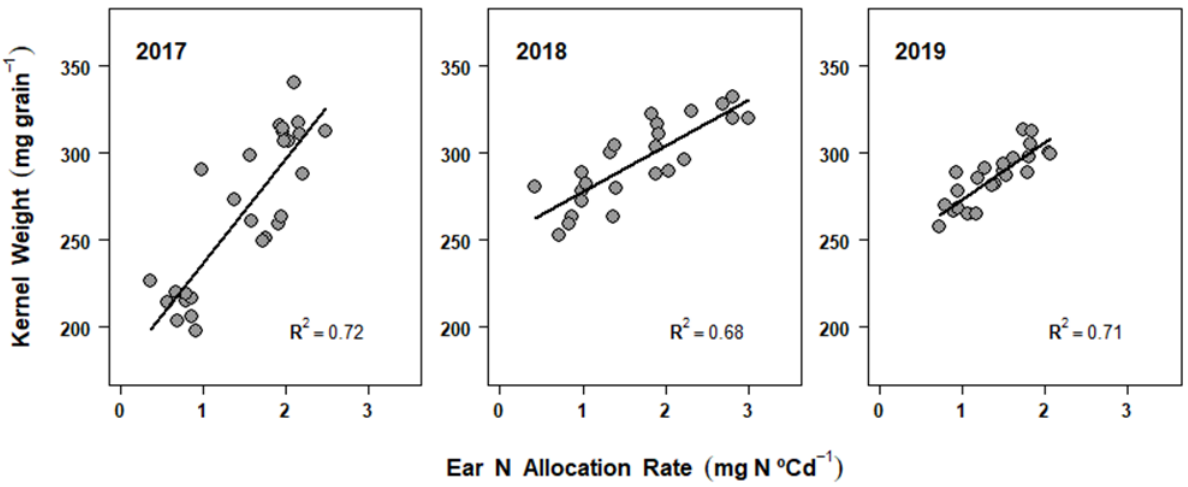

Figure 3.7. Relationship between ear N allocation rate during the lag phase ($ENAR_{R1.R3}$) and kernel weight in maize. Each panel shows data from a field experiment where N rate treatments were combined with timing application treatments (season 2017, Exp. 1) or plant density treatments (seasons 2018 and 2019, Exp. 2 and Exp. 3, respectively). Points represent data on a per plot basis. Lines represent the linear fit obtained by regression analysis. R^2 for each significant regression ($p<0.05$) is shown.

CHAPTER 4. DRY MATTER GAINS IN MAIZE KERNELS ARE DEPENDENT ON THEIR RATE OF NITROGEN ACCUMULATION DURING GRAIN FILLING

4.1 Abstract

Maize kernel weight (KW) has become a more variable trait as a result of sink strength increases by genetic improvement. Allocation of N assimilates to kernels during grain filling may be constraining the much more abundant accumulation of carbohydrates. The main objective of this work was to study dry matter (DM) and N accumulation dynamics in maize kernels during grain fill under a wide soil N availability gradient. The same maize hybrid was grown in three field experiments with a combination of fertilizer N rates, N timing applications, and plant densities. Linear plateau models were fitted to kernel DM and N accumulation data collected over 9-10 weeks from the early R3 stage. Increases in N supply, regardless of application timing or plant density, changed kernel DM accumulation dynamics by either increasing both the effective grain-filling rate (EGFR) and grain filling duration (GFD), or by increasing GFD alone. Kernel N content increased consistently under higher N availability because of gains in both kernel N accumulation rate (KNAR) and duration (KNAD). Kernels actively accumulated N until late in the season, as shown by the similar GFD and KNAD values reached (averaging ~1140ºCd^{-1} and ~1120ºCd^{-1}, respectively). While EGFR was less impacted by N rate differences, KNAR was much more responsive, showing a strong correlation with final KW (r=0.87). These results contribute to a better understanding of physiological mechanisms underlying the direct role of kernel N accumulation in limiting DM allocations, and therefore final KW, during grain filling.

Abbreviations: DM, dry matter**;** KN, kernel number; KW, kernel weight; GY, grain yield; EGFR, effective grain filling rate; GFD, grain filling duration; KNc, kernel N concentration; KNC, kernel N content; KNAR, kernel N accumulation rate; KNAD, kernel N accumulation duration; TT, thermal time; PG, plant growth; PNU, plant N uptake.

Keywords: kernel weight, grain-filling duration, effective grain-filling rate, kernel N content, kernel N accumulation duration, kernel N accumulation rate

4.2 Introduction

Maize grain yield is defined by the product of kernel number (KN) and kernel weight (KW). Although KN is considered the main grain yield determinant (Otegui, 1995; Chapman and Edmeades, 1999; Borrás et al., 2004) because it is more responsive to changes in environmental conditions (Tollenaar, 1977; Westgate and Boyer, 1986a; Andrade and Ferreiro, 1996; Sadras, 2007), grain yield can still be affected by variations in KW (Borrás and Gambín, 2010). In addition, as a result of genetic improvement in sink strength, modern genotypes have shown more KW variation than their older counterparts (Echarte et al., 2006; Chen et al., 2016a). Furthermore, several recent studies with current maize hybrids reported that final KW was proportionally more responsive than KN, and thus, more closely related to grain yield variations, under differences in planting dates (Bonelli et al., 2016; Zhou et al., 2016) and soil N availability (Chapter 3). Therefore, the prospect of KW becoming a more important driver behind in-field grain yield variability warrants a closer look into the physiological mechanisms that play a role when post-flowering stress conditions limit KW.

Final KW is the result of physiological processes taking place throughout the grain-filling period (i.e., from silking to maturity). Once potential KW is defined through endosperm cell division (with negligible dry weight gain) in the lag phase (Jones et al., 1985, 1996), kernels then enter the effective grain-filling phase, where they actively accumulate dry matter (DM) at a constant rate until reaching physiological maturity (Johnson and Tanner, 1972). Both the rate and the duration of DM accumulation (i.e., effective grain-filling rate -EGFR-, and grain-filling duration -GFD-, respectively) thus constitute the determining factors of final KW (Johnson and Tanner, 1972; Poneleit and Egli, 1979). In addition, around mid-filling, kernel water content increases to reach a maximum and then it decreases as dry matter accumulation continues (Westgate and Boyer, 1986b; Borrás et al., 2003). Both maximum kernel water content and EGFR are also related to potential KW (Jones et al., 1996; Borrás and Westgate, 2006). Whether kernels achieve this previously established potential size has previously been reported to depend on the availability of assimilates per kernel (i.e., source-sink relationship) during the linear phase (Tollenaar, 1977; Borrás et al., 2004). The main source of assimilates for the growing kernels is current net photosynthesis (estimated as plant growth gain during grain filling) (Rajcan and Tollenaar, 1999b; Borrás et al., 2004), while stem reserves play a role when sink demands are higher than photosynthetic source capacity (Uhart and Andrade, 1995; D'Andrea et al., 2016).

Individual KW is a genetically determined trait (Reddy and Daynard, 1983), and it varies among genotypes via different combinations of EGFR and GFD (Gambín et al., 2007; Borrás et al., 2009). However, environmental conditions during the linear phase, such as extreme temperatures (Rattalino Edreira et al., 2014) or water stress (Wang et al., 2019), also change final KW. Furthermore, at the crop level, decreases in KW under low N conditions have been associated with reductions in post-silking biomass accumulation (i.e. photosynthetic source capacity) and with changes in source-sink ratio (Uhart and Andrade, 1995; Hisse et al., 2019). On a per-kernel basis, DM dynamics have been described for numerous experimental conditions, but few studies have investigated how kernel growth parameters (i.e., GFD and EGFR) might be affected by contrasting N availability scenarios. For example, KW changes under different N supply have been related more to changes in grain-filling rate (Wei et al., 2019) or changes in both the EGFR and the GFD (Melchiori and Caviglia, 2008; Liu et al., 2011). However, because maize response to N is often a function of N timing and plant density, further research into the physiological determinants of final KW under a wide per-plant and per-kernel N availability gradient could help identify underlying mechanisms and management combinations for achieving higher KW.

While carbohydrates dominate the DM accumulated by kernels during grain filling, N assimilates are also actively demanded by these sink tissues (Crawford et al., 1982). N allocated to the kernels comes from post-silking N uptake and/or N remobilization from leaves and stems (Pan et al., 1986; Ciampitti and Vyn, 2013), and it is used for the synthesis of both storage proteins and enzymes required to convert soluble sugars and amino acids into starch and proteins, respectively (Singletary and Below, 1990; Cazetta et al., 1999). Despite its crucial role in achieving final KW, kernel N accumulation over time has not been studied in the same detail as DM. Recent studies have looked into kernel N accumulation from a descriptive perspective by plotting linear interpolations between five (Chen et al., 2016b) or seven (Ning et al., 2021) consecutive sampling dates over the grain-filling period. While both of these studies provided valuable insight into kernel N dynamics, the N availability ranges were limited to 2-3 N rates (without a secondary factor), and the lack of kernel samplings beyond 50-58 days after silking (DAS) prevented a deeper analysis of possible peaks or plateaus that may further explain the relationship of final KW with final kernel N content. Given the tight interactions between C and N source-sink dynamics (Paul and Foyer, 2001; Fernie et al., 2020), describing kernel N accumulation via well-known

characterization parameters should help in better understanding physiological mechanisms associated with DM accumulation, and ultimately final KW.

To the best of our knowledge, there have been no prior studies focused on maize kernels that sequentially determined both DM and N dynamics at weekly time intervals under a wide range of in-field N availability conditions. Therefore, the objectives of this chapter were: 1) to study kernel DM and N kernel dynamics during the linear phase of grain filling, 2) to determine N effects on the parameters thus obtained, and 3) to study the relationships between the parameters underlying the two processes.

4.3 Materials and Methods

4.3.1 Field Experiments

Three experiments were carried out in order to study dry matter and N dynamics in maize kernels. One common genotype (hybrid DKC63-60RIB GENSS, Dekalb, commercially released in 2015) was used in the three studies. Experiment 1 (2017) was conducted at the Purdue Rice Farm (LaCrosse, IN), while Experiment 2 (2018) and Experiment 3 (2019) were located at the Purdue Agronomy Center of Research and Education in West Lafayette, IN. All experiments followed a split-plot, randomized complete block design, involving N rate treatments, applied in the form of 28% urea ammonium nitrate (UAN), alongside a secondary factor such as N timing application (Experiment 1) or plant density (Experiments 2 and 3) to create a wide range of N availability conditions. Since experimental conditions for each experiment have already been described in Chapter 3, Table 4.1 provides a brief summary. In the case of Experiment 1, plots also received 17 kg N ha^{-1} and 6 kg P ha^{-1} as band-applied starter fertilizer (19-17-0), and supplementary sprinkler irrigation (through a center pivot system) when needed. In all cases, plots were kept weed-free and pesticide management practices followed Purdue University recommendations.

4.3.2 Measurements

Over the course of the growing season, phenological stages were recorded according to the scale by Ritchie and Hanway (1982). Stages were determined based on the day when 50% of 20 previously marked plants per plot reached that stage. At V4 stage, plant populations were

determined by counting four 4 sub-areas for each plot. Additionally, another 60 plants per plot (from the respective center pair of rows in each experiment) were tagged around V12 stage, and their respective silking dates were recorded individually. Phenology records were accompanied by weather data obtained for each growing season. Data from two nearby weather stations ("Wanatah 2 WNW", La Porte, IN and "Knox WWTP", Starke, IN; both NOAA National Centers for Environmental Information) were averaged to account for Experiment 1. For Experiments 2 and 3, weather data were retrieved from the on-site station ("ACRE-West Lafayette") (INClimate - The Indiana State Climate Office). Data obtained for each season included air temperature (maximum and minimum) and precipitation (Chapter 3, Table 3.1).

Above-ground biomass was sampled at the onset (R3 stage) and at the end (R6 stage) of the effective grain-filling period. In each sampling, 10 plants were cut-off at ground level from center rows in each plot. Plants were separated into their different components (leaf plus husks, stem plus tassels, ear, cob, grain), dried at 60°C to constant weight, and weighed to determine component dry matters. After weighing, samples were ground (to pass a 1-mm sieve) and sent for N concentration analysis by combustion methods (Etheridge et al., 1998) to A&L Laboratories, IN (Exp. 1) and to Ward Laboratories, NE (Exp. 2 and 3). To ensure data consistency between labs, back-up sub-samples of ground plant tissue from 2017 were submitted to Ward Laboratories and vice versa, back-up ground material from 2018/2019 was submitted to A&L Laboratories. Reported concentrations from duplicate samples were similar. At each sampling stage, total-plant growth or total-plant N uptake was calculated by adding up DM or N content from all the respective separate components. In addition, plant growth and plant N uptake during the whole grain-filling period were calculated by subtracting total-plant DM and N between R6 and R3 stages.

To account for grain-filling dynamics, an intense ear sampling was performed. Beginning at R3 stage (12-17 DAS), four ears from previously tagged plants (i.e., of known silking date) were sampled from each plot on a weekly basis (i.e., 7-8 days apart). Overall, there were nine (Experiments 1 and 2) and ten (Experiment 3) sampling dates (i.e., weeks), thus making a total of 2796 ears processed: 972 in Experiment 1, 864 in Experiment 2, and 960 in Experiment 3. From the center section of each ear, 15 intact kernels were collected, weighed immediately after (i.e., fresh weight), and then weighed again after drying for 24 hours at 100ºC (i.e., dry weight). An additional grain sub-sample was taken from the same ears once they were dried until constant

weight at 60ºC. A composite sample was formed with the four ears of the same plot. From this composite sample, kernels were ground and analyzed for N concentration following the same procedure as that of the other plant tissue samples explained above. Therefore, for each plot at each sampling date, they were four DM points, and only one N concentration value. Kernel N content was calculated by multiplying the plot N concentration value over the four DM points, thus obtaining four N content values per plot per sampling date.

Grain yield (GY) was determined from different plants. For Exp. 1, GY was obtained by an 8-row combine harvesting the 8-center rows of each plot, and the yield monitor data was appropriately curated to consider values from only the zones where the combine reached a stable harvesting flow, as explained in Chapter 3. For Exp. 2 and 3, GY was hand-harvested from a 3 m^2 plot area that was properly bordered. In all experiments, GY was expressed on a per area basis and adjusted to 15.5% moisture content. Kernel number (KN) and kernel weight (KW) were both estimated from the R6 biomass sample. KN resulted from counting all kernels in the 10-ear R6 sample, whereas 5 sub-samples of 200 kernels per plot were weighed to estimate KW.

4.3.3 Calculations and Statistical Analysis

All analysis were conducted using R programming language (R Core Team, 2019). With each experiment's data set, a linear plateau model was fitted to compare DM and N accumulation dynamics between combinations of treatments on a thermal time (TT, ºC days) basis, following the Equations 4.1 and 4.2:

$$KW \text{ or } KNC = a + b\,TT, \qquad when\ TT \leq c \qquad \text{Equation 4.1}$$

$$KW \text{ or } KNC = bc, \qquad when\ TT > c, \qquad \text{Equation 4.2}$$

where *a* is the *y*-intercept (mg), *b* is the rate of the grain filling (EGFR, mg ºC day^{-1}) or the rate of N accumulation in grain (KNAR, mg N ºC day^{-1}), and *c* is the total duration of grain filling (GFD, ºC $days^{-1}$) or the total duration of N accumulation in grain (KNAD, ºC $days^{-1}$). The models were fitted via nonlinear regression analysis (function *nls* in R), using the self-starting function *SSlinp* within the package *nlraa* (Miguez, 2021). Parameters of different treatment combinations were compared by overlapping their respective approximate 95% confidence intervals. Thermal time accumulation started at silking of each plant, using the average of maximum and minimum daily air temperature and a base temperature of 0ºC (Muchow, 1990).

N rate, N timing application, plant density, and interaction effects on individual variables were tested by ANOVA, following the respective split-plot structure of each experiment (i.e., whole plots nested within blocks, subplots nested within whole plots). Means separation was tested by least significant difference (LSD) at α=0.05. Both ANOVA and LSD were conducted using the package *agricolae* (de Mendiburu, 2020). Finally, relationships between parameters were studied via Pearson's correlation analysis.

4.4 Results

4.4.1 Grain Yield, Kernel Number per Plant, Kernel Weight and Final Kernel N Content

GY, its components, and grain N content (KNC) at R6 consistently responded to N rate treatments across all experiments (Tables 4.2, 4.3, and 4.4), without showing significant interactions with either application timing (Experiment 1) or plant density (Experiments 2 and 3). While N application timing main effects were never significant in Exp. 1, plant density sub-treatment effects were detected in some parameters in Exp. 2 and 3. However, KW was only affected by density in Exp. 2 (Table 4.3). The highest gains in GY (~10.4 Mg ha^{-1}), KW (~100 mg $grain^{-1}$), and KNC (2.4 mg N $grain^{-1}$) from 0N to 224N occurred in Exp. 1 (Table 4.2). Although the highest treatment means of both GY and KW in Exp. 1 and Exp. 2 were similar (15.7 and 16.6 Mg ha^{-1}, respectively), the GY and KW means did not decline as much under 0N in the latter study (Table 4.3), probably due to a bigger contribution from soil mineralization. Conversely, though Exp. 3 was conducted in the same location (but not in the same field) as Exp. 2, the significant delay in planting constrained the realization of the hybrid's GY potential by lowering both KNP and KW (Table 4.4). Despite these seasonal differences average GY increased 8.1 Mg ha^{-1} in response to N (i.e., from 0N to 224N) over the 3-year period. While kernel N concentrations (KNc) were similar in Exp. 2 and 3, lower KNC values were observed across N rates in Exp. 3 due to a lower overall KW.

4.4.2 Plant Growth and N Uptake During the Effective Grain-Filling Period

As expected, total-plant DM production and N uptake at the onset of the effective grain-filling period (PG_{R3} and PNU_{R3}, respectively), as well as total-plant DM and N accumulation over the whole effective grain-filling period ($PG_{R3.R6}$ and $PNU_{R3.R6}$), responded positively to soil N

availability in all experiments (Tables 4.2, 4.3 and 4.4), except for $PNU_{R3.R6}$ in the lower yielding Exp. 3. In addition, interaction effects between application timings and N rate (Exp. 1) or between N rate and plant density (Exp. 2 and 3) were never significant. While in Exp. 1 the timing of fertilizer application did not impact PG_{R3}, PNU_{R3}, $PG_{R3.R6}$ and $PNU_{R3.R6}$ (Table 4.2), most of these parameters were reduced at higher plant density in Exp. 2 (i.e., PG_{R3}, PNU_{R3} and $PG_{R3.R6}$, Table 4.3) and Exp. 3 (i.e., PG_{R3} and PNU_{R3}, Table 4.4).

In terms of photosynthetic source capacity, $PG_{R3.R6}$ reached similar maximum values in Exp 1 and 2, regardless of lower starting biomass (i.e., at R3) in the latter (Tables 4.2 and 4.3). Under higher N rates, Exp. 3 produced just half the $PG_{R3.R6}$ (compared to Exp. 2) while having similar R3 biomass (Tables 4.3 and 4.4). Under increases in N rate, both PNU_{R3} and $PNU_{R3.R6}$ gains were greater in Exp. 1 (1.52 and 0.81 g N $plant^{-1}$, respectively), while being lower in Exp. 3 (0.96 g N $plant^{-1}$ and non-significant, respectively). The remarkably lower biomass production and N uptake present in Exp. 3 were consistent with a less favorable growing season due to delayed planting.

4.4.3 Dry Matter Accumulation Dynamics in Kernels

Kernel DM accumulation under the different treatments resulted from either a combination of changes in both the effective grain filling rate (EGFR) and the grain filling duration (GFD) (Exp. 1, Fig. 4.1) or changes in GFD only (Exp. 2 and Exp. 3, Fig. 4.3 and 4.5, respectively). Averaging across treatments, maize reached maximum kernel weights at 1088 ºC day^{-1} in 2017, 1160 ºC day^{-1} in 2018, and 1165 ºC day^{-1} in 2019, which corresponded with 52, 51, and 53 days after silking, respectively.

In Exp. 1, the major factor affecting KW variability was N rate, regardless of when the fertilizer was applied (Table 4.2); thus, we pooled data from the three application timings to run nonlinear regression analysis by N rate alone (Fig. 4.1). DM accumulation by kernels showed three distinct patterns, depending on the amount of total N that plants received throughout the growing season, because of positive changes in both EGFR and GFD. EGFR increased gradually with N supply: 11% from 0N to 112N, 12% from 112N to 224N, and 24% from 0N to 224N (Fig. 4.1 and Fig. 4.7). Additionally, N supply increased GFD (extending it by 110-143 ºC day^{-1}, approximately similar to an actual 4-5-day increase under these climatic conditions), but no GFD differences were found between 112N and 224N.

When nonlinear regression analysis was applied to Exp. 2 and Exp. 3 datasets, DM accumulation dynamics in kernels were not differentially affected by plant density x N rate combinations, with both densities showing a similar response as N rate increased. Furthermore, plant density never differentially influenced grain filling parameters under the same N rate. Therefore, DM accumulation dynamics were analyzed in terms of the N rate gradient only, pooling data from both density treatments. Changes in kernel DM dynamics in both Exp. 2 and Exp. 3 were entirely explained by differences in GFD, while no N rate effects were detected on EGFR (overall equaled 0.35 mg ºC day^{-1} in both seasons) (Fig. 4.3, 4.5 and 4.7). In Exp. 2, two distinct grain filling patterns were identified based on the amount of plant N available: kernels gained DM until 1109-1131 ºC day^{-1} (0N-84N, respectively) or until 1186-1212 ºC day^{-1} (168N-224N, respectively) (Fig. 4.3). Conversely, in Exp. 3, GFD was not different from 0N to 168N, but it significantly increased under 224N (average increase of 70 ºC day^{-1}) (Fig. 4.5).

4.4.4 Nitrogen Accumulation Dynamics in Kernels

Kernel N accumulation followed a pattern similar to that of grain DM accumulation, with an active, linear import of N assimilates for the major part of the grain-filling period and then a plateau near physiological maturity in all three experiments (Fig. 4.2, 4.4 and 4.6). Furthermore, differences in kernel N accumulation dynamics were always realized through changes in both kernel N accumulation rate (KNAR) and kernel N accumulation duration (KNAD). In Exp. 1, N accumulation was once again studied considering N rate treatments without splitting the data into timing applications due to the lack of impact this experimental factor had on final KNC (Table 4.2). Increases in N rate produced a similar KNAD variation as that found for GFD, while KNAR presented a much bigger relative gain (compared to EGFR) under changes in N supply: 72% from 0N to 112N, 34% from 112N to 224N, and 131% from 0N to 224N (Fig. 4.2 and Fig. 4.7).

In Exp. 2 and Exp. 3, N rate effects on kernel N accumulation dynamics were also studied independently of plant density treatments, similarly to DM dynamics. Kernel N accumulation patterns detected in these two experiments were somewhat similar to those of Exp. 1, with N supply increasing final KNC by changing both KNAR and KNAD (Fig. 4.7). However, relative gains in the parameters were different from season to season. In Exp. 2, KNAR increased gradually until 168N, showing a 14% increase from 0N to 84N, a 34% increase from 84N to 168N, and a 53% increase from 0N to 168N (Fig. 4.4 and 4.7). In Exp. 3, KNAR changed from 0N-84N to 168N-

224N, with average gains of 10-20% (Fig. 4.6 and 4.7). In terms of KNAD, in Exp. 2 kernel N accumulation plateaued at similar times from 0N to 168N, increasing significantly only when the N rate was 224N (Fig. 4.4 and Fig. 4.7). Conversely, gains in KNAD were detected at both 168N and 224N treatments in Exp. 3 (Fig 4.6 and 4.7).

4.4.5 Relationships Between Parameters

To examine relationships between variables, pairwise Pearson's correlation analysis was applied among the DM and N grain-filling parameters estimated by nonlinear regression and the N rate means of GY, KNP, KW, KNC, PG_{R3}, $PG_{R3.R6}$, PNU_{R3}, and $PNU_{R3.R6}$ (Table 4.5). As expected, GY was correlated (at different degrees) with all variables. The parameters that were highly correlated with KW, but not at all significantly with final KNP, included EGFR, GFD and KNAR. Final KW was slightly more strongly associated with EGFR than with GFD. Similarly, KNC was correlated with both KNAD and KNAR, but the stronger association was with the latter. Given the similarities between kernel DM and N allocation dynamics, GFD and KNAD were strongly correlated, further supporting the fact that N was actively imported alongside carbohydrate assimilates by kernels until late in the reproductive period. The association between EGFR and KNAR was also highly significant, with the correlation being somewhat higher than that of the durations. Interestingly, final KW showed a stronger association with KNAR, suggesting that the N flux to the kernel can become a limitation to the realization of final KW. Finally, $PNU_{R3.R6}$ was not related to any of the DM or N grain-filling parameters, while GFD, KNAD and KNAR were all significantly associated with PNU_{R3}.

4.5 Discussion

Given the increasing relevance of KW variability in explaining GY limitations in modern maize genotypes (Cerrudo et al., 2013; Bonelli et al., 2016; Chen et al., 2016a; Mueller et al., 2019), a comprehensive study was conducted in order to better understand how soil N availability affected this yield component. An intensive ear sampling was performed for 9-10 weeks beginning at 200-300 $^{o}C\ day^{-1}$ after silking to estimate KW defining parameters (i.e., effective grain filling rate -EGFR- and grain filling duration -GFD-) (Johnson and Tanner, 1972; Frey, 1981) and compare them among different N supply treatments. Furthermore, kernel N accumulation

dynamics were also characterized via similar parameters (i.e., kernel N accumulation N rate -KNAR- and kernel N accumulation duration -KNAD-) in order to determine possible interactions with DM allocation, given that kernels are active N sink tissues as well (Crawford et al., 1982; Below et al., 2000).

4.5.1 Overview of Responses to N Timing Application and Plant Density Treatments

Across experiments, N rate treatments produced the strongest effects on both DM and N accumulation in kernels (Fig. 4.1-4.7), regardless of: a) the time when the fertilizer was applied (Exp. 1), b) the competition for resources by changes in plant density (Exp. 2 and 3), and c) their respective interactions with N rate (all non-significant, Tables 4.2, 4.3 and 4.4). While late-season, split N applications have been associated with higher N recovery efficiencies due to increased post-silking N uptake (Mueller et al., 2017), split applications explored in Exp. 1 did not produce any benefits in either R3 N uptake or post-R3 N uptake when compared to the at-planting N application (Table 4.2), explaining in part the lack of N timing effect on both final KNC and kernel N accumulation dynamics (i.e., rate and duration). The lack of N timing effect on KW (as well as on KN) represented a more common outcome, as these management practices are less likely to increase final GY (Mueller et al., 2017; Fernandez et al., 2019). To the best of our knowledge, no other studies had previously tested kernel DM accumulation parameters during grain fill (i.e., GFD and EFGR) under differences in N timing applications alone or combined with N rate.

In terms of plant density effects, usually associated with source-sink balances reflecting assimilate availability for the kernels to grow, decreases in KW by changes in EGFR and/or GFD under higher plant densities (i.e., less resources per kernel) have been well documented (Poneleit and Egli, 1979; Borrás et al., 2003; Sala et al., 2007). Nevertheless, in our study, the higher plant density only reduced final KW in Exp. 2, with no effect on KNC (Table 4.3), while the opposite pattern was found in Exp. 3 (i.e., no effect on KW and reduced KNC under higher plant stand, Table 4.4). Despite the latter inconsistency, when nonlinear regression models were fit into kernel DM and N data discriminating by N rate x plant density treatment combination, both Exp. 2 and 3 showed the same pattern: DM and N accumulation dynamics increased with N rate at both plant densities, with no plant density differences in these parameters under the same N rate. Conversely, our results differed from a recent report where grain-filling parameters were determined under combinations of three N rates (ranging from 0 to 360 kg N ha^{-1}) and two plant densities (6.8 vs 9.8

plant m^{-2}) (Wei et al., 2019). In that study, KW was changed by plant population, N rate, and their respective interaction, with the effect of density being the strongest, and EGFR proving to be the most affected parameter. Nevertheless, the lack of plant density effect in our results could be explained by the fact that plant density effects can be proportionally different on GFD and EGFR depending on the position in the ear from where the kernels were collected (Chen et al., 2013). In the latter study, much larger decreases in KW due to increases in plant density were registered in kernels coming from the basal and apical ear sections than those coming from the middle (where all our kernel samples were collected). This differential response can be explained by differences in pollination timing along the rachis, where middle-section kernels start growth earlier, thus having the advantage of enough assimilate supply even under limiting conditions (Chen et al., 2013).

4.5.2 N Rate Effects on Kernel Dry Matter and N Accumulation Dynamics

Final KW was significantly increased by N rate in all three experiments (Tables 4.2, 4.3 and 4.4). This strong, consistent response is in line with the concept that modern, high-yielding maize hybrids have more flexible KWs than older genotypes (Echarte et al., 2006; Chen et al., 2016a). This is further supported by the fact that the hybrid used in our study, commercially released in 2015, achieved high yields of 15.7-16.6 Mg ha^{-1} in two out of three seasons (2017 and 2018, respectively), while averaging an increase of 8.1 Mg ha^{-1} in response to N (i.e., from 0N to 224N) over the complete 3-year experimental period. In addition, GY variability was largely explained by KW in all experiments, as shown by the r=0.9 from correlation analysis (Table 4.5).

However, the most novel kernel DM and Kernel N findings in our research came about because of the intensive individual kernel sampling during the linear grain-filling period in all three experiments. The subsequent modeling of kernel dynamics of simultaneous DM and N gains in response to N rate treatments provided new clarity on the underlying rate and duration processes.

Accordingly, kernel DM accumulation dynamics were demonstrably affected by N rate treatments (Fig. 4.1, 4.3 and 4.5). However, depending on the season, two different mechanisms were detected: DM accumulation in kernels responded to N supply either via changes in both EGFR and GFD (Exp. 1, Fig. 4.1 and 4.7), or via changes in GFD alone (Exp. 2 and 3, Fig. 4.3, 4.5, and 4.7). Similarly to Exp. 1, Melchiori and Caviglia (2008) reported that changes in KW resulted from changes in both parameters, though EGFR was more related to KW than GFD in one

growing season, and the opposite pattern was detected the following year. In our study, correlation analysis denoted that both parameters were highly associated with KW, though the fact that GFD was improved with N rates in all three experiments might explain its slightly higher Pearson's coefficient (Table 4.5). In addition, Liu et al. (2011) also found that EGFR and GFD were increased under N fertilization, thus enhancing final KW. Furthermore, these authors reported that positive N nutrition effects on KW were even bigger when fertilization included P and K.

EGFR is associated with potential sink capacity defined earlier in the reproductive season (Jones et al., 1985, 1996). Therefore, changes in this parameter would reflect N treatment effects on potential KW determination that happened during the lag phase (Chapter 3) rather than responses to actual growing conditions during the linear period. This could be further supported by the lack of correlation between EGFR and all whole-plant parameters (neither DM nor N) (Table 4.5).

Changes in kernel DM accumulation in response to the actual N conditions of the linear period could then be explained by the differences found in GFD (Fig. 4.7). Once the potential KW is set in the lag phase (and, as a consequence, a particular EGFR defined), DM deposition in kernels would depend on the availability of assimilates per kernel during the grain-filling period (Borrás et al., 2004). Therefore, under higher N supply, indirect N effects on KW via larger GFD could be explained by a longer leaf N retention (i.e., delayed remobilization) (DeBruin et al., 2017; Mueller et al., 2019), a greater post-silking N uptake, and an extended photosynthetic capacity. Modern hybrids are able to retain N longer (i.e., increased leaf area duration) due to their greater use of stem N in early reproductive stages (Mueller et al., 2019; Fernandez et al., 2020). In our study, this mechanism was initially supported by the gains detected in all four whole-plant variables under higher N rate: R3 biomass, post-R3 plant growth, R3 N uptake and post-R3 N uptake (Tables 4.2, 4.3 and 4.4). Moreover, another evidence came from the correlation analysis since GFD proved to be highly associated with both $PG_{R3.R6}$ and PNU_{R3} (Table 4.5).

KNC was also strongly affected by soil N supply (Tables 4.2, 4.3 and 4.4), thus mirroring both KW and GY responses. Given the importance of this physiological parameter, abundant research has been done around the sources of KNC (Crawford et al., 1982; Rajcan and Tollenaar, 1999a; Pommel et al., 2006; Ciampitti and Vyn, 2013; Yang et al., 2016). However, the dynamics of N accumulation on a per-kernel basis (i.e., KNAD and KNAR) have been less frequently considered in field experiments. Moreover, from the few cases where KNC was determined

periodically during the grain-filling period (Chen et al., 2016b; Ning et al., 2017, 2021), only one study had formally modeled these data as a function of days after silking (Ning et al., 2017). Therefore, to the best of our knowledge, our study represented the first effort to describe KNC over the grain-filling period by estimating KNAD and KNAR characterization parameters on a thermal-time basis.

Overall, kernel N accumulation followed a pattern similar to that of DM (Fig. 4.2, 4.4 and 4.6): kernels actively imported N assimilates for most of the grain-filling period, until N accumulation reached a plateau near physiological maturity. While kernel N accumulation dynamics were strongly affected by N rate treatments (similarly to DM dynamics), one consistent mechanism was detected across experiments: both parameters (KNAR and KNAD) increased with N rate (Fig. 4.7). Furthermore, final KNC was correlated with both KNAD and KNAR, but the stronger association was with the latter (Table 4.5).

A strong association between GFD and KNAD was observed in the correlation analyses between DM and N parameters. This supported the fact that N was actively imported by kernels in tandem with carbohydrate assimilates until late in the reproductive period. The association between EGFR and KNAR was also significant, showing a correlation slightly higher than that between the durations (Table 4.5). The strong relationship between kernel DM and N accumulation rates detected in our study is consistent with the fact that transport rates of total carbohydrates and amino acids into the endosperm are linearly related during the effective grain-filling period (Seebauer et al., 2010).

Finally, the tight interaction between kernel DM and N accumulation dynamics was further confirmed by another key finding in our study: final KW was highly correlated with KNAR (r=0.96). The latter suggested that the N flux to the kernel during the linear period clearly limits the realization of final KW. This agrees with a similar conclusion (i.e., that kernel C accumulation in N deficient plants might be limited by kernel N availability) reached by Ning et al. (2021) because, in their case, kernel C:N ratios increased as final KW dropped under low N supply conditions. Besides the stoichiometric hypothesis proposed by these authors, limitation of DM accumulation in kernels by N deficiency could also be related to the portion of allocated N that is used within the kernel tissues as substrate for synthesis of enzymes (Cazetta et al., 1999; Below et al., 2000).

Overall, our results provide new complementary evidences towards a better understanding of the physiological mechanisms behind KW determination as affected by N availability. By following an intensive ear sampling protocol, we were able to accurately estimate parameters such as kernel N accumulation rate and duration, that helped us further characterize the intertwined interactions between DM and N during the effective grain-filling period.

4.6 References

Andrade, F. H., and Ferreiro, M. A. (1996). Reproductive growth of maize, sunflower and soybean at different source levels during grain filling. *F. Crop. Res.* 48, 155–165.

Below, F. E., Cazetta, J. O., and Seebauer, J. R. (2000). Carbon/nitrogen interactions during ear and kernel development of maize. *Crop Sci.*, 15–24. doi:10.2135/cssaspecpub29.c2.

Bonelli, L. E., Monzon, J. P., Cerrudo, A., Rizzalli, R. H., and Andrade, F. H. (2016). Maize grain yield components and source-sink relationship as affected by the delay in sowing date. *F. Crop. Res.* 198, 215–225. doi:10.1016/j.fcr.2016.09.003.

Borrás, L., and Gambín, B. L. (2010). Trait dissection of maize kernel weight: Towards integrating hierarchical scales using a plant growth approach. *F. Crop. Res.* 118, 1–12. doi:10.1016/j.fcr.2010.04.010.

Borrás, L., Slafer, G. A., and Otegui, M. E. (2004). Seed dry weight response to source-sink manipulations in wheat, maize and soybean: A quantitative reappraisal. *F. Crop. Res.* 86, 131–146. doi:10.1016/j.fcr.2003.08.002.

Borrás, L., and Westgate, M. E. (2006). Predicting maize kernel sink capacity early in development. *F. Crop. Res.* 95, 223–233. doi:10.1016/j.fcr.2005.03.001.

Borrás, L., Westgate, M. E., and Otegui, M. E. (2003). Control of kernel weight and kernel water relations by post-flowering source-sink ratio in maize. *Ann. Bot.* 91, 857–867. doi:10.1093/aob/mcg090.

Borrás, L., Zinselmeier, C., Senior, M. L., Westgate, M. E., and Muszynski, M. G. (2009). Characterization of grain-filling patterns in diverse maize germplasm. *Crop Sci.* 49, 999–1009. doi:10.2135/cropsci2008.08.0475.

Cazetta, J. O., Seebauer, J. R., and Below, F. E. (1999). Sucrose and nitrogen supplies regulate growth of maize kernels. *Ann. Bot.* 84, 747–754. doi:10.1006/anbo.1999.0976.

Cerrudo, A., Di Matteo, J., Fernandez, E., Robles, M., Olmedo Pico, L., and Andrade, F. H. (2013). Yield components of maize as affected by short shading periods and thinning. *Crop Pasture Sci.* 64, 580–587. doi:10.1071/CP13201.

Chapman, S. C., and Edmeades, G. O. (1999). Selection improves drought tolerance in tropical maize populations: II. Direct and correlated responses among secondary traits. *Crop Sci.* 39, 1315–1324. doi:10.2135/cropsci1999.3951315x.

Chen, K., Camberato, J. J., Tuinstra, M. R., Kumudini, S. V., Tollenaar, M., and Vyn, T. J. (2016a). Genetic improvement in density and nitrogen stress tolerance traits over 38 years of commercial maize hybrid release. *F. Crop. Res.* 196, 438–451. doi:10.1016/j.fcr.2016.07.025.

Chen, Q., Mu, X., Chen, F., Yuan, L., and Mi, G. (2016b). Dynamic change of mineral nutrient content in different plant organs during the grain filling stage in maize grown under contrasting nitrogen supply. *Eur. J. Agron.* 80, 137–153. doi:10.1016/J.EJA.2016.08.002.

Chen, Y., Hoogenboom, G., Ma, Y., Li, B., and Guo, Y. (2013). Maize kernel growth at different floret positions of the ear. *F. Crop. Res.* 149, 177–186. doi:10.1016/J.FCR.2013.04.028.

Ciampitti, I. A., and Vyn, T. J. (2013). Grain nitrogen source changes over time in maize: A review. *Crop Sci.* 53, 366–377. doi:10.2135/cropsci2012.07.0439.

Crawford, T. W., Rendig, V. V., and Broadbent, F. E. (1982). Sources, fluxes, and sinks of nitrogen during early reproductive growth of maize (Zea mays L.). *Plant Physiol.* 70, 1654–1660. doi:10.1104/pp.70.6.1654.

D'Andrea, K. E., Piedra, C. V., Mandolino, C. I., Bender, R., Cerri, A. M., Cirilo, A. G., et al. (2016). Contribution of reserves to kernel weight and grain yield determination in maize: Phenotypic and genotypic variation. *Crop Sci.* 56, 697–706. doi:10.2135/cropsci2015.05.0295.

de Mendiburu, F. (2020). agricolae: Statistical Procedures for Agricultural Research. R package version 1.3-2. https://CRAN.R-project.org/package=agricolae.

DeBruin, J. L., Schussler, J. R., Mo, H., and Cooper, M. (2017). Grain yield and nitrogen accumulation in maize hybrids released during 1934 to 2013 in the US Midwest. *Crop Sci.* 57, 1431–1446. doi:10.2135/cropsci2016.08.0704.

Echarte, L., Andrade, F. H., Sadras, V. O., and Abbate, P. (2006). Kernel weight and its response to source manipulations during grain filling in Argentinean maize hybrids released in different decades. *F. Crop. Res.* 96, 307–312. doi:10.1016/j.fcr.2005.07.013.

Etheridge, R. D., Pesti, G. M., and Foster, E. H. (1998). A comparison of nitrogen values obtained utilizing the Kjeldahl nitrogen and Dumas combustion methodologies (Leco CNS 2000) on samples typical of an animal nutrition analytical laboratory. *Anim. Feed Sci. Technol.* 73, 21–28. doi:10.1016/S0377-8401(98)00136-9.

Fernandez, J. A., DeBruin, J., Messina, C. D., and Ciampitti, I. A. (2019). Late-season nitrogen fertilization on maize yield: A meta-analysis. *F. Crop. Res.*, 107586. doi:10.1016/J.FCR.2019.107586.

Fernandez, J. A., Messina, C. D., Rotundo, J., and Ciampitti, I. A. (2020). Integrating nitrogen and water-soluble carbohydrates dynamics in maize: A comparison between hybrids from different decades. *Crop Sci.*, 1–14. doi:10.1002/csc2.20338.

Fernie, A. R., Bachem, C. W. B., Helariutta, Y., Neuhaus, H. E., Prat, S., Ruan, Y. L., et al. (2020). Synchronization of developmental, molecular and metabolic aspects of source–sink interactions. *Nat. Plants* 6, 55–66. doi:10.1038/s41477-020-0590-x.

Frey, N. M. (1981). Dry matter accumulation in kernels of maize. *Crop Sci.* 21, 118–122. doi:10.2135/cropsci1981.0011183x002100010032x.

Gambín, B. L., Borrás, L., and Otegui, M. E. (2007). Kernel water relations and duration of grain filling in maize temperate hybrids. *F. Crop. Res.* 101, 1–9. doi:10.1016/j.fcr.2006.09.001.

Hisse, I. R., D'Andrea, K. E., and Otegui, M. E. (2019). Source-sink relations and kernel weight in maize inbred lines and hybrids: Responses to contrasting nitrogen supply levels. *F. Crop. Res.* 230, 151–159. doi:10.1016/J.FCR.2018.10.011.

INClimate - The Indiana State Climate Office Purdue Mesonet. https://ag.purdue.edu/indiana-state-climate/. Available at: https://iclimate.org/.

Johnson, D. R., and Tanner, J. W. (1972). Calculation of the rate and duration of grain filling in corn (Zea mays L.). *Crop Sci.* 12, 485–486. doi:10.2135/cropsci1972.0011183x001200040028x.

Jones, R. J., Roessler, J., and Ouattar, S. (1985). Thermal environment during endosperm cell division in maize: effects on number of endosperm cells and starch granules. *Crop Sci.* 25, 830–834. doi:10.2135/cropsci1985.0011183x002500050025x.

Jones, R. J., Schreiber, B. M. N., and Roessler, J. A. (1996). Kernel sink capacity in maize: Genotypic and maternal regulation. *Crop Sci.* 36, 301–306. doi:10.2135/cropsci1996.0011183X003600020015x.

Liu, K., Ma, B. L., Luan, L., and Li, C. (2011). Nitrogen, phosphorus, and potassium nutrient effects on grain filling and yield of high-yielding summer corn. *J. Plant Nutr.* 34, 1516–1531. doi:10.1080/01904167.2011.585208.

Melchiori, R. J. M., and Caviglia, O. P. (2008). Maize kernel growth and kernel water relations as affected by nitrogen supply. *F. Crop. Res.* 108, 198–205. doi:10.1016/j.fcr.2008.05.003.

Miguez, F. (2021). nlraa: An R package for Nonlinear Regression Applications in Agricultural Research. Available at: https://cran.r-project.org/package=nlraa.

Muchow, R. C. (1990). Effect of high temperature on grain-growth in field-grown maize. *F. Crop. Res.* 23, 145–158. doi:10.1016/0378-4290(90)90109-O.

Mueller, S. M., Camberato, J. J., Messina, C., Shanahan, J., Zhang, H., and Vyn, T. J. (2017). Late-split nitrogen applications increased maize plant nitrogen recovery but not yield under moderate to high nitrogen rates. *Agron. J.* 109, 2689. doi:10.2134/agronj2017.05.0282.

Mueller, S. M., Messina, C. D., and Vyn, T. J. (2019). Simultaneous gains in grain yield and nitrogen efficiency over 70 years of maize genetic improvement. *Sci. Rep.* 9, 9095. doi:10.1038/s41598-019-45485-5.

Ning, P., Fritschi, F. B., and Li, C. (2017). Temporal dynamics of post-silking nitrogen fluxes and their effects on grain yield in maize under low to high nitrogen inputs. *F. Crop. Res.* 204, 249–259. doi:10.1016/j.fcr.2017.01.022.

Ning, P., Maw, M. J. W., Yang, L., and Fritschi, F. B. (2021). Carbon accumulation in kernels of low-nitrogen maize is not limited by carbon availability but by an imbalance of carbon and nitrogen assimilates. *J. Plant Nutr. Soil Sci.*, 1–10. doi:10.1002/jpln.202000112.

NOAA National Centers for Environmental Information Climate Data Online (CDO). https://www.ncdc.noaa.gov/cdo-web/. Available at: https://www.ncdc.noaa.gov/cdo-web/.

Otegui, M. E. (1995). Prolificacy and grain yield components in modern Argentinian maize hybrids. *Maydica* 40, 371–376.

Pan, W. L., Camberato, J. J., Jackson, W. A., and Moll, R. H. (1986). Utilization of previously accumulated and concurrently absorbed nitrogen during reproductive growth in maize. *Plant Physiol.* 82, 247–253. doi:10.1104/pp.82.1.247.

Paul, M. J., and Foyer, C. H. (2001). Sink regulation of photosynthesis. *J. Exp. Bot.* 52, 1383–1400. doi:10.1093/jexbot/52.360.1383.

Pommel, B., Gallais, A., Coque, M., Quilleré, I., Hirel, B., Prioul, J. L., et al. (2006). Carbon and nitrogen allocation and grain filling in three maize hybrids differing in leaf senescence. *Eur. J. Agron.* 24, 203–211. doi:10.1016/j.eja.2005.10.001.

Poneleit, C. G., and Egli, D. B. (1979). Kernel growth rate and duration in maize as affected by plant density and genotype. *Crop Sci.* 19, 385–388. doi:10.2135/cropsci1979.0011183x001900030027x.

R Core Team (2019). R: A language and environment for statistical computing. R Foundation for Statistical Computing, Vienna, Austria. https://www.R- project.org/.

Rajcan, I., and Tollenaar, M. (1999a). Source: Sink ratio and leaf senescence in maize: II. Nitrogen metabolism during grain filling. *F. Crop. Res.* 60, 255–265. doi:10.1016/S0378-4290(98)00143-9.

Rajcan, I., and Tollenaar, M. (1999b). Source:sink ratio and leaf senescence in maize: I. Dry matter accumulation and partitioning during grain filling. *F. Crop. Res.* 60, 255–265. doi:10.1016/s0378-4290(98)00143-9.

Rattalino Edreira, J. I., Mayer, L. I., and Otegui, M. E. (2014). Heat stress in temperate and tropical maize hybrids: Kernel growth, water relations and assimilate availability for grain filling. *F. Crop. Res.* 166, 162–172. doi:10.1016/j.fcr.2014.06.018.

Reddy, V., and Daynard, T. (1983). Endosperm characteristics associated with rate of grain filling and kernel size in corn. *Maydica* 28, 339–355. doi:10.11693/hyhz20181000233.

Ritchie, S. W., and Hanway, J. J. (1982). How a corn plant develops. Iowa State University of Science and Technology. Cooperative Extension Service, Iowa, EEUU. Special Report N°48. 1982.

Sadras, V. O. (2007). Evolutionary aspects of the trade-off between seed size and number in crops. *F. Crop. Res.* 100, 125–138. doi:10.1016/j.fcr.2006.07.004.

Sala, R. G., Westgate, M. E., and Andrade, F. H. (2007). Source/sink ratio and the relationship between maximum water content, maximum volume, and final dry weight of maize kernels. *F. Crop. Res.* 101, 19–25. doi:10.1016/j.fcr.2006.09.004.

Seebauer, J. R., Singletary, G. W., Krumpelman, P. M., Ruffo, M. L., and Below, F. E. (2010). Relationship of source and sink in determining kernel composition of maize. *J. Exp. Bot.* 61, 511–519. doi:10.1093/jxb/erp324.

Singletary, G. W., and Below, F. E. (1990). Nitrogen-induced changes in the growth and metabolism of developing maize kernels grown in vitro. *Plant Physiol.* 92, 160–167. doi:10.1104/pp.92.1.160.

Tollenaar, M. (1977). Sink-source relationships during reproductive development in maize. A review. *Maydica* 22, 49–75.

Uhart, S. A., and Andrade, F. H. (1995). Nitrogen and carbon accumulation and remobilization during grain filling in maize under different source/sink ratios. *Crop Sci.* 35, 183–190. doi:10.2135/cropsci1995.0011183X003500010034x.

Wang, J., Kang, S., Du, T., Tong, L., Ding, R., and Li, S. (2019). Estimating the upper and lower limits of kernel weight under different water regimes in hybrid maize seed production. *Agric. Water Manag.* 213, 128–134. doi:10.1016/j.agwat.2018.09.014.

Wei, S., Wang, X., Li, G., Qin, Y., Jiang, D., and Dong, S. (2019). Plant density and nitrogen supply affect the grain-filling parameters of maize kernels located in different ear positions. *Front. Plant Sci.* 10, 180. doi:10.3389/fpls.2019.00180.

Westgate, M. E., and Boyer, J. S. (1986a). Reproduction at low silk and pollen water potentials in maize. *Crop Sci.* 26, 951–956. doi:10.2135/cropsci1986.0011183x002600050023x.

Westgate, M. E., and Boyer, J. S. (1986b). Water status of the developing grain of maize. *Agron. J.* 78, 714–719. doi:10.2134/agronj1986.00021962007800040031x.

Yang, L., Guo, S., Chen, Q., Chen, F., Yuan, L., and Mi, G. (2016). Use of the stable nitrogen isotope to reveal the source-sink regulation of nitrogen uptake and remobilization during grain filling phase in maize. *PLoS One* 11, 1–16. doi:10.1371/journal.pone.0162201.

Zhou, B., Yue, Y., Sun, X., Wang, X., Wang, Z., Ma, W., et al. (2016). Maize grain yield and dry matter production responses to variations in weather conditions. *Agron. J.* 108, 196–204. doi:10.2134/agronj2015.0196.

4.7 Tables and Figures

Table 4.1. Characteristics of the field experiments. Each experiment was conducted under a split-plot arrangement of treatments. Respective whole plot and sub-plot factors are detailed for each experiment.

	Location	**Planting Date**	**Plant Density**	**N Rate**	**N Timing Application**	**Plot Size**	**Reps**
Experiment 1	LaCrosse, IN	16 May, 2017	8.3 plants m^{-2}	*Sub-plot*: 0 112 kg N ha^{-1} 224 kg N ha^{-1}	*Main plot:* At planting Split between planting and V6 Last 56 kg N ha^{-1} applied at V12	12 rows 0.76 m row width 228 m row length	3
Experiment 2	West Lafayette, IN	8 May, 2018	*Sub-plot:* 7.9 plants m^{-2} 10.4 plants m^{-2}	*Main plot:* 0 84 kg N ha^{-1} 168 kg N ha^{-1} 224 kg N ha^{-1}	At planting	4 rows 0.76 m row width 14.5 m row length	3
Experiment 3	West Lafayette, IN	3 June, 2019	*Sub-plot:* 7.9 plants m^{-2} 10.4 plants m^{-2}	*Main plot:* 0 84 kg N ha^{-1} 168 kg N ha^{-1} 224 kg N ha^{-1}	At planting	4 rows 0.76 m row width 14.5 m row length	3

Table 4.2. ANOVA for grain yield (GY, Mg ha^{-1}, 15.5% moisture), kernel number per plant (KNP, grain $plant^{-1}$), kernel weight (KW, mg $grain^{-1}$), kernel N concentration (KNc, %), kernel N content (KNC, mg N $grain^{-1}$), plant growth at R3 (PG_{R3}, g $plant^{-1}$), plant growth during the effective grain filling period ($PG_{R3.R6}$, g $plant^{-1}$), plant N uptake at R3 (PNU_{R3}, g N $plant^{-1}$), and plant N uptake during the effective grain filling ($PNU_{R3.R6}$, g N $plant^{-1}$) in Experiment 1 (LaCrosse, IN, 2017).

	GY	**KNP**	**KW**	**KNc**	**KNC**	**PG_{R3}**	**$PG_{R3.R6}$**	**PNU_{R3}**	**$PNU_{R3.R6}$**
N Timing Application									
Planting	10.5	483	261.1	1.05	2.82	170	61	1.58	0.47
Planting_V6	11.3	468	274.4	1.08	3.05	168	71	1.64	0.56
Planting_V12	11.2	492	263.4	1.08	2.92	166	65	1.60	0.50
N Rate **(kg N ha^{-1})**									
0N	5.3 c	314 b	213.3 c	0.80 c	1.71 c	124 b	15 c	0.72 c	0.15 c
112N	11.9 b	560 a	271.3 b	1.11 b	3.02 b	186 a	78 b	1.85 b	0.43 b
224N	15.7 a	569 a	314.3 a	1.29 a	4.07 a	193 a	103 a	2.24 a	0.96 a
F-test									
N Timing (T)	ns	ns	ns	ns	ns	ns	ns	ns	ns
N Rate (N)	<.001	<.001	<.001	<.001	<.001	<.001	<.001	<.001	<.001
T x N	ns	ns	ns	ns	ns	ns	ns	ns	ns

ns: not significant at α=0.05, p-value for F-test is >0.05. Means separation determined by Fisher's least significant difference (LSD) at α=0.05. Same letter or absence of letter means no significant difference was found among levels. For all variables, three replicates were collected (n=3, N=27).

Table 4.3. ANOVA for grain yield (GY, Mg ha^{-1}, 15.5% moisture), kernel number per plant (KNP, grain $plant^{-1}$), kernel weight (KW, mg $grain^{-1}$), kernel N concentration (KNc, %), kernel N content (KNC, mg N $grain^{-1}$), plant growth at R3 (PG_{R3}, g $plant^{-1}$), plant growth during the effective grain filling period ($PG_{R3.R6}$, g $plant^{-1}$), plant N uptake at R3 (PNU_{R3}, g N $plant^{-1}$), and plant N uptake during the effective grain filling ($PNU_{R3.R6}$, g N $plant^{-1}$) in Experiment 2 (West Lafayette, IN, 2018).

	GY	**KNP**	**KW**	**KNc**	**KNC**	**PG_{R3}**	**$PG_{R3.R6}$**	**PNU_{R3}**	**$PNU_{R3.R6}$**
N Rate **(kg N ha^{-1})**									
0N	7.4 d	255 c	267.7 b	0.86 c	2.29 c	119 c	29 b	0.77 c	0.13 b
84N	11.4 c	356 b	283.9 b	0.95 b	2.70 b	143 b	54 b	1.20 b	0.20 b
168N	15.3 b	475 a	309.6 a	1.13 a	3.50 a	164 ab	87 a	1.94 a	0.28 b
224N	16.6 a	505 a	318.3 a	1.15 a	3.65 a	165 a	110 a	2.03 a	0.64 a
Plant Density **(plant m^{-2})**									
7.9D	12.8	455 a	301.7 a	1.03	3.13	163 a	86 a	1.70 a	0.37
10.4D	12.5	340 b	288.0 b	1.01	2.95	131 b	54 b	1.26 b	0.25
F-test									
N Rate (N)	<.001	<.001	0.002	<.001	<.001	0.005	0.004	<.001	0.026
Density (D)	ns	<.001	0.010	ns	ns	<.001	0.001	0.002	ns
N x D	ns	ns	ns	ns	ns	ns	ns	ns	ns

ns: not significant at α=0.05, p-value for F-test is >0.05. Means separation determined by Fisher's least significant difference (LSD) at α=0.05. Same letter or absence of letter means no significant difference was found among levels. For all variables, three replicates were collected (n=3, N=24).

Table 4.4. ANOVA for grain yield (GY, Mg ha^{-1}, 15.5% moisture), kernel number per plant (KNP, grain $plant^{-1}$), kernel weight (KW, mg $grain^{-1}$), kernel N concentration (KNc, %), kernel N content (KNC, mg N $grain^{-1}$), plant growth at R3 (PG_{R3}, g $plant^{-1}$), plant growth during the effective grain filling period ($PG_{R3.R6}$, g $plant^{-1}$), plant N uptake at R3 (PNU_{R3}, g N $plant^{-1}$), and plant N uptake during the effective grain filling ($PNU_{R3.R6}$, g N $plant^{-1}$) in Experiment 3 (West Lafayette, IN, 2019).

	GY	**KNP**	**KW**	**KNc**	**KNC**	**PG_{R3}**	**$PG_{R3.R6}$**	**PNU_{R3}**	**$PNU_{R3.R6}$**
N Rate **(kg N ha^{-1})**									
0N	7.5 c	288 c	264.9 c	0.88 c	2.34 c	127 b	26 b	0.88 b	0.10
84N	9.5 b	342 b	282.3 b	0.95 bc	2.68 bc	131 b	47 a	1.06 b	0.20
168N	11.0 ab	406 a	295.3 ab	1.06 ab	3.12 ab	169 a	47 a	1.66 a	0.19
224N	12.2 a	424 a	299.2 a	1.16 a	3.48 a	167 a	60 a	1.84 a	0.20
Plant Density **(plant m^{-2})**									
7.9D	10.0	405 a	287.6	1.03	2.97 a	162 a	50	1.51 a	0.20
10.4D	10.1	325 b	283.2	1.00	2.84 b	135 b	39	1.21 b	0.14
F-test									
N Rate (N)	0.004	<.001	0.008	0.008	0.004	<.001	0.011	0.002	ns
Density (D)	ns	<.001	ns	ns	0.012	<.001	ns	0.012	ns
N x D	0.024	ns	ns	ns	ns	ns	ns	ns	ns

ns: not significant at α=0.05, p-value for F-test is >0.05. Means separation determined by Fisher's least significant difference (LSD) at α=0.05. Same letter or absence of letter means no significant difference was found among levels. For all variables, three replicates were collected (n=3, N=24).

Table 4.5. Correlation analysis between physiological parameters obtained in Exp. 1, 2 and 3 (N=11). Data included: a) main N rate means of grain yield (GY, Mg ha^{-1}, 15.5% moisture), kernel number per plant (KNP, grain $plant^{-1}$), kernel weight (KW, mg $grain^{-1}$), kernel N content (KNC, mg N $grain^{-1}$), plant growth at R3 (PG_{R3}, g $plant^{-1}$), plant growth during the effective grain filling period ($PG_{R3.R6}$, g $plant^{-1}$), plant N uptake at R3 (PNU_{R3}, g N $plant^{-1}$), and plant N uptake during the effective grain filling ($PNU_{R3.R6}$, g N $plant^{-1}$); b) estimators of effective grain-filling rate (EGFR, mg $^{o}Cday^{-1}$), grain-filling duration (GFD, $^{o}Cday^{-1}$), kernel N accumulation rate (KNAR, mg N ^{o}C day^{-1}), and kernel N accumulation duration (KNAD, $^{o}Cday^{-1}$) obtained by nonlinear regression. Pairwise Pearson's coefficients (r) are located above the diagonal. Significance results are located below the diagonal.

	GY	**KNP**	**KW**	**KNC**	**EGFR**	**GFD**	**KNAD**	**KNAR**	**PG_{R3}**	**$PG_{R3.R6}$**	**PNU_{R3}**	**$PNU_{R3.R6}$**
GY		0.84	0.90	0.95	0.63	0.74	0.66	0.84	0.80	0.97	0.93	0.74
KNP	**		0.61	0.83	0.31	0.42	0.64	0.60	0.95	0.90	0.94	0.81
KW	***	*		0.92	0.88	0.91	0.70	0.96	0.65	0.82	0.81	0.56
KNC	***	**	***		0.72	0.79	0.79	0.90	0.86	0.91	0.96	0.75
EGFR	*	ns	***	*		0.80	0.47	0.89	0.41	0.53	0.53	0.37
GFD	**	ns	***	**	**		0.75	0.90	0.49	0.63	0.67	0.27
KNAD	*	*	*	**	ns	**		0.69	0.75	0.62	0.79	0.46
KNAR	**	ns	***	***	***	***	*		0.66	0.74	0.80	0.49
PG_{R3}	**	***	*	***	ns	ns	**	*		0.81	0.95	0.73
$PG_{R3.R6}$	***	***	**	***	ns	*	*	**	**		0.92	0.83
PNU_{R3}	***	***	**	***	ns	*	**	**	***	***		0.75
$PNU_{R3.R6}$	**	**	ns	**	ns	ns	ns	ns	*	**	**	

(ns): p>0.05, (*): p<0.05, (**): p<0.01, (***): p<0.001.

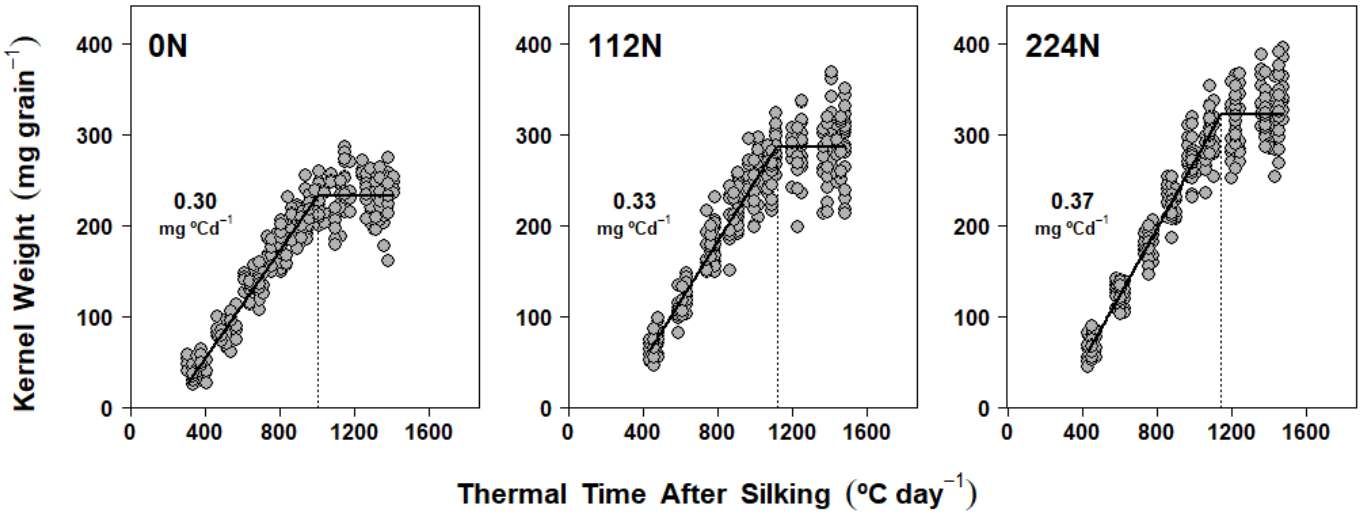

Figure 4.1. Dry matter accumulation in maize kernels in Experiment 1 (LaCrosse, 2017). Each panel shows data obtained from plants grown under one N rate (0, 112, 224 kg N ha^{-1}) applied at three different application timings. Each point represents data from individual kernels. Full lines represent the linear-plateau models that best fitted the data via nonlinear regression analysis. Dotted vertical lines point to the end of the grain-filling duration (GFD). Effective grain-filling rate (EGFR) is shown above each model.

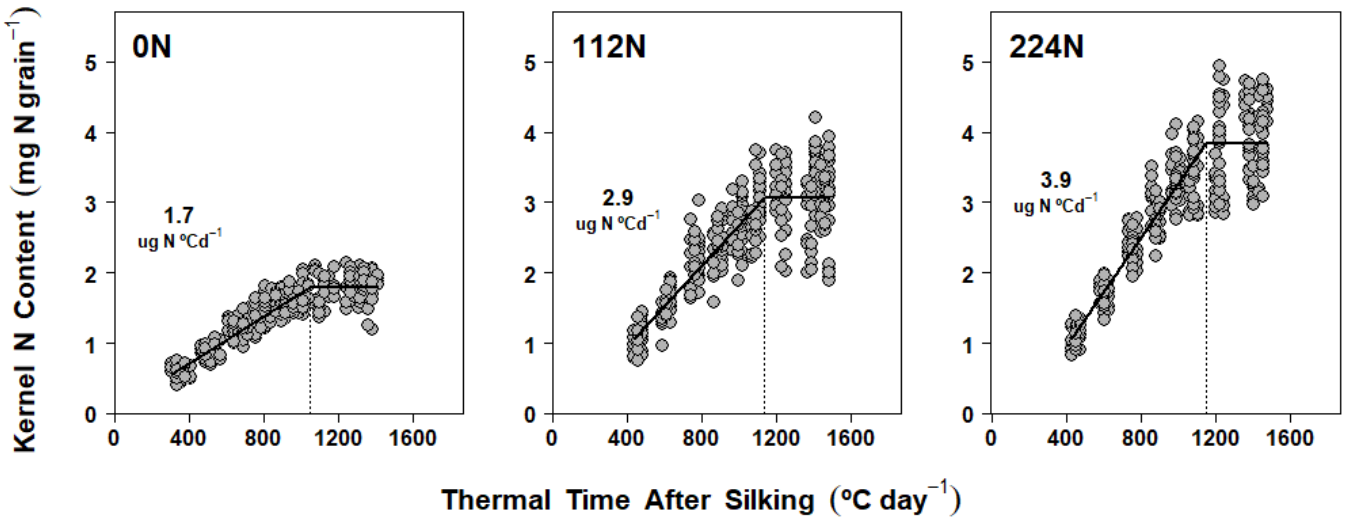

Figure 4.2. N accumulation in maize kernels in Experiment 1 (LaCrosse, 2017). Each panel shows data obtained from plants grown under one N rate (0, 112, 224 kg N ha^{-1}) applied at three different application timings. Each point represents data from individual kernels. Full lines represent the linear-plateau models that best fitted the data via nonlinear regression analysis. Dotted vertical lines point to the end of the kernel N accumulation duration (KNAD). Kernel N accumulation rate (KNAR) is shown above each model.

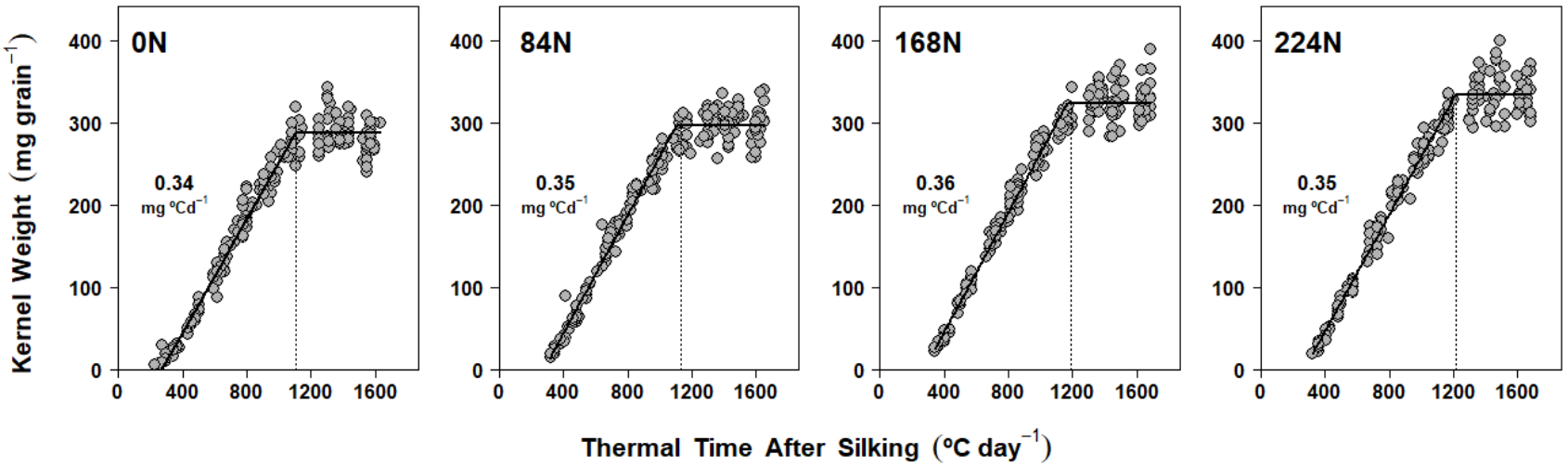

Figure 4.3. Dry matter accumulation in maize kernels in Experiment 2 (West Lafayette, 2018). Each panel shows data obtained from plants grown under one N rate (0, 84, 168, 224 kg N ha^{-1}) at two different plant densities. Each point represents data from individual kernels. Full lines represent the linear-plateau models that best fitted the data via nonlinear regression analysis. Dotted vertical lines point to the end of the grain-filling duration (GFD). Effective grain-filling rate (EGFR) is shown above each model.

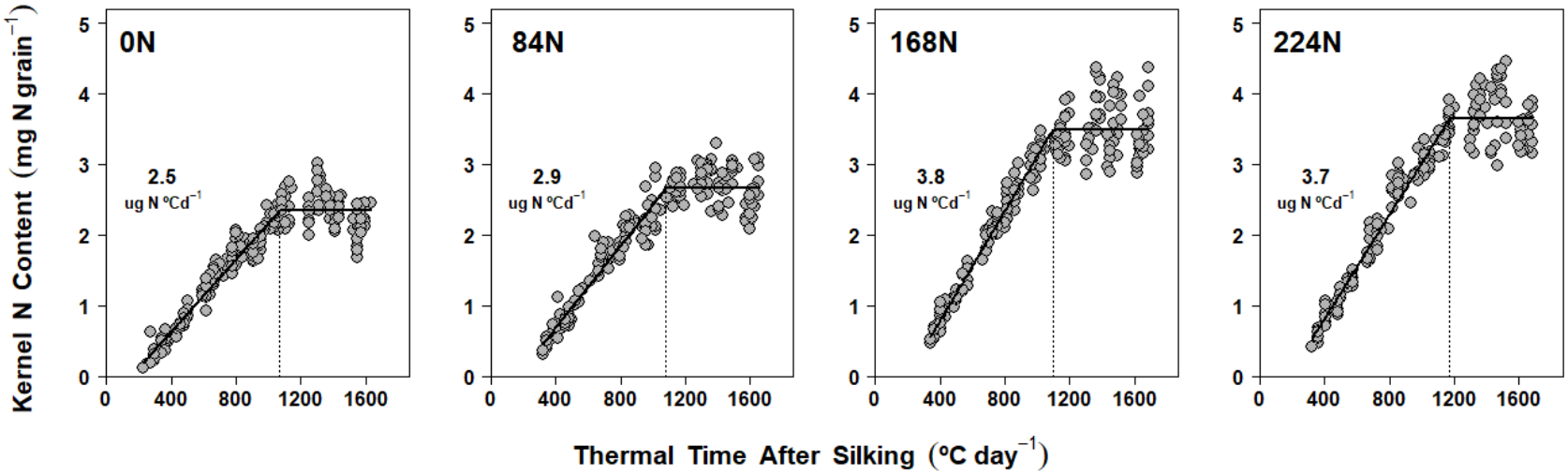

Figure 4.4. N accumulation in maize kernels in Experiment 2 (West Lafayette, 2018). Each panel shows data obtained from plants grown under one N rate (0, 84, 168, 224 kg N ha^{-1}) at two different plant densities. Each point represents data from individual kernels. Full lines represent the linear-plateau models that best fitted the data via nonlinear regression analysis. Dotted vertical lines point to the end of the kernel N accumulation duration (KNAD). Kernel N accumulation rate (KNAR) is shown above each model.

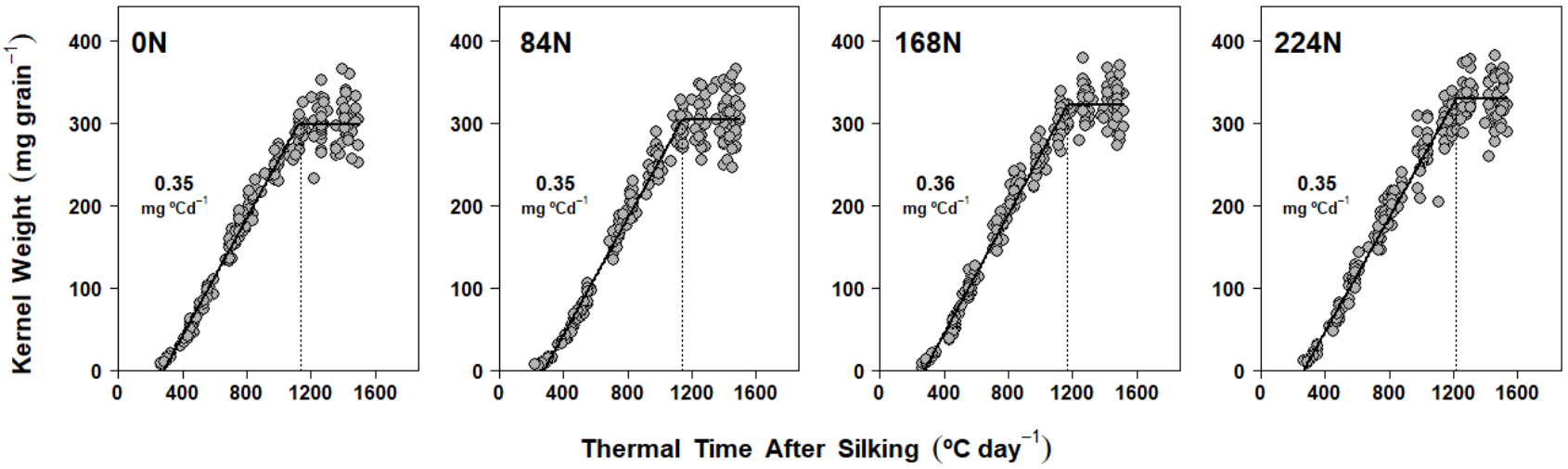

Figure 4.5. Dry matter accumulation in maize kernels in Experiment 3 (West Lafayette, 2019). Each panel shows data obtained from plants grown under one N rate (0, 84, 168, 224 kg N ha^{-1}) at two different plant densities. Each point represents data from individual kernels. Full lines represent the linear-plateau models that best fitted the data via nonlinear regression analysis. Dotted vertical lines point to the end of the grain-filling duration (GFD). Effective grain-filling rate (EGFR) is shown above each model.

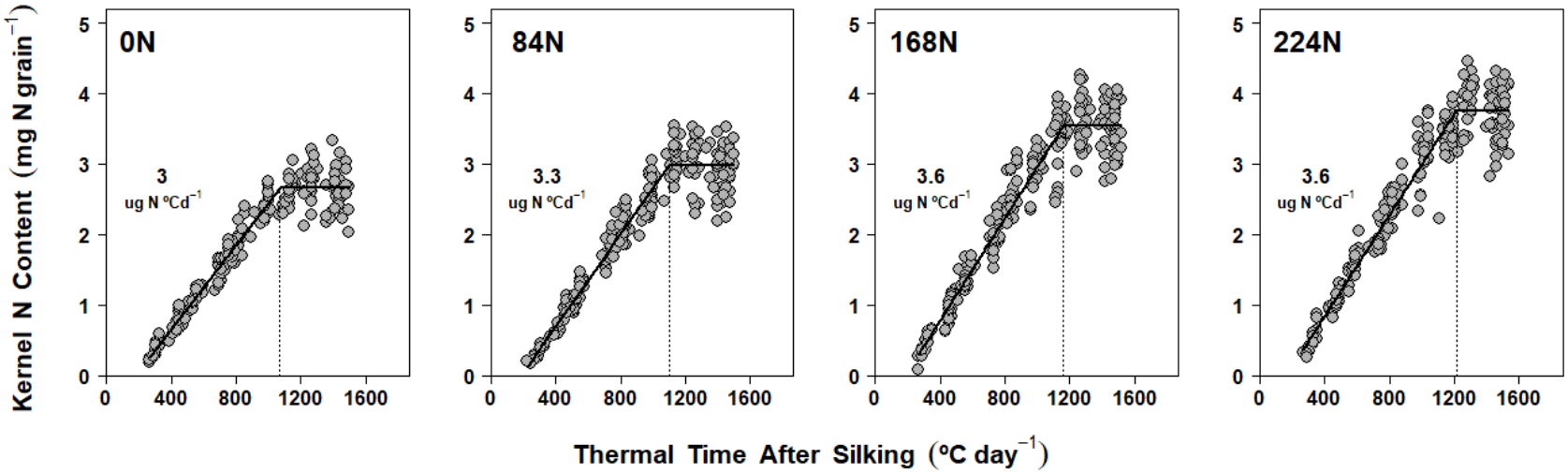

Figure 4.6. N accumulation in maize kernels in Experiment 3 (West Lafayette, 2019). Each panel shows data obtained from plants grown under one N rate (0, 84, 168, 224 kg N ha^{-1}) at two different plant densities. Each point represents data from individual kernels. Full lines represent the linear-plateau models that best fitted the data via nonlinear regression analysis. Dotted vertical lines point to the end of the kernel N accumulation duration (KNAD). Kernel N accumulation rate (KNAR) is shown above each model.

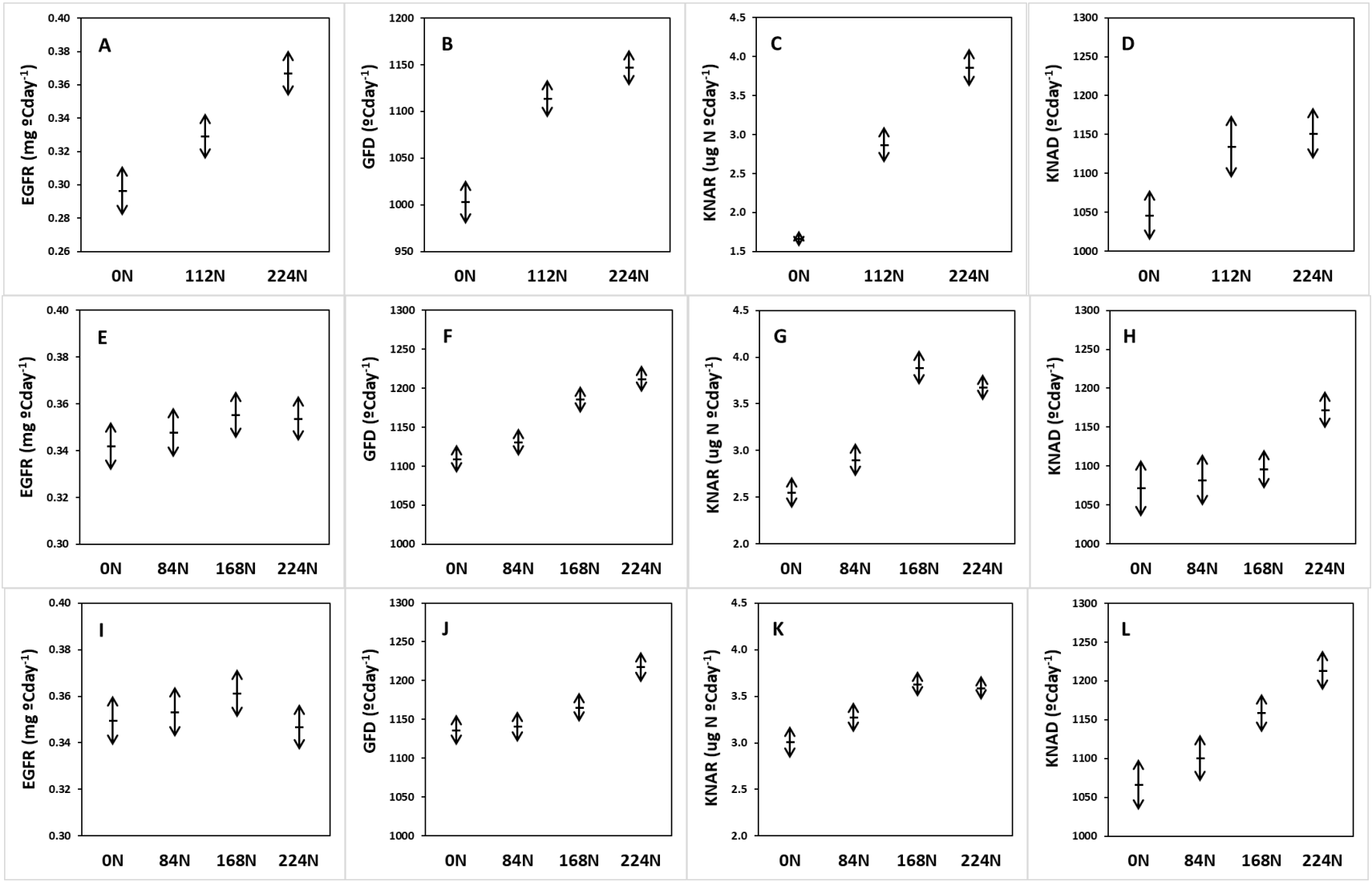

Figure 4.7. Confidence intervals (95%) of the kernel DM and N parameters estimated by nonlinear regression (EGFR: effective grain-filling rate, GFD: grain-filling duration, KNAR: kernel N accumulation rate, KNAD: kernel N accumulation duration). Panels A-D: Experiment 1 (LaCrosse, 2017). Panels E-H: Experiment 2 (West Lafayette, 2018). Panels I-L: Experiment 3 (West Lafayette, 2019).

CHAPTER 5. GENERAL DISCUSSION

5.1 Novel Contributions to Science

This dissertation investigated the physiological determinants of maize kernel weight (KW) as affected by soil N availability over the course of four seasons of field studies. Though historically considered a stable grain yield (GY) component, KW was chosen as the focus of this research due to: 1) its increased importance in the genetic improvement of U.S. temperate germplasm over the last 3-4 decades, which marked a significant shift from the conventional breeding approach based primarily on kernel number (KN) increases; and 2) its increased responsiveness to changes in post-silking growing conditions, which turned it into a more important driver behind within- or between-field GY variability. Therefore, recent evidence of higher KW variability, and its ultimate impact on GY in modern maize hybrids, laid the foundation for this research.

Given that N availability is one of the most common yield-limiting factors affecting maize production worldwide, this dissertation used a combination of N rates, N timing applications, plant densities and locations in order to explore a wide gradient in N supply to the plants. Despite the abundant publications reporting maize responses to N availability from diverse perspectives, N effects on GY components have usually been related to KN and the indirect role of N in building up the photosynthetic capacity for dry matter (DM) production and partitioning to reproductive structures during the critical period of yield determination. Similarly, N effects on KW, though much less explored, have been typically acknowledged more with respect to nitrogen's role in maintaining functional photosynthetic capacity long enough so as to ensure an adequate flux of carbohydrates (i.e., source capacity) for kernel growth. Conversely, we took a more integrative, novel approach to study N effects on KW by returning to the physiological roots of kernel growth and development and tackling not only source capacity, but also sink capacity (potential and actual) on a per kernel basis. Therefore, all three main chapters of this dissertation focused on analyzing N effects in one of those components: Chapter 2, overall DM and N source dynamics; Chapter 3, determination of potential KW; Chapter 4, realization of final KW.

Beginning with source dynamics, Chapter 2 introduces the first field study of this dissertation which was conducted during the 2016 and 2017 growing seasons. This experiment

involved five N rates between 0 and 280 kg N ha^{-1}, each applied at three different timings. Aside from the wider-than-usual N rate gradient, this experiment's novelty lay in its approach for capturing DM and N reproductive dynamics according to the specific growth dynamics of kernels, the main reproductive sink tissues allocating both C and N. Biomass samples of plant components were taken not only at the conventional R1 and R6 stages, but also at early R3 which marked the end of the lag phase and the onset of the effective grain-filling period. By calculating post-silking DM production (PostDM), post-silking N uptake (PostN), and DM and N remobilization (RemDM and RemN, respectively) separately from R1-R3 and then from R3-R6, we were able to detect key differential partitioning patterns between these two grain-filling phases. One novel finding about the lag phase was the fact that, proportionally, N assimilates were almost entirely partitioned to the reproductive tissues, while significant portions of DM were also allocated to the vegetative tissues. This suggested that the ear was a much stronger sink for N than for DM, a first hint at possible direct N effects in potential KW determination. Additionally, and as expected, increases in N rate positively affected N remobilization and DM accumulation during the linear phase.

The impact of N availability on the determination of potential KW during the lag phase was then explored in Chapter 3. Data collection involved three seasons of field experiments using a single commercial hybrid. Experiment 1 involved a treatment sub-set from the above described 2017 growing season (0, 112, and 224 kg N ha^{-1} applied at the three original timings). Experiments 2 (2018) and 3 (2019) involved four N rates (0, 84, 168, and 224 kg N ha^{-1}, all applied at planting) and two plant densities (7.9 and 10.4 plants m^{-2}). Given that the number of endosperm cells (ECN) formed during the lag phase determines the potential storage capacity of kernels, we measured ECN at 9, 10, 13, and (or) 17 days after silking (DAS). An intensive ear sampling (513 ears collected over the 3-year period) from plants of known silking date was performed, and kernels thus extracted were subject to a precise laboratory procedure involving dissection, dyeing, and enzymatic digestion of endosperm tissues. ECN responded positively to N rate treatments, without detection of any N application timing, plant density, or interaction effects. Furthermore, ECN was highly correlated with both final KW and ear N allocation rate from R1 to R3 across experiments. Because plant nutritional status, and specifically N availability, effects on grain development during the lag phase had usually been studied utilizing in-vitro cultured kernels, our results represented novel findings regarding the direct role of N in kernel sink capacity establishment. Additional original contributions to the physiological mechanisms of KW determination obtained

in all three experiments were: GY variability was largely explained by KW, no trade-offs were detected between KW and KN, and plant growth rate per kernel during the critical period (an indicator of assimilate availability) had no impact on final KW.

The investigations in Chapter 4 proved how the realization of final KW can be limited by N availability during the effective grain-filling period. To do so, another intensive ear sampling from plants of known silking date was carried out in the same experiments described in Chapter 3. This time, ears were collected for kernel removal every 7-8 days for 9-10 weeks from the beginning of R3 stage (2796 ears sampled over the 3-year period). Given that N assimilates are also actively demanded by the kernels during the linear phase, another novel approach taken in this dissertation was to analyze kernel N accumulation dynamics alongside the more common DM filling patterns. While linear plateau models have frequently been used to fit kernel DM data over accumulated thermal time after silking, this was the first time (to the best of our knowledge) that this analysis was performed on kernel N data. This allowed us to describe N accumulation in kernels by similar parameters than those used for DM dynamics (i.e., rate and duration). Relationships between those parameters were also examined to evaluate possible DM and N interactions during kernel growth. Final DM accumulation in kernels changed under soil N availability differences by either increasing both the effective grain-filling rate (EGFR) and grain filling duration (GFD), or by increasing GFD alone. Conversely, kernel N content (KNC) increased consistently under higher N availability because of gains in both kernel N accumulation rate (KNAR) and duration (KNAD). In addition, KNAR was highly responsive to increases in N rate treatments across experiments, being strongly correlated with KW (r=0.96). This novel finding implies that kernel DM accumulation during the linear phase, and therefore final KW, was limited by N assimilate allocation to kernels. Furthermore, KNAR was highly correlated with plant N uptake at R3 (PNU_{R3}), rather than with total post-R3 PNU ($PNU_{R3.R6}$), thus indicating that kernel N demand during the linear grain-filling period was predominantly fulfilled by remobilization of pre-R3 N stored in vegetative tissues.

Overall, this dissertation contributes significantly to a better understanding of the physiological mechanisms that determine final KW in maize at high yield potential by presenting new evidences for the distinct indirect and direct roles that N plays during the reproductive period. The high yield context for our mechanism studies was clear from the high GY (15.7-16.6 Mg ha^{-1}) achieved in two out of three years (2017 and 2018, respectively), plus the average 8.1 Mg ha^{-1}

GY increase in response to N (i.e., from 0N to 224N) over the 3-year period. Indirectly, leaf N is responsible for post-silking photosynthesis, the major source of carbohydrates for the kernels, while stem N reserves help delay leaf senescence by acing as the main reserve buffer for early N remobilization to developing ears. Directly, N assimilates are highly demanded during the lag phase by reproductive tissues to fulfill the endosperm cell division requirements that establish potential KW. Similarly, during the linear phase, N assimilate availability appeared to limit DM deposition in kernels as differences in final KW were explained by changes in both rate and duration of kernel N accumulation. Finally, the strong, consistent response of KW to N rate treatments found across experiments further confirms the importance of this component in explaining GY variability in modern, high-yielding genotypes.

5.2 Major Implications to Agriculture

Results coming from this research have implications in both crop management and breeding. From an agronomic stand point, the importance of KW in explaining GY variability means that management practices should ensure optimum physiological conditions during the grain-filling period. While maize GY potential is normally attributed to plant status in the period bracketing silking, our research proved that KW determination can be as much responsible for GY losses as KN. Therefore, N fertilization practices should be applied with the goal of not only increasing KN, but also KW by enhancing its potential during the lag phase (i.e., higher ECN) and then ensuring its potential being fulfilled through extended canopy photosynthetic capacity (i.e., longer GFD). Furthermore, the fact that kernels actively import N until physiological maturity and that KNAR can limit DM deposition confirms the fact that a specific fertility balance must be reached during the reproductive stages in order to avoid GY reductions due to unrealized KW gains. That is why plant nutrition status, which is typically assessed with ear leaves at R1, should be re-assessed to consider new indicators developed for plant tissue sampling at the R3 stage. Additionally, given KW's greater sensitivity to changes in grain-filling growing conditions, any other management factors (besides N nutrition) that can work towards maintaining a healthy canopy for as long as possible should be considered worth adding into the seasonal management plan. Among those, supplementary irrigation and crop protection practices (fungicides, insecticides, etc.) ensuring plant health beyond R1 could mean the difference between achieving potential GY or not.

From a crop breeding perspective, this research showed that GY components of KN and KW did not behave under the rather typical inverse relationship (i.e., no trade-offs detected). Furthermore, we demonstrated that potential KW definition was much more dependent on N assimilate availability to the ear than to DM availability during the lag phase (even though DM availability appears to dominate KN determination). Therefore, there could be a breeding opportunity for increasing both components at the same time by manipulating conditions during the lag phase. For that, plant breeders should focus on understanding how the flexibility in KW under situations of moderate to high KN works, by employing studies using wide genotype x environment combinations.

5.3 Research Limitations

The study described in Chapter 1 had an experimental complication of having utilized two different genotypes (because of commercial seed supply reasons), one in each season. The consequence was that certain conclusions are confounded between environment (year) and hybrid. To avoid any further genotypic inconsistencies, the same hybrid utilized in the 2017 growing season was then planted in both seasons of the second field study. However, given the well-documented genotypic variability that exits for GY, biomass and N uptake responses to N availability in maize, one of the major limitations of this research is that only one hybrid was used for the analyses in Chapters 3 and 4. Furthermore, there is also ample genotypic variability in final KW via different combinations of EGFR and/or GFD, which may further constrain the possibility of extrapolating some of our results.

Differences in the experimental conditions and combination of treatments applied from one field study to the other represent another limitation. When considering Chapters 3 and 4, only two N rates (0 and 224N) were common across the 3 years being reported, and the 2017 study was the only one that had starter fertilizer applied. If, nevertheless, location effects were to be tested using these two N rates, further constraints derive from the lack of a common plant density and the fact that 2017 site was provided with supplementary irrigation.

In terms of the experimental factors tested *per se*, the original goal was to explore a wide N gradient by combining N rates with N timing applications and plant densities. Unfortunately, the N timing application effect had nil to minor consequences across the number of parameters evaluated. In turn, while plant density treatments had proportionally more impact on specific

variables than N application timings, neither of these two complementary experimental factors interacted with N rate. However, N rate and timing interactions are known to be occasionally significant for post-R1 N uptake situations in other experiments, including those conducted in Indiana. We cannot conclude that N timing treatments would never be consequential for ECN and KW determination because to do so would have needed testing of many more hybrids and environments.

Regarding kernels sampled for Chapter 3 and 4, only one ear position was explored. Differences in pollination timing associated with the kernel position along the rachis were avoided by focusing sampling efforts in only the middle sector. However, for the same reason, our results are limited to that ear region. Additionally, for Chapter 4, kernel N concentration values came from a composite sample of the same plot's four ears taken at each sampling date during grain fill. Thus, kernel N content was calculated by multiplying four individual kernel DM values by one common kernel N concentration. An improved method would imply analyzing each's ear kernel N concentration separately.

Although all kernels used for Chapters 3 and 4 were intended to be sampled intact and from the center of the ears, a few inconsistencies were found in the form of occasional outliers when the respective data analyses were performed. While outlying values were still detectable, this situation speaks to the high level of training that people undertaking kernel sampling should have. Thus, this methodology is labor intensive and time consuming, making it difficult to replicate every single season.

5.4 Future Research Suggestions

As mentioned above, the major conclusions of this research are constrained to just a single hybrid. Therefore, future research should test whether the conclusions reached in this dissertation are maintained under a large pool of modern genotypes. Most benefit would be derived if genotypic variability in KW, GFR, and/or EGFD were present within the hybrids selected for such study. Furthermore, since KW increases in the last 3-4 decades of U.S. genetic improvement seemed to have been the result of indirect breeding efforts (rather than an actual goal of targeting this complex trait), another research suggestion is to perform an ERA study on KW determinants comparing the hybrid we used in this research (plus other modern hybrids) against older-era genetic materials.

In terms of experimental factors, N rate treatments should be tested in combination with a wider range of plant densities in order to detect possible interactions that were missed in this research. Furthermore, water availability should also be considered as an important secondary factor to investigate, given the significant role that water availability plays in the growth and development of maize kernels.

Finally, considering parameter selection decisions, accumulation of other nutrients (besides N) in maize kernels during the effective grain-filling period should be analyzed in order to detect similar potential nutrient interactions with kernel DM allocation that can influence KW realization. Furthermore, stoichiometry relationships among macro- and micro-nutrients should be studied to find possible thresholds for optimum DM accumulation in kernels. In addition, measurement of activity of phytohormones, such as cytokinins and ABA, and enzymes, such as invertases, could enhance the conclusions of this research by addressing mechanisms of KW determination from a molecular physiology standpoint. Additionally, acknowledging that the results in this dissertation are limited to kernels found in the center of the ear, and given that pollination timing differs along the rachis, measurements of both ECN and DM/N accumulation dynamics in kernels from different ear regions should improve scientific understanding of how much potential and final KW variation comes from alternate kernel positions within the same ear.

APPENDIX A. CHAPTER 2 SUPPLEMENTARY MATERIAL

Table A.1. Soil fertility data from experimental sites in 2016 and 2017 (LaCrosse, IN). Soil composite samples were taken to the 20-cm depth across all four reps near planting time. Values represent the average of four reps.

	Season 2016	**Season 2017**
Buffered pH	6.9	6.5
Organic Matter (%)	2.0	2.0
P ICP M3 (ppm)	44	40
K M3 (ppm)	131	119
Mg M3 (ppm)	342	209
Ca M3 (ppm)	1138	873
S M3 (ppm)	6	13
Zn DTPA (ppm)	0.4	0.7

Table A.2. Soil N availability data from experimental sites in 2016 and 2017 (LaCrosse, IN). Soil samples were taken at three depths across the three 0N plots (one per each N timing application whole plot) in each one of the four reps at planting time before any fertilizer application. Values represent the average of four reps.

	Whole Plot 0N	**Depth**	**Season 2016**	**Season 2017**
N from NO_3^- (ppm)	Planting	0-15cm	4.6	4.0
		15-30cm	2.8	2.5
		30-60cm	2.7	2.5
	Planting_V6	0-15cm	5.7	3.7
		15-30cm	2.8	2.7
		30-60cm	2.6	2.5
	Planting_V12	0-15cm	4.0	2.7
		15-30cm	2.5	1.8
		30-60cm	2.1	2.2
N from NH_4^+ (ppm)	Planting	0-15cm	1.5	8.3
		15-30cm	0.5	2.4
		30-60cm	0.4	2.4
	Planting_V6	0-15cm	1.3	11.9
		15-30cm	0.6	4.0
		30-60cm	0.4	3.6
	Planting_V12	0-15cm	1.2	9.4
		15-30cm	0.4	3.0
		30-60cm	0.3	3.5

Table A.3. Soil N availability from NO_3^- (ppm) and NH_4^+ (ppm) at V6 stage for experiments in 2016 and 2017 (LaCrosse, IN). Soil samples were taken at three depths across all combinations of N timing application by N rate treatments. Values represent the average of four reps.

Whole Plot	Sub-plot	Depth	Season 2016		Season 2017	
			NO_3^-	NH_4^+	NO_3^-	NH_4^+
Planting	0N	0-15cm	7.8	1.4	3.4	3.9
		15-30cm	3.6	0.6	2.8	3.5
		30-60cm	5.3	0.4	3.1	2.7
	112N	0-15cm	12.2	1.4	4.5	4.7
		15-30cm	4.8	0.8	3.8	4.1
		30-60cm	6.6	0.3	4.0	3.1
	168N	0-15cm	10.5	1.3	11.4	4.5
		15-30cm	6.3	0.9	7.4	3.8
		30-60cm	8.2	0.5	8.8	3.1
	224N	0-15cm	21.5	1.6	9.1	3.9
		15-30cm	6.4	0.7	7.7	5.5
		30-60cm	8.2	0.5	10.4	6.2
	280N	0-15cm	12.5	1.7	23.6	10.5
		15-30cm	4.7	0.8	12.9	5.6
		30-60cm	7.6	0.6	13.4	5.0
Planting_V6	0N	0-15cm	6.4	1.2	3.4	3.6
		15-30cm	3.8	0.5	3.2	3.8
		30-60cm	5.8	0.5	3.6	3.9
	112N	0-15cm	12.3	1.5	5.4	4.2
		15-30cm	5.0	0.8	4.9	3.9
		30-60cm	7.3	2.3	5.2	3.4
	168N	0-15cm	8.9	1.3	8.1	4.8
		15-30cm	5.2	0.8	5.8	4.0
		30-60cm	8.2	0.4	5.7	2.7
	224N	0-15cm	7.6	1.7	19.8	7.4
		15-30cm	4.6	1.1	10.9	4.4
		30-60cm	5.4	0.5	8.5	3.6
	280N	0-15cm	13.3	1.8	7.3	5.5
		15-30cm	4.9	11.6	7.0	7.2
		30-60cm	6.1	0.4	6.3	4.0
Planting_V12	0N	0-15cm	4.8	1.7	4.3	3.9
		15-30cm	3.1	0.6	3.4	3.3
		30-60cm	3.9	0.3	3.6	3.3
	112N	0-15cm	8.6	1.7	4.7	3.4
		15-30cm	4.5	0.9	3.3	3.3
		30-60cm	5.5	0.3	3.6	2.8
	168N	0-15cm	9.8	1.9	14.8	4.8
		15-30cm	4.1	0.5	9.6	3.9
		30-60cm	6.1	0.2	9.8	2.4
	224N	0-15cm	18.4	2.6	5.8	3.8
		15-30cm	6.2	1.0	4.0	4.7
		30-60cm	9.0	0.3	4.1	3.4
	280N	0-15cm	11.7	1.6	11.0	4.3
		15-30cm	5.1	0.8	7.2	4.1
		30-60cm	7.2	0.8	8.5	3.2

APPENDIX B. CHAPTER 3 SUPPLEMENTARY MATERIAL

Table B.1. ANOVA for endosperm cell number (ECN) determined at 13 days after silking (DAS) in Experiment 1 (LaCrosse, IN, 2017).

	ECN at 13 DAS	
N Timing Application		
Planting	22.3×10^6	
Planting_V6	24.2×10^6	
Planting_V12	21.3×10^6	
N Rate (kg N ha^{-1})		
0N	7.1×10^6	c
112N	22.8×10^6	b
224N	37.8×10^6	a
F-test		
N Timing (T)	ns	
N Rate (N)	<.001	
T x N	ns	

ns: not significant at α=0.05, p-value for F-test is >0.05. Means separation determined by Fisher's least significant difference (LSD) at α=0.05. Same letter or absence of letter means no significant difference was found among levels. For all variables, three replicates were collected (n=3, N=27).

Table B.2. ANOVA for ECN determined at 9 and 17 DAS in Experiment 2 (West Lafayette, IN, 2018).

	ECN at 9 DAS		**ECN at 17 DAS**	
N Rate (kg N ha^{-1})				
0N	4.64×10^5	c	106.9×10^6	b
84N	6.06×10^5	b	122.5×10^6	a
168N	6.74×10^5	a	130.4×10^6	a
224N	6.76×10^5	a	131.2×10^6	a
Plant Density (plants m^{-2})				
7.9D	5.98×10^5		124.5×10^6	
10.4D	6.12×10^5		120.9×10^6	
F-test				
N Rate (N)	<.001		0.018	
Plant Density (D)	ns		ns	
N x D	ns		ns	

ns: not significant at α=0.05, p-value for F-test is >0.05. Means separation determined by Fisher's least significant difference (LSD) at α=0.05. Same letter or absence of letter means no significant difference was found among levels. For all variables, three replicates were collected (n=3, N=24).

Table B.3. ANOVA for ECN determined at 10 and 17 DAS in Experiment 3 (West Lafayette, IN, 2019).

	ECN at 10 DAS		ECN at 17 DAS	
N Rate (kg N ha^{-1})				
0N	9.3 x 10^5	b	75.7 x 10^6	b
84N	12.6 x 10^5	a	80.2 x 10^6	a
168N	13.0 x 10^5	a	88.4 x 10^6	a
224N	12.9 x 10^5	a	84.9 x 10^6	a
Plant Density (plants m^{-2})				
7.9D	12.4 x 10^5		82.9 x 10^6	
10.4D	11.5 x 10^5		81.7 x 10^6	
F-test				
N Rate (N)	0.026		0.047	
Plant Density (D)	ns		ns	
N x D	ns		ns	

ns: not significant at α=0.05, p-value for F-test is >0.05. Means separation determined by Fisher's least significant difference (LSD) at α=0.05. Same letter or absence of letter means no significant difference was found among levels. For all variables, three replicates were collected (n=3, N=24).

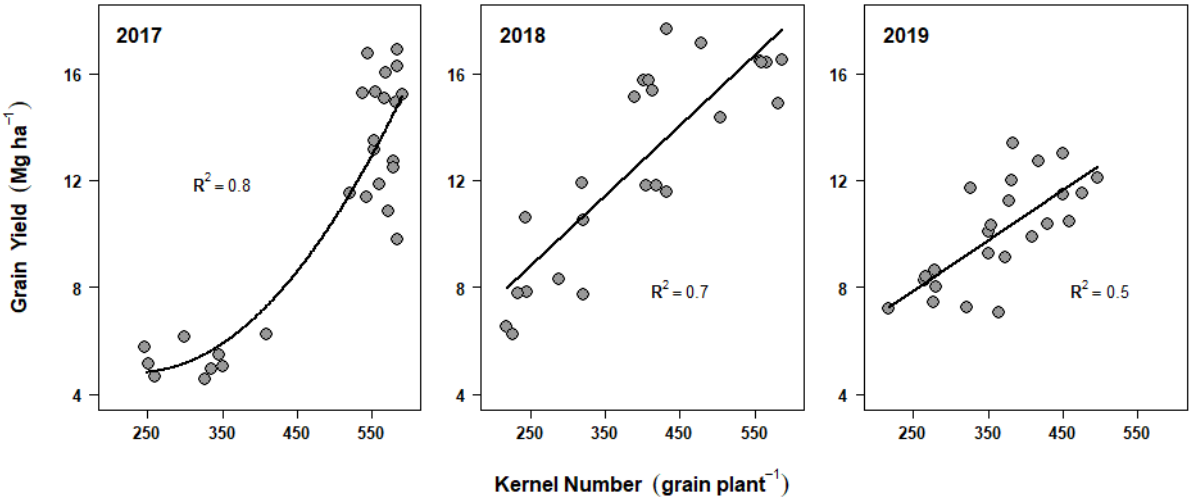

Figure B.1. Relationship between kernel number per plant and grain yield. Each panel shows data from a field experiment where N rate treatments were combined with timing application treatments (season 2017, Exp. 1) or plant density treatments (seasons 2018 and 2019, Exp. 2 and Exp. 3, respectively). Points represent data on a per plot basis. Lines represent the best fit obtained by regression analysis. R^2 for each significant regression ($p<0.05$) is shown.